AD-A235 604

RL-TR-91-47
In-House Report
March 1991

OPTICAL PERFORMANCE ANALYSIS OF THE PRECISION OPTICAL RESEARCH AND TRACKING FACILITY (PORTF)

Paul L. Repak

APPROVED FOR PUBLIC RELEASE; DISTRIBUTION UNLIMITED.

DTIC
ELECTE
MAY 10 1991
S D
E

Rome Laboratory
Air Force Systems Command
Griffiss Air Force Base, NY 13441-5700

91 5 10 007

This report has been reviewed by the Rome Laboratory Public Affairs Office (PA) and is releasable to the National Technical Information Service (NTIS). At NTIS it will be releasable to the general public, including foreign nations.

RL-TR-91-47 has been reviewed and is approved for publication.

APPROVED:

JAMES W. CUSACK, Chief
Electro-Optical Surveillance Division
Directorate of Surveillance

APPROVED:

JAMES W. YOUNGBERG, Lt Col, USAF
Deputy Director
Directorate of Surveillance

FOR THE COMMANDER:

JAMES W. HYDE III
Directorate of Plans and Programs

If your address has changed or if you wish to be removed from the Rome Laboratory mailing list, or if the addressee is no longer employed by your organization, please notify RL(OCSP) Griffiss AFB NY 13441-5700. This will assist us in maintaining a current mailing list.

Do not return copies of this report unless contractual obligations or notices on a specific document require that it be returned.

REPORT DOCUMENTATION PAGE

Form Approved
OMB No. 0704-0188

Public reporting burden for this collection of information is estimated to average 1 hour per response, including the time for reviewing instructions, searching existing data sources, gathering and maintaining the data needed, and completing and reviewing the collection of information. Send comments regarding this burden estimate or any other aspect of this collection of information, including suggestions for reducing this burden, to Washington Headquarters Services, Directorate for information Operations and Reports, 1215 Jefferson Davis Highway, Suite 1204, Arlington, VA 22202-4302, and to the Office of Management and Budget, Paperwork Reduction Project (0704-0188), Washington, DC 20503.

1. AGENCY USE ONLY (Leave Blank)	2. REPORT DATE	3. REPORT TYPE AND DATES COVERED
	March 1991	In-House Oct 89 - Oct 90

4. TITLE AND SUBTITLE
OPTICAL PERFORMANCE ANALYSIS OF THE PRECISION OPTICAL RESEARCH AND TRACKING FACILITY (PORTF)

5. FUNDING NUMBERS
PE - 62702F
PR - 4506
TA - PR
WU - OJ

6. AUTHOR(S)
Paul L. Repak

7. PERFORMING ORGANIZATION NAME(S) AND ADDRESS(ES)
Rome Laboratory (OCSP)
Griffiss AFB NY 13441-5700

8. PERFORMING ORGANIZATION REPORT NUMBER
RL-TR-91-47

9. SPONSORING/MONITORING AGENCY NAME(S) AND ADDRESS(ES)
Rome Laboratory (OCSP)
Griffiss AFB NY 13441-5700

10. SPONSORING/MONITORING AGENCY REPORT NUMBER
N/A

11. SUPPLEMENTARY NOTES
Rome Laboratory Project Engineer: Paul L. Repak/OCSP/(315) 330-4481
Rome Laboratory (RL) was formerly Rome Air Development Center (RADC).

12a. DISTRIBUTION/AVAILABILITY STATEMENT
Approved for public release; distribution unlimited.

12b. DISTRIBUTION CODE

13. ABSTRACT (Maximum 200 words)

The Precision Optical Research and Tracking Facility (PORTF) is the field optical site operated by the Directorate of Surveillance at Rome Laboratory (RL/OC). This report discusses the optical configuration of PORTF and practical optical component set-up considerations. Results are documented from computer analyses performed by the author at Rome Laboratory which simulate the complete primary optical system. Common alignment errors in the optical train and focal plane were investigated with a goal of determining allowable tolerances in the opto-mechanical alignment of the components. The tolerance limits may be used as a baseline during telescope alignment exercises to determine the alignment accuracies needed to produce acceptable images.

14. SUBJECT TERMS
Optical Simulation, Raytracing, Telescope

15. NUMBER OF PAGES
122

16. PRICE CODE

17. SECURITY CLASSIFICATION OF REPORT	18. SECURITY CLASSIFICATION OF THIS PAGE	19. SECURITY CLASSIFICATION OF ABSTRACT	20. LIMITATION OF ABSTRACT
UNCLASSIFIED	UNCLASSIFIED	UNCLASSIFIED	SAR

TABLE OF CONTENTS

PARAGRAPH	TITLE	PAGE
1.0	Background	1
2.0	Optical design	2
3.0	Sensor coupling	5
4.0	Optical alignment and induced errors	9
4.1	On-axis objects at various ranges	9
4.1.1	Case I: Object at infinity, aligned on axis	10
4.1.2	Case II: Object at 3 miles, aligned on axis	11
4.1.3	Case III: Object at 5,000 feet, aligned on axis	12
4.1.4	Case IV: Object at 500 feet, aligned on axis	13
4.2	Piston and defocus errors	13
4.2.1	Case V: Secondary mirror axially displaced 0.1 mm	14
4.2.2	Case VI: Focal plane detector displaced 1.0 mm	15
4.3	Lateral and tilt alignment errors	17
4.3.1	Case VII: Secondary mirror centration error 1.0 mm	17
4.3.2	Case VIII: Secondary mirror centration error 0.3 mm	19
4.3.3	Case IX: Secondary mirror tilt error 35 arc-seconds	19
4.3.4	Case X: Secondary mirror tilt error 2 arc-minutes	20

CONTENTS (cont'd)

PARAGRAPH	TITLE	PAGE
5.0	Off-axis object image quality	22
5.1	Case XI: Object 20 arc-seconds off-axis	22
5.2	Case XII: Object 2 arc-minutes off-axis	24
5.3	Case XIII: Object 5 arc-minutes off-axis	24
5.4	Case XIV: Object 7.5 arc-minutes off-axis	25
6.0	Summary of analysis results	27
References		29
APPENDIX		A1-A14

LIST OF FIGURES

FIGURE	CAPTION	PAGE
1.	Primary Optical Layout	3
2.	PORTL Optical Prescription	4
3.	Image Coupling Optics	6
4.	Encircled energy for on-axis objects at various ranges	10
5.	Encircled energy for off-axis view angles	26

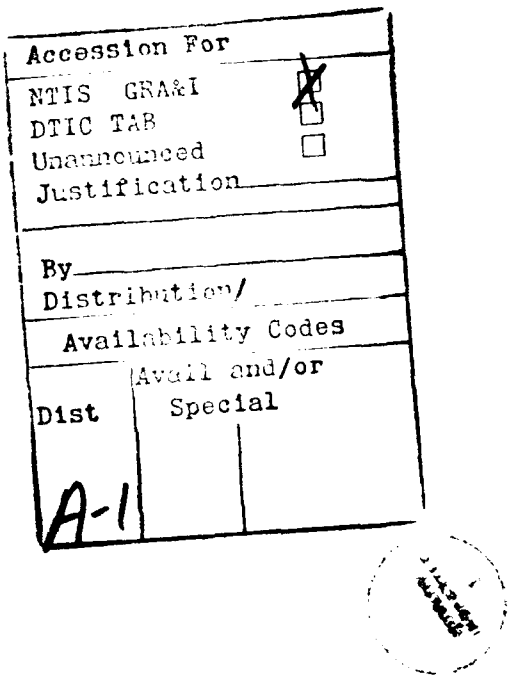

OPTICAL PERFORMANCE ANALYSIS OF THE PRECISION OPTICAL RESEARCH AND TRACKING LABORATORY (PORTL)

1.0 Background:

The Precision Optical Research and Tracking Laboratory, PORTL, is the field site for the Electro-Optical Applications Branch of the Rome Air Development Center (RADC/OCSP). PORTL's mission is to function as an in-house laboratory capable of research on ground, airborne, and space based surveillance concepts satisfying US Air Force and DoD requirements. Use by investigators from organizations external to RADC is encouraged and is designed to enhance the site's mission and status while providing a low cost high quality facility for a variety of research projects.

The PORTL facility was established in the early 1970's as a field site near Verona, NY for supporting emerging concepts in ground based surveillance. Among the research projects performed at PORTL were the Real Time Atmospheric Correction (RTAC) measurements which were the forerunner of the Compensated Imaging System (CIS) currently in place at the Air Force Maui Optical Station (AMOS). The past several years have seen the site dedicated to conceptual studies of atmospheric turbulence supported by measurements of atmospheric turbulence at optical frequencies. The equipment has the potential for future users to perform signature collection, imaging, and tracking of satellites and other exoatmospheric targets through a turbulent atmosphere and to evaluate emerging surveillance technologies. The site also has the capability of bistatic tracking and collection of target data simultaneously with the established infrared and radar surveillance facilities located at RADC, some 15 miles away. Each has tracked and recorded aircraft images and signatures in the Griffiss AFB air traffic area and beyond.

The optical system sensitivity and tolerance to misalignments and optical path errors has until now not been analyzed in detail. The purpose of the current

study was to establish a baseline of what tolerances are acceptable and what alignment conditions must be met in order to collect useful observational data. Knowledge of acceptable alignment errors is information required by optical engineers at the site when performing adjustments or modifications to the primary optical system. The analysis approach was to exercise the optical ray trace and analysis code, *POLYPAGOS*[1], which runs on a DEC VAX 8650. The optimal prescription of PORTL was perturbed in *POLYPAGOS* software by slightly adjusting positions of the secondary mirror in tilt and piston. Analyses of off-axis and near focus objects were made and compared to the expectations given in the telescope manual.

2. 0 Optical design:

The main observing instrument is a rigidly mounted 1 meter Cassegrain telescope with a coelostat style tracking mount to direct light into the telescope pupil. The coelostat tracking system contains two 1.45 m diameter mirrors in an altitude-azimuth mount directing light to a fixed vertically mounted Cassegrain telescope. This arrangement offers great flexibility in experimental setup and operation, as the focal plane is fixed in relation to the optical bench for all observing positions. An image derotation "K" mirror assembly is included in the assembly to derotate image rotation caused by azimuthal track (see Figure 1).

The telescope is a classical 2-mirror Cassegrain with a 120 inch focal length, f/3 parabolic primary and a hyperbolic secondary yielding a final focal ratio of f/18. Details of the optical prescription are shown in Figure 2. A focussing servo moves the secondary with respect to the primary away from the infinity focus position to allow focussing on objects at finite distances. As the object distance decreases, the downward movement of the focal plane can be exactly nullified by moving the secondary mirror away from the primary mirror. According to the telescope design parameters, at the secondary mirror's limit of travel of approximately 2.5 inches from the infinity focus position, objects at 500 feet range will be in best focus. Any object at less than approximately three miles range will no longer be diffraction limited, as non-correctable spherical aberration enlarges

the blur circle significantly at closer ranges[2]. At this close 500 ft range spherical aberration causes a path error of about three waves and the effective linear resolution is the same as that for objects at a range of 6,000 feet[3]. These configurations will be analyzed later in Section 4.

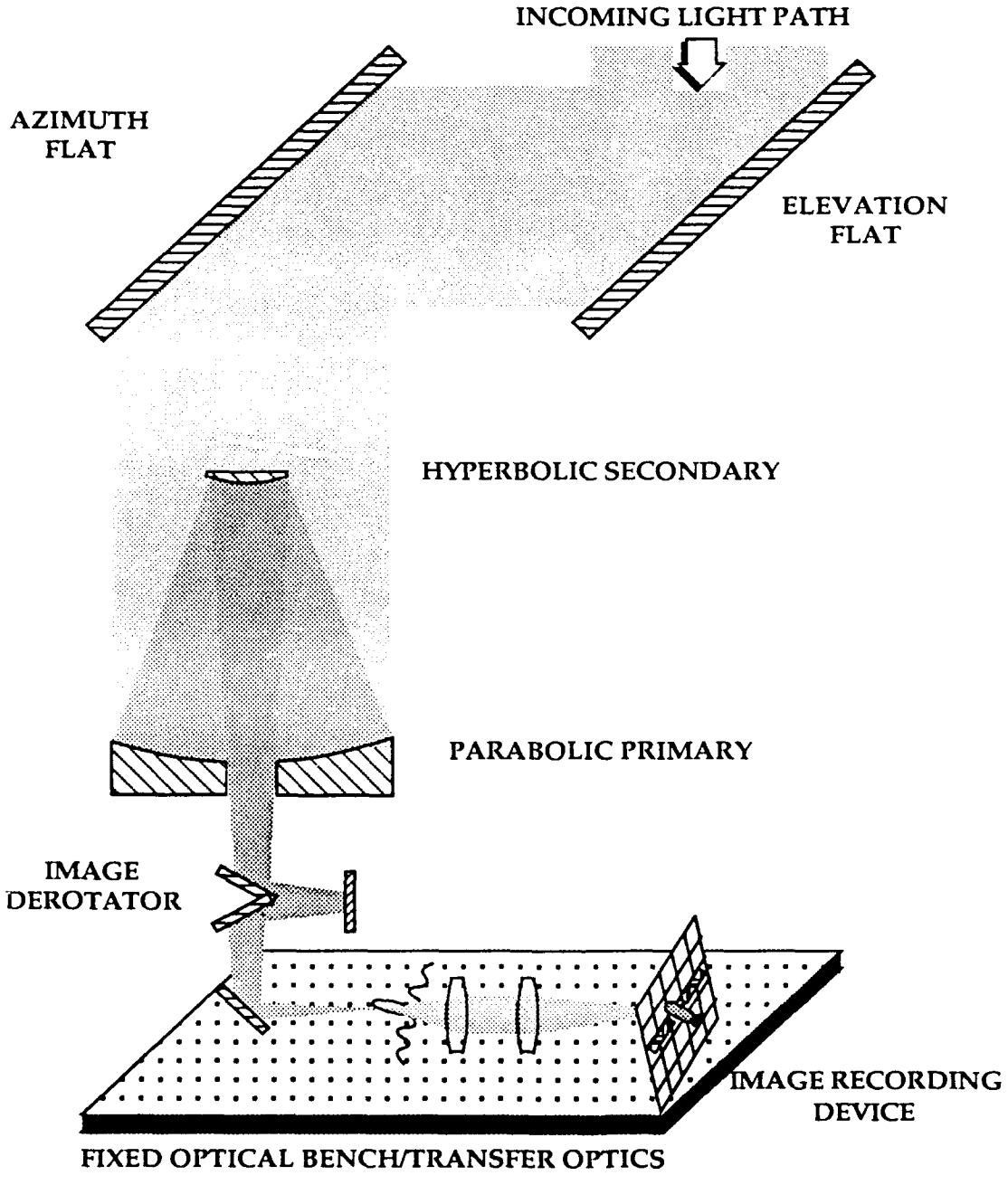

Figure 1. Primary Optical Layout

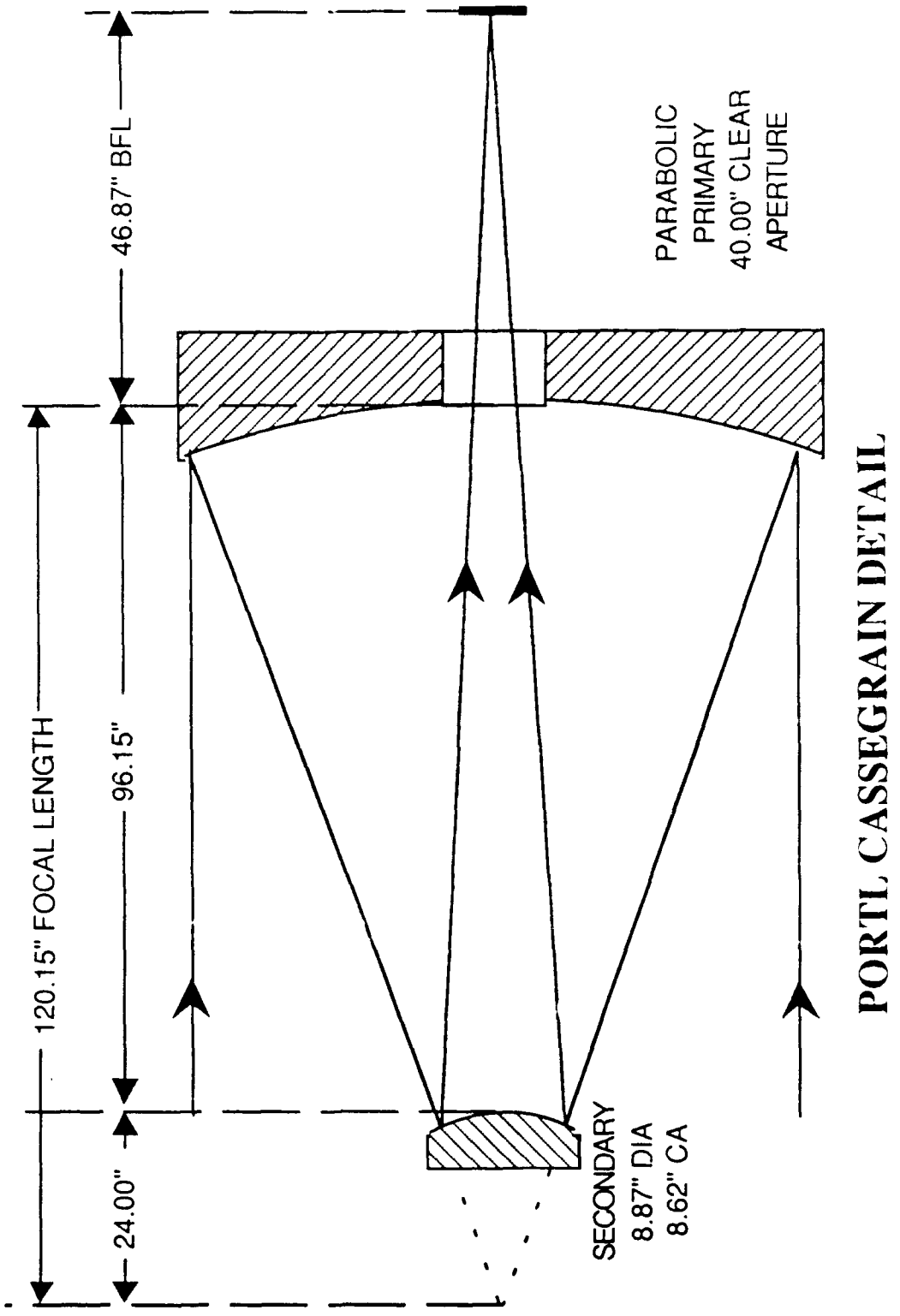

Figure 2. PORTL Optical Prescription

In the absence of a distorting atmosphere and assuming diffraction limited optics, the diameter of the Airy disc for a point object may be found from the well known relationship:

$$a = 2.44\lambda(F\#)$$

In the case of the F/18 PORTL telescope, the primary image will thus have a spot size of 24.16 μm at a visible wavelength of 0.55 μm . For the purposes of optical analysis, this will be the alignment baseline to which deviations in the system configuration are compared.

3. 0 Sensor coupling:

Efficient coupling of the collected photons to a detection device is a straightforward procedure in principle, but one which demands careful planning. One of the goals of PORTL is to record images with diffraction limited information content by both direct imaging and by methods of post detection processing (e.g. speckle imaging). When using two-dimensional solid state detectors, the sampling induced by the spatial extent of the pixel size must be matched to the Nyquist sampling criterion for subsequent image recovery. This essentially calls for at least two detection pixels per Airy disk (diffraction spot). Figure 3 shows the basic coupling optics scheme, which relays the primary image through a collimator for filtering, and then re-images onto the detector focal plane. The collimator assembly is generally required for insertion of filters or other auxiliary optics as well as for Airy disk to pixel matching, and will be a part of most optical configurations.

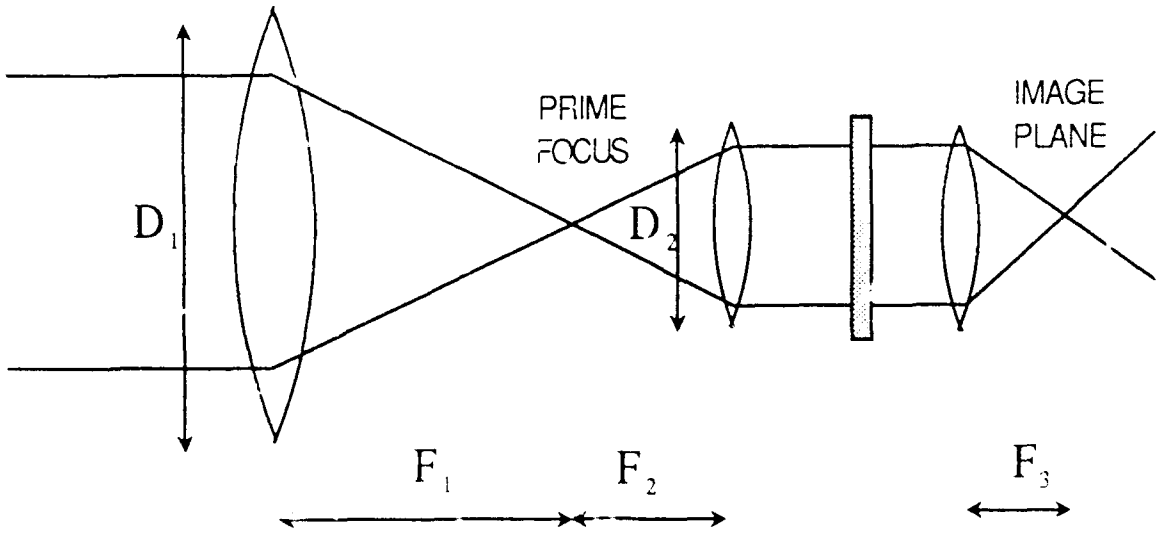

Figure 3. Image Coupling Optics

To determine the required coupler specifications, again recall that according to the Nyquist criteria a diffraction limited spot will require a detector element size 'ds' of at no larger than:

$$ds = \frac{2.44\lambda(F\#)}{2}$$

Where F# is the focal ratio (F/D) of the PORTL primary/secondary optical system. The coupling optics must have a magnification equal to the ratio of prime focus telescope image size to the given pixel size (3). To derive the transfer optical prescriptions, refer to Figure 3 and note that the first requirement is to match the primary focal ratio with that of the first collimating optic. This condition will just fill the collimator with the after focus re-expanding cone of light from the telescope:

$$\frac{F_1}{D_1} = \frac{F_2}{D_2} \qquad \text{thus } D_2 = \frac{D_1 F_2}{F_1}$$

In this f/18 case, so as to collect all of the available light in the image, we require for the collimator the relationship:

$$\frac{F_2}{D_2} \leq 18$$

A front collimator lens with a focal ratio of F/18 will be just filled by the primary telescope light beam; a collimator front focal ratio greater than F/18 would spill light outside the collection aperture of the collimator and the light would be lost. The collimated light will next be filtered, if required, and then refocussed by the rear collimator lens onto the detector focal plane. The effective diameter of the rear collimator lens is predetermined by the diameter of the light beam at the entrance to the first collimation lens (see Figure 3). Now the Airy disc size ' Δx ' at the detector is found by:

$$\Delta x = \frac{2.44\lambda F_3}{2D_3} = \frac{2.44\lambda F_3}{2D_2} \qquad \text{(since when collimated } D_3 = D_2\text{)}$$

Optimal detection efficiency requires matching the pixel size on the detector to the Airy disc. Rearranging and combining the above equations, we obtain the required relative focal lengths of the collimator lenses in terms of the primary focal ratio and detector pixel size which will just cover two pixels with a diffraction limited spot:

$$\frac{F_3}{F_2} = \frac{2\Delta x}{2.44\lambda}\frac{D_1}{F_1}$$

PORTL has two different representative CCD camera system focal planes; one with a pixel size Δx of 18.6 μm and another with 9.9 μm. Substituting into the equation above, we find that the two collimator lenses need have focal lengths in the ratio $F_3/F_2 = 1.54$ or 0.82, respectively, in each of the two cases. Not at all a stressing combination of translation lenses.

Difficulty arises when trying to account for the reality of atmospheric turbulence and efficiently placing all of the available light on a single pixel. Speckle imaging techniques, for example, require extremely short exposures (on the order of several milliseconds) and consequently very few photons may be recorded during any one exposure. Because of the paucity of photons, extremely efficient coupling is required. The image resolution on the focal plane is now determined not by the primary telescope diameter, but rather by the atmospheric turbulence parameter R_0. At PORTL, R_0 may range down to three cm. Effectively then, the focal ratio of the telescope changes by the ratio of the primary diameter to R_0 and the transfer optics which match the Airy disk to the pixel element size must be modified. At R_0 = 3 cm, the system focal ratio effectively changes to:

$$\frac{F_1}{D_1} \Rightarrow \frac{F_1}{D_1} R_0 = \frac{F_i}{D_i} \quad .03$$

Substituting into the previous equation above, we find that the requirements on the collimator lenses are that the front and rear lenses must have focal lengths in the ratios of F_3/F_2 = 0.05 or 0.02 respectively for each of the two CCD cases. Given the additional requirement of an F# of near F/18 on the first collimator lens, the F ratio requirement of twenty or fifty to one on the rear lens is clearly unreasonable, especially if high quality and reasonably priced optics are desired. There is no easy way out of this situation, as no combination of auxiliary optics will get around the fundamental facts stemming from a small R_0. All that can be done is to approach the required specifications with available coupling optics as much as possible and accept some loss of performance.

4.0 Optical alignment and induced errors:

The alignment tolerances of PORTL have been analyzed using the optical analysis program *POLYPAGOS* running on a VAX computer. Cases were run with piston, tilt and decentration errors between the primary and secondary mirrors. The overall theoretical optical performance was analyzed in the perfectly aligned and misaligned cases and serve as an indicator as to the types of tolerable misalignments. Output data and plots and resulting from each case are presented in the Appendix. In all cases, the results do not consider the effects of atmospheric turbulence, which will tend to overwhelm all but the worst focal plane errors. Because of this fact, care should be exercised when interpreting what efforts are required to adequately align the optical system.

4.1 On-axis objects at various ranges:

Although the PORTL telescope system is an infinity corrected system, it can be used at finite object distances by moving the secondary mirror to refocus, keeping the focal plane at a constant position relative to the optical bench. This was tested in *POLYPAGOS* by comparing the infinity focus position performance with objects located at 3 miles, 5,000 feet, and 500 feet range.

A number of analysis tools are available with *POLYPAGOS* to determine optical quality. Here, the primary means of comparison is a combination of geometric spot diagram, optical path difference (OPD) variance, Strehl ratio, point spread function (PSF) intensity distribution, and modulation transfer function (MTF) contrast distribution. In addition, especially when comparison of analyses are difficult to interpret, an encircled energy plot of the diffraction spot is another means to graphically show energy density of the image. Figure 4 is such a plot, for the on-axis ranges investigated. One can immediately notice that although the Cassegrain telescope system is adaptable to focus on finite range objects, the energy distribution in the image plane will dramatically change. This is simply a consequence of utilizing a finite conjugate design in non-optimum configurations.

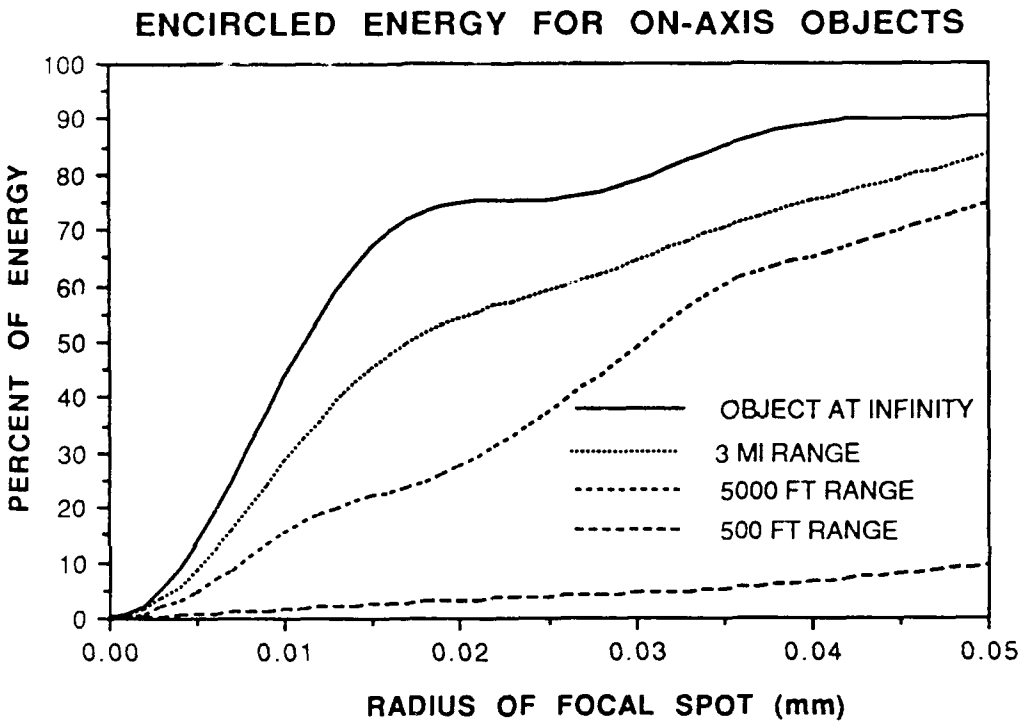

Figure 4. Encircled energy for on-axis objects at various ranges

4.1.1 Case I, Object at infinity, aligned on axis:

As a baseline, the theoretical performance of the telescope was checked with *POLYPAGOS* on the RADC Surveillance Directorate's VAX computer using the optical prescription (Figure 2) as given in the original PORTL Operation and Maintenance Manual[2]. The geometric spot diagram was evaluated for a point displaced slightly from the paraxial focus position (by 0.6 μm) for computational and plotting purposes, so that the geometric spot of this "perfectly aligned" layout would be of finite size, rather than a theoretical calculated single geometric point (see Figure A-1a). All other calculations were performed with proper alignments and focal positions. Examination of the defocussed spot shows a perfectly symmetrical pattern with the central hole due in this case to the defocus

displacement. *POLYPAGOS* calculates the focal length of this nominal F/18 system at 18.186143 meters, and the back focal length is at 1.1904971 meters. Residual Optical Path Difference (OPD) errors calculated for this system are very low, as shown in the following extract from the program output:

```
OPD STATISTICS NORMALIZED TO WAVELENGTH  1 EQUAL TO   0.5550000E-03

                    MAXIMUM VALUE =   0.1493165E-03
                    MINIMUM VALUE =   0.3727777E-06
                    AVERAGE VALUE =   0.5250004E-04
                    RMS DEVIATION =   0.4430233E-04

                    STREHL RATIO  =  0.99999992E+00
```

Carrying out the diffraction analysis, the calculated optical point spread function of this optimally aligned system (see Figure A-1b) has a Strehl ratio of 1.00 and shows a classical Airy disk which agrees well with the theoretical spot size (to the first null) of:

$$2.44\lambda(F\#) = 2.44(0.55)(18) = 24.16\mu m$$

The Modulation Transfer Function (MTF) displays a shoulder fall off (see Figure A-1d) which is normal for this Cassegrainian optical system, due to the central hole of the primary mirror and blockage of the secondary mirror.

4.1.2 Case II, Object at 3 miles, aligned on axis:

According to the original telescope Operation and Maintenance Manual[2], the secondary may be moved to accommodate decreasing object distances and the system will be diffraction limited for an object distance of approximately 3 miles or more. This was checked by moving the object distance to 3 miles and adjusting the secondary mirror position (by 1.98 mm) such that the focal plane would fall in the same place relative to the fixed optical bench as it did in Case I.

Note that the 3 mile range calculated geometric spot diagram has increased in size to ~60 μm, while the central Airy disk indicated in PSF in Figure A-2b is still approximately 24 μm in size. However, the shape of the outer diffraction

rings is becoming distorted and more energy is appearing in the outside the central Airy disk regions. Compare the encircled energy plot of this case to that of an object at infinity in Figure 4. This range does appear to be the closest for which the system is still approximately diffraction limited if one considers the central disk of the PSF. However, with a *POLYPAGOS* calculated Strehl ratio of 0.63, the peak intensity is only 2/3 that for an object focussed at infinity. Aberrations, primarily spherical, begin to affect the OPD and the RMS OPD is approximately 1/10 wave, as the calculated OPD statistics show:

```
OPD STATISTICS NORMALIZED TO WAVELENGTH  1 EQUAL TO   0.5550000E-03

                    MAXIMUM VALUE =   0.3553567E+00
                    MINIMUM VALUE =   0.8930380E-03
                    AVERAGE VALUE =   0.1246840E+00
                    RMS DEVIATION =   0.1051865E+00

                    STREHL RATIO  =  0.63665132E+00
```

4.1.3 Case III, Object at 5,000 feet, aligned on axis:

A number of experiments have been carried out over the ground range at the Verona Test Site. In particular, a shed 5,000 feet down range is used to house sensors of various types. The optical quality of the system was calculated for this range, neglecting the effects of atmospheric turbulence (which may be significant over this ground path).

To allow the focal plane to remain fixed, the secondary mirror position from the primary mirror must be increased by 5.95 mm when the object distance is 5,000 ft. From Figure A-3a, the geometric spot has increased to 0.14 mm in diameter, significantly wider than the infinity focus case of 0.024 mm. The OPD peak to valley is more than one wave and the Airy disk has dramatically decreased in intensity with a Strehl ratio of 0.085 and widened to 0.034 mm. The encircled energy contained within the Airy disk is a small fraction of the infinity focus case (see Figure 4) and the RMS OPD has grown to 1/3 wave.

```
OPD STATISTICS NORMALIZED TO WAVELENGTH  1 EQUAL TO   0.5550000E-03

                    MAXIMUM VALUE =   0.1067907E+01
                    MINIMUM VALUE =   0.2687821E-02
                    AVERAGE VALUE =   0.3747147E+00
                    RMS DEVIATION =   0.3161013E+00

                    STREHL RATIO  =  0.85482516E-01
```

4.1.4 Case IV, Object at 500 feet, aligned on axis:

The PORTL optical system was originally designed to focus down to 500 feet in range by adjusting the secondary mirror position up to 2.5 inches farther away from the primary mirror than the infinity focus case with three waves of degradation[3]. The actual distance *POLYPAGOS* calculated for the secondary movement to focus on an object at 500 feet down range is 2.35 inches (60 mm). Spherical aberration at this range dominates the image (see A-4). Though a central intensity spot exists, its energy content is overwhelmed by the energy in the wings. This is confirmed by both Figure 4, and the Strehl ratio in the output excerpt shown below. There are three waves of average wavefront degradation as reported in the telescope operations manual, but the peak to valley is more than 10 waves.

```
OPD STATISTICS NORMALIZED TO WAVELENGTH  1 EQUAL TO   0.5550000E-03

                    MAXIMUM VALUE =   0.1036575E+02
                    MINIMUM VALUE =   0.2761718E-01
                    AVERAGE VALUE =   0.3647775E+01
                    RMS DEVIATION =   0.3071220E+01

                    STREHL RATIO  =  0.91381485E-02
```

4.2 Piston and defocus errors:

One claimed advantage of PORTL is its ability to maintain a constant focal position, regardless of object range. This depends upon on-axis movement of the

secondary mirror, but it is unknown what effect any errors in secondary mirror axial travel will have on focal plane positioning. It was also unknown exactly how precisely the focal plane detector must be positioned to obtain a good image.

Simple defocus cases in piston of either the secondary mirror r the focal plane detector were analyzed to determine what accuracy might be needed in axial placement of these components. Errors may occur in two ways; the secondary may be misplaced, or the secondary may be in the proper position but the focal plane position may not be accurately found. In all cases in this section, observed objects are assumed to be point objects on axis at infinite range.

4.2.1 Case V, Secondary mirror axially displaced 0.1 mm:

To determine what effect a misplaced secondary mirror with respect to the fixed focal plane would have on system optical quality, an analysis was performed on the system with a small piston displacement of the secondary. This might easily be caused by unknown or inaccurate placement of the secondary mirror motor drive, or lack of resolution in the secondary motor positioning screw.

If the secondary is displaced from its infinity focus position to 0.1 mm further away from the primary mirror, the calculated prime focus position moves inward by as much as 3.6 mm. If the focal plane detector is moved to this new position, the resultant Strehl ratio is 0.9989 that of the non-displaced case, the RMS OPD error is 0.005, and no significant error or loss of signal strength or spatial resolution results.

```
OPD STATISTICS NORMALIZED TO WAVELENGTH  1 EQUAL TO   0.5550000E-03

                    MAXIMUM VALUE =   0.1767595E-01
                    MINIMUM VALUE =   0.4413392E-04
                    AVERAGE VALUE =   0.6214910E-02
                    RMS DEVIATION =   0.5244469E-02

                    STREHL RATIO  =  0.99891690E+00
```

(focal plane displaced for best focus)

Little or no image degradation would be evident for this amount of piston error. If the focal plane detector is not displaced by this critical 3.6 mm, however, the quality of the image is significantly degraded. The RMS OPD error rises to 0.7 wave and the Strehl ratio plummets to 0.016. The PSF at this position shows very high sidelobe structure due to the defocus error (see Figure A-5b) and any resulting image would be quite blurry.

```
OPD STATISTICS NORMALIZED TO WAVELENGTH  1 EQUAL TO   0.5550000E-03

                    MAXIMUM VALUE =  -0.1309739E+00
                    MINIMUM VALUE =  -0.2612913E+01
                    AVERAGE VALUE =  -0.1374002E+01
                    RMS DEVIATION =   0.7187316E+00

                    STREHL RATIO  =  0.16280299E-01
```

(focal plane *not* displaced for best focus)

A *POLYPAGOS* analysis on a full 1.0 mm displacement of the secondary mirror results in a focus shortened by 36 mm (36 times the piston error). The PSF calculation for the displaced focal plane image in this case is still within the diffraction limited regime, with a Strehl ratio of 0.89. The required 36 mm displacement of the focal plane closer to the primary mirror is probably not a practical adjustment to be made, however.

4.2.2 Case VI, Focal plane detector displaced 1.0 mm:

This case is similar to the one in Case V, but with the focal plane incorrectly placed. If the secondary mirror is correctly positioned for infinity focus but the focal plane detector is displaced in focus by 1.0 mm, the image will suffer an OPD error of 0.2 wave and a Strehl ratio drop to 0.15.

```
OPD STATISTICS NORMALIZED TO WAVELENGTH  1 EQUAL TO   0.5550000E-03

                    MAXIMUM VALUE =   0.7207678E+00
                    MINIMUM VALUE =   0.3589105E-01
                    AVERAGE VALUE =   0.3781459E+00
                    RMS DEVIATION =   0.1983299E+00

                    STREHL RATIO  =  0.1491[illegible]17E+00
```

(focal plane displaced 1.0 mm)

From both the geometric spot diagram and the PSF, (Figure A-6a and A-6b) the point image size is as large as 60 μm and the spatial resolution as indicated in the MTF has dropped to 1/3 of its former value. The high and complex sidelobe structure of the PSF indicates a very poor image would result from this defocus error.

At half this focal plane defocus error, analysis for a displacement of 0.5 mm gives a nearly diffraction limited spot size with an RMS OPD error of 0.1 waves and a Strehl ratio of 0.67.

This may be quite acceptable for most purposes and thus 0.5 mm may be considered to be near the focal plane position resolution requirement. However, the presence of other alignment and aberration errors would most likely modify this finding, making the tolerable focal plane placement more restrictive.

```
OPD STATISTICS NORMALIZED TO WAVELENGTH  1 EQUAL TO   0.5550000E-03

                    MAXIMUM VALUE =   0.3606993E+00
                    MINIMUM VALUE =   0.1794276E-01
                    AVERAGE VALUE =   0.1890681E+00
                    RMS DEVIATION =   0.9917019E-01

                    STREHL RATIO  =  0.6675[illegible]257E+00
```

(focal plane displaced 0.5 mm)

4.3 Lateral and tilt alignment errors:

The secondary mirror assembly is motor driven axially and rides on a focus drive screw. The next series of analyses will investigate the accuracy required for good imaging by proper centration and tilt of the secondary mirror. The secondary mirror is aligned laterally with the primary mirror by aligning a centering dot on the secondary with crossed wires on the coelostat base casting[2]. The wires previously had been centered by plumb line with the primary mirror to within 0.06 inch (1.5 mm). The procedure does not indicate how accurate the centering dot must be placed on the secondary, but obviously its position is critical to the lateral displacement of the secondary mirror in the optical train.

Equally important is the tilt error of the secondary mirror relative to the primary. Tilt is also corrected visually with the crossed wire technique, by looking at the reflection of the primary mirror in the secondary mirror. The claimed accuracy of this method is 25 arc-seconds, and manufacturing error may account for a total of 35 arc-seconds tolerance in tilt[2].

4.3.1 Case VII, Secondary mirror centration error 1.0 mm:

This case presumes that the secondary mirror can be optically centered with the primary mirror to within 1.0 mm lateral displacement orthogonal to the optical axis in an arbitrary 'Y' direction. Note that this optical centering technique of the secondary and primary mirrors is not strictly limited by the 1.5 mm plumb line tolerance given for the primary/coelostat alignment, but is limited by one's ability to visually center reflected images of the cross wires and the mechanical tolerance of the spider vane adjustment screws. The opto-mechanical centering tolerance is not referenced in the original operations and maintenance manual, but sample cases are checked here for resultant focal plane quality.

The geometric spot diagram for this case in Figure A-7a shows a considerable spread of the focused rays in the direction of secondary mirror

displacement. Peak to valley OPD error is more than four waves. Diffraction analysis results in a Strehl ratio of 0.17. The PSF in the 'Y' direction is distorted, as shown in the separate 'X' and 'Y' plots of Figures A-7b and A-7c. Notice that the orthogonal X,Y plot slices miss the pronounced double sidelobe which is evident in the contour and isometric plots of Figures A-7d and A-7e. This is due to an induced tilt (in radians) and lateral displacement (in mm) of the exit pupil, as calculated by *POLYPAGOS* :

```
        TILT AND DISPLACEMENT OF EXIT PUPIL IN X- AND Y-DIRECTIONS

    XTILT              YTILT              XDISP              YDISP
0.00000000E+00    -0.13651317E-02    0.00000000E+00    0.95262474E+00

 OPD STATISTICS NORMALIZED TO WAVELENGTH  1 EQUAL TO   0.5550000E-03
                  MAXIMUM VALUE =   0.2054531E+01
                  MINIMUM VALUE =  -0.2106614E+01
                  AVERAGE VALUE =  -0.1217140E-01
                  RMS DEVIATION =   0.7564407E+00

                   STREHL RATIO  =  0.17232760E+00
```

Clearly, the secondary mirror must be centered to better than 1.0 mm for good image quality. The MTF and hence the image contrast has also markedly deteriorated (see Figure A-7f and A-7g), to no better than 60 lines/mm in the 'X' direction and 40 lines/mm in the 'Y' direction (vs. ~100 lines/mm in Case I). Note also the narrowness and complex structure of the isometric surface plot MTF of Figure A-6h.

It turns out that if the secondary mirror is tilted by the amount calculated for the tilt of the exit pupil shown above, then the effects of the lateral displacement can be in large part compensated for, with the Strehl ratio rising to 0.92 and the large sidelobes of the PSF disappearing. The secondary mirror support structure does not have any way to introduce a known tilt compensation, however. Even if it did, the lateral displacement would have to be known in advance and it would be much easier to correct for that error directly.

4.3.2 Case VIII, Secondary mirror centration error 0.3 mm:

With a secondary mirror centration error of only 0.3 mm in the 'Y' direction the situation is much improved. The spreading of the geometric and diffraction spots is reduced, the peak to valley OPD error is down to 1.2 waves, and the Strehl ratio is up to 0.80. Tilt and displacement in the 'Y' direction are consequently reduced as well.

```
TILT AND DISPLACEMENT OF EXIT PUPIL IN X- AND Y-DIRECTIONS

 XTILT                YTILT                XDISP              YDISP
[illegible]E+00     -0.40953965E-03      0.00000000E+00    0.28580633E+00

PD STATISTICS NORMALIZED TO WAVELENGTH  1 EQUAL TO    0.5550000E-03
                 MAXIMUM VALUE =    0.6219635E+00
                 MINIMUM VALUE =   -0.6263791E+00
                 AVERAGE VALUE =   -0.1047652E-02
                 RMS DEVIATION =    0.2269244E+00

                 STREHL RATIO  =   0.79978107E+00
```

Note in the surface contour of Figure A-8d that the first sidelobe maximum is much higher on the displaced 'Y' side than the opposite side, but the peaks so evident in Case VII are now missing.

4.3.3 Case IX, Secondary mirror tilt error 35 arc-seconds:

The alignment procedure described in Paragraph 4.2.5 of the Telescope Operation and Maintenance Manual[2], if followed correctly, results in a total possible error of 35 arc-seconds. This misalignment effectively tilts and displaces the exit pupil. The result is an OPD peak to valley of 0.4 waves, with an RMS value of 0.78 waves and a Strehl of 0.97 as shown below:

```
TILT AND DISPLACEMENT OF EXIT PUPIL IN X- AND Y-DIRECTIONS

      XTILT                YTILT                XDISP                YDISP
 0.00000000E+00      -0.33936958E-03      0.00000000E+00      0.23633851E+00

 OPD STATISTICS NORMALIZED TO WAVELENGTH  1 EQUAL TO  0.5550000E-03
                    MAXIMUM VALUE =   0.2154005E+00
                    MINIMUM VALUE =  -0.2150315E+00
                    AVERAGE VALUE =  -0.2698514E-04
                    RMS DEVIATION =   0.7824396E-01

                    STREHL RATIO  =  0.97331620E+00
```

The image plane pattern observed (see Appendix 9) is very similar to that produced by the decentration error of Case VIII. The image in this case is only slightly degraded, thus the claimed 35 arc-second alignment tolerance by itself is quite acceptable.

4.3.4 Case X, Secondary mirror tilt error 2 arc-minutes:

A 2 arc-minute tip/tilt error in the secondary mirror cell position should be readily observable during the prescribed alignment procedure. If the error in secondary mirror tilt is as much as 2 arc-minutes, *POLYPAGOS* calculates the following results:

```
TILT AND DISPLACEMENT OF EXIT PUPIL IN X- AND Y-DIRECTIONS

      XTILT                YTILT                XDISP                YDISP
 0.00000000E+00      -0.11635528E-02      0.00000000E+00      0.81197746E+00

 OPD STATISTICS NORMALIZED TO WAVELENGTH  1 EQUAL TO   0.5550000E-03

                    MAXIMUM VALUE =   0.7384166E+00
                    MINIMUM VALUE =  -0.7373202E+00
                    AVERAGE VALUE =  -0.9818558E-03
                    RMS DEVIATION =   0.2682668E+00

                    STREHL RATIO  =  0.72855208E+00
```

From the graphics displayed in Appendix 10, one can see that even a 2 arc-minutes tilt error in the secondary mirror does not severely degrade the imaging quality of the optical system. With a Strehl ratio down to 0.72, however, much greater tilts are probably not acceptable.

5.0 Off-axis object image quality:

All of the analyses presented in Section 4 above was the result of imaging a point object on axis with mechanical misalignments of the telescope's optical components. To determine how well the optical system images extended objects or point objects off-axis, *POLYPAGOS* was used to calculate a number of cases in which the object does not lie on the extended optical axis. In all cases investigated in this section, the proper opto-mechanical alignment of the telescope is assumed. All targets are points at infinite range lying off the extended optical axis. Knowledge of off-axis object imaging performance is important in determining the useful field of view when separate multiple targets are being observed, and analysis may be extended to large objects at finite ranges (though these cases were not analyzed here).

5.1 Case XI, Object 20 arc-seconds off-axis:

Assume atmospheric turbulence restricts R_0 to approximately 3 cm. Applying the diffraction equation to a 3 cm aperture yields a diffraction resolution of 10 arc-seconds. This case calculates the image quality for a full 1.0 meter aperture with an object at 20 arc-seconds off-axis, to see if the telescope introduces distortions at this atmospherically defined minimum field-of-view. Note in the output given below that looking off-axis induces a small effective tilt and displacement in the exit pupil.

TILT AND DISPLACEMENT OF EXIT PUPIL IN X- AND Y-DIRECTIONS

XTILT	YTILT	XDISP	YDISP
0.00000000E+00	0.20360477E-03	0.00000000E+00	0.43556002E-04

OPD STATISTICS NORMALIZED TO WAVELENGTH 1 EQUAL TO 0.5550000E-03

MAXIMUM VALUE =	0.8364583E-02
MINIMUM VALUE =	-0.9318628E-02
AVERAGE VALUE =	-0.1767882E-03
RMS DEVIATION =	0.3255870E-02
STREHL RATIO =	0.99958199E+00

From the graphics analysis in Appendix 11, there is virtually no difference in image quality between this case and the optimum alignment of Case I. The optical quality of the telescope should not interfere with resolution of objects at this angular separation.

5.2 Case XII, Object 2 arc-minutes off-axis:

At 2 arc-minutes, an object in orbit at 200 km range would have a lateral extent of 116 m, while at the 5,000 foot Verona site test shed 2 arc-minutes cover 35 in. *POLYPAGOS* analysis results below and the graphics in Appendix 12 show that an object of twice this size (centered on axis, four arc minutes total field-of-view) would still have almost imperceptible image distortion with the PORTL telescope.

TILT AND DISPLACEMENT OF EXIT PUPIL IN X- AND Y-DIRECTIONS

XTILT	YTILT	XDISP	YDISP
0.00000000E+00	0.24432394E-02	0.00000000E+00	-0.78691602E-03

OPD STATISTICS NORMALIZED TO WAVELENGTH 1 EQUAL TO 0.5550000E-03

MAXIMUM VALUE =	0.3534891E-01
MINIMUM VALUE =	-0.1773379E+00
AVERAGE VALUE =	-0.3182876E-01
RMS DEVIATION =	0.4263380E-01
STREHL RATIO =	0.98189519E+00

5.3 Case XIII, Object 5 arc-minutes off-axis:

At 5 arc-minutes off axis the situation begins to noticeably change. The Strehl ratio has dropped to 0.61 and The OPD RMS is becoming significant at 0.15.

TILT AND DISPLACEMENT OF EXIT PUPIL IN X- AND Y-DIRECTIONS

XTILT	YTILT	XDISP	YDISP
0.00000000E+00	0.61080942E-02	0.00000000E+00	-0.30606090E-02

OPD STATISTICS NORMALIZED TO WAVELENGTH 1 EQUAL TO 0.5550000E-03

MAXIMUM VALUE =	-0.1637963E-01
MINIMUM VALUE =	-0.7048112E+00
AVERAGE VALUE =	-0.1980895E+00
RMS DEVIATION =	0.1450887E+00
STREHL RATIO =	0.60682295E+00

From Figure A-13a the extent of the geometric spot size in the off-axis direction is now approaching the diffraction spot size of 24 μm. The Y-axis slice PSF is becoming slightly wider than the X-axis slice, and the contour map shows an unsymmetrical secondary ring emerging. Similarly, resolution and spatial contrast is reduced in the 'Y' direction as seen in the MTF plots. This analysis shows that 5 arc-minutes is likely near or just beyond the limit of the acceptable off-axis angle viewing angle for which the PORTL telescope design is diffraction limited.

5.4 Case XIV, Object 7.5 arc-minutes off-axis:

At 7.5 arc-minutes off-axis, the geometric spot diagram is 2-3 times size of the on-axis diffraction spot and the PSF is highly distorted in both 'X' and 'Y' directions (see Appendix 14) with a Strehl ratio of 0.16. The calculated resolution has dropped to only approximately 20 lines/mm from the original 100.

TILT AND DISPLACEMENT OF EXIT PUPIL IN X- AND Y-DIRECTIONS

XTILT	YTILT	XDISP	YDISP
0.00000000E+00	0.91620772E-02	0.00000000E+00	-0.59750319E-02

OPD STATISTICS NORMALIZED TO WAVELENGTH 1 EQUAL TO 0.5550000E-03

MAXIMUM VALUE = -0.3758385E-01
MINIMUM VALUE = -0.1383756E+01
AVERAGE VALUE = -0.4445489E+00
RMS DEVIATION = 0.2820486E+00

STREHL RATIO = 0.16111941E+00

Figure 5 is an encircled energy plot for the off-axis viewing cases. It clearly shows that between 2 and 5 arc-minutes off-axis large changes occur in the energy density of the image plane spot. At 7.5 arc-minutes off-axis the distortion has become so extreme that the energy in the central spot is no longer a prominent feature, an indication of significant image distortion.

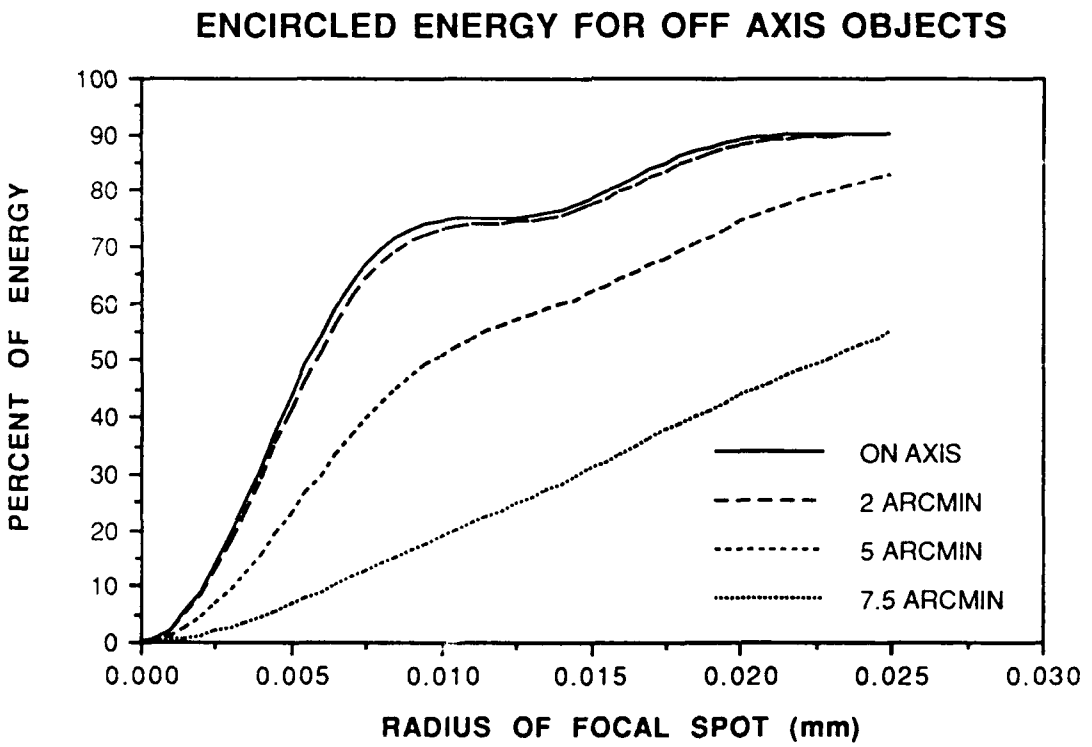

Figure 5. Encircled energy for off-axis view angles

6.0 Summary of analysis results:

Simulation and optical analysis of the PORTL telescope system is meant as a starting point in alignment and characterization of the instrument's optical and imaging properties. Final experimentation must be performed on the telescope itself to verify the findings resulting from analyses. The analyses do serve as a beginning to tell the engineer which parameters have special tolerance requirements, and indicate the care needed in meeting the alignment specifications. These analyses also do not generally account for the degrading effects of the atmosphere on a distant object, or on the effects of localized dome turbulence. Turbulence effects may in fact overwhelm the finer points of image formation so that some of the tolerances derived in the absence of an atmosphere may be lessened.

As a minimum, the following facts are evident when considering optical performance of PORTL:

A. The optimally aligned system produces an Airy diffraction spot of an infinite range on-axis object of 24 μm in diameter.

B. The system may be focussed at closer ranges (down to 500 feet), but at considerable expense in the intensity of the central diffraction spot. The lost energy in the Airy spot appears in the wings of the diffraction pattern and results in a smudging of the image and loss of spatial resolution and contrast.

C. A small error in axial piston placement of the secondary mirror results in a focal plane best focus displacement of 36 times the secondary error.

D. The focal plane should be placed (image focussed) to within 0.5 mm to achieve a Strehl ratio of at least 0.67.

E. The secondary mirror must be centered on the optical axis to within 0.3 mm for a Strehl of 0.80.

F. The secondary mirror must be aligned in tip/tilt to no more than 2 arc-minutes for a Strehl of 0.73.

G. An imaged object should be no more than 5 arc-minutes off-axis for diffraction limited performance at a Strehl ratio of 0.61.

The following table summarizes the error sources and provides acceptable tolerance limits, based on POLYPAGOS simulation results. The limits are somewhat subjective, based upon the point at which the point spread function begins to depart significantly from the theoretical diffraction limit of the optimally aligned telescope system. Each tolerance level must be considered individually, as combinations of errors will in general compound the degradation of the image. Only through experimentation with the instrument itself, will the engineer be able to determine the absolute acceptable tolerance of alignment and focussing errors.

ERROR SOURCE	TOLERANCE
Spherical Aberration (near object focus)	Object > 5,000 ft range
Coma (Off axis object)	Object < 5 arc-min off axis
Focal Plane Piston (focus error)	< 0.5 mm
Secondary Centration	<0.3 mm
Secondary Tip/Tilt	< 2 arc-min

REFERENCES

[1] Brewer, S., POLYPAGOS: Polychromatic Program for the Analysis of General Optical Systems, SAMSO-TR-70-411, Space and Misssile Systems Organization, Air Force Systems Command, Los Angeles Air Force Station, CA, 1970.

[2] Operation & Maintenance Manual for a 40-Inch Aperture F/18 Cassegrain Telescope, Report No. F(2)-872-047-014-2227, Owens-Illinois Fecker Systems Division, Pittsburgh, PA.

[3] Technical Proposal for a 40-Inch Aperture Cassegrain Telescope, Report No. F(1)-1222-047-014-2044, Owens-Illinois Fecker Systems Division, Pittsburgh, PA, 1972.

APPENDIX

POLYPAGOS OPTICAL CONFIGURATION TEST CASES

GRAPHICAL OUTPUT

APPENDIX CONTENTS

CASE	FIGURE	TITLE	PAGE
I.	**Object at infinity, aligned on axis**		
	A-1a	Geometric spot diagram	A1-1
	A-1b	PSF X-axis slice	A1-2
	A-1c	PSF 3-D surface map	A1-2
	A-1d	MTF X-axis slice	A1-3
	A-1e	MTF 3-D surface map	A1-3
II.	**Object at 3 miles, aligned on axis**		
	A-2a	Geometric spot diagram	A2-1
	A-2b	PSF X-axis slice	A2-2
	A-2c	PSF 3-D surface map	A2-2
	A-2d	MTF X-axis slice	A2-3
	A-2e	MTF 3-D surface map	A2-3

APPENDIX CONTENTS (cont'd)

CASE	FIGURE	TITLE	PAGE
III.	**Object at 5,000 feet, aligned on axis**		
	A-3a	Geometric spot diagram	A3-1
	A-3b	PSF X-axis slice	A3-2
	A-3c	PSF 3-D surface map	A3-2
	A-3d	MTF X-axis slice	A3-3
	A-3e	MTF 3-D surface map	A3-3
IV.	**Object at 500 feet, aligned on axis**		
	A-4a	Geometric spot diagram	A4-1
	A-4b	PSF X-axis slice	A4-2
	A-4c	PSF 3-D surface map	A4-2
	A-4d	MTF X-axis slice	A4-3
	A-4e	MTF 3-D surface map	A4-3

APPENDIX CONTENTS (cont'd)

CASE	FIGURE	TITLE	PAGE
V.	**Secondary mirror axially displaced 0.1 mm**		
	A-5a	Geometric spot diagram	A5-1
	A-5b	PSF X-axis slice	A5-2
	A-5c	PSF 3-D surface map	A5-2
	A-5d	MTF X-axis slice	A5-3
	A-5e	MTF 3-D surface map	A5-3
VI.	**Focal plane detector displaced 1.0 mm**		
	A-6a	Geometric spot diagram	A6-1
	A-6b	PSF X-axis slice	A6-2
	A-6c	PSF 3-D surface map	A6-2
	A-6d	MTF X-axis slice	A6-3
	A-6e	MTF 3-D surface map	A6-3

APPENDIX CONTENTS (cont'd)

CASE	FIGURE	TITLE	PAGE
VII.	**Secondary mirror centration error 1.0 mm**		
	A-7a	Geometric spot diagram	A7-1
	A-7b	PSF X-axis slice	A7-2
	A-7c	PSF Y-axis slice	A7-2
	A-7d	PSF surface contour	A7-3
	A-7e	PSF 3-D surface map	A7-3
	A-7f	MTF X-axis slice	A7-4
	A-7g	MTF Y-axis slice	A7-4
	A-7h	MTF 3-D surface map	A7-5

APPENDIX CONTENTS (cont'd)

CASE	FIGURE	TITLE	PAGE
VIII.	**Secondary mirror centration error 0.3 mm**		
	A-8a	Geometric spot diagram	A8-1
	A-8b	PSF X-axis slice	A8-2
	A-8c	PSF Y-axis slice	A8-2
	A-8d	PSF surface contour	A8-3
	A-8e	PSF 3-D surface map	A8-3
	A-8f	MTF X-axis slice	A8-4
	A-8g	MTF Y-axis slice	A8-4
	A-8h	MTF 3-D surface map	A8-5
IX.	**Secondary mirror tilt error 35 arc-seconds**		
	A-9a	Geometric spot diagram	A9-1
	A-9b	PSF X-axis slice	A9-2
	A-9c	PSF Y-axis slice	A9-2
	A-9d	PSF surface contour	A9-3
	A-9e	PSF 3-D surface map	A9-3
	A-9f	MTF X-axis slice	A9-4
	A-9g	MTF Y-axis slice	A9-4
	A-9h	MTF 3-D surface map	A9-5

APPENDIX CONTENTS (cont'd)

CASE	FIGURE	TITLE	PAGE
X.		**Secondary mirror tilt error 2 arc-minutes**	
	A-10a	Geometric spot diagram	A10-1
	A-10b	PSF X-axis slice	A10-2
	A-10c	PSF Y-axis slice	A10-2
	A-10d	PSF 3-D surface map	A10-3
	A-10e	MTF X-axis slice	A10-4
	A-10f	MTF Y-axis slice	A10-4
	A-10g	MTF 3-D surface map	A10-5
XI.		**Object 20 arc-seconds off-axis**	
	A-11a	Geometric spot diagram	A11-1
	A-11b	PSF X-axis slice	A11-2
	A-11c	PSF Y-axis slice	A11-2
	A-11d	PSF 3-D surface map	A11-3
	A-11e	MTF X-axis slice	A11-4
	A-11f	MTF Y-axis slice	A11-4
	A-11g	MTF 3-D surface map	A11-5

APPENDIX CONTENTS (cont'd)

CASE	FIGURE	TITLE	PAGE
XII. Object 2 arc-minutes off-axis			
	A-12a	Geometric spot diagram	A12-1
	A-12b	PSF X-axis slice	A12-2
	A-12c	PSF Y-axis slice	A12-2
	A-12d	PSF 3-D surface map	A12-3
	A-12e	MTF X-axis slice	A12-4
	A-12f	MTF Y-axis slice	A12-4
	A-12g	MTF 3-D surface map	A12-5
XIII. Object 5 arc-minutes off-axis			
	A-13a	Geometric spot diagram	A13-1
	A-13b	PSF X-axis slice	A13-2
	A-13c	PSF Y-axis slice	A13-2
	A-13d	PSF surface contour	A13-3
	A-13e	PSF 3-D surface map	A13-3
	A-13f	MTF X-axis slice	A13-4
	A-13g	MTF Y-axis slice	A13-4
	A-13h	MTF 13-D surface map	A13-5

APPENDIX CONTENTS (cont'd)

CASE	FIGURE	TITLE	PAGE
XIV. Object 7.5 arc-minutes off-axis			
	A-14a	Geometric spot diagram	A14-1
	A-14b	PSF X-axis slice	A14-2
	A-14c	PSF Y-axis slice	A14-2
	A-14d	PSF surface contour	A14-3
	A-14e	PSF 3-D surface map	A14-3
	A-14f	MTF X-axis slice	A14-4
	A-14g	MTF Y-axis slice	A14-4
	A-14h	MTF 14-D surface map	A14-5

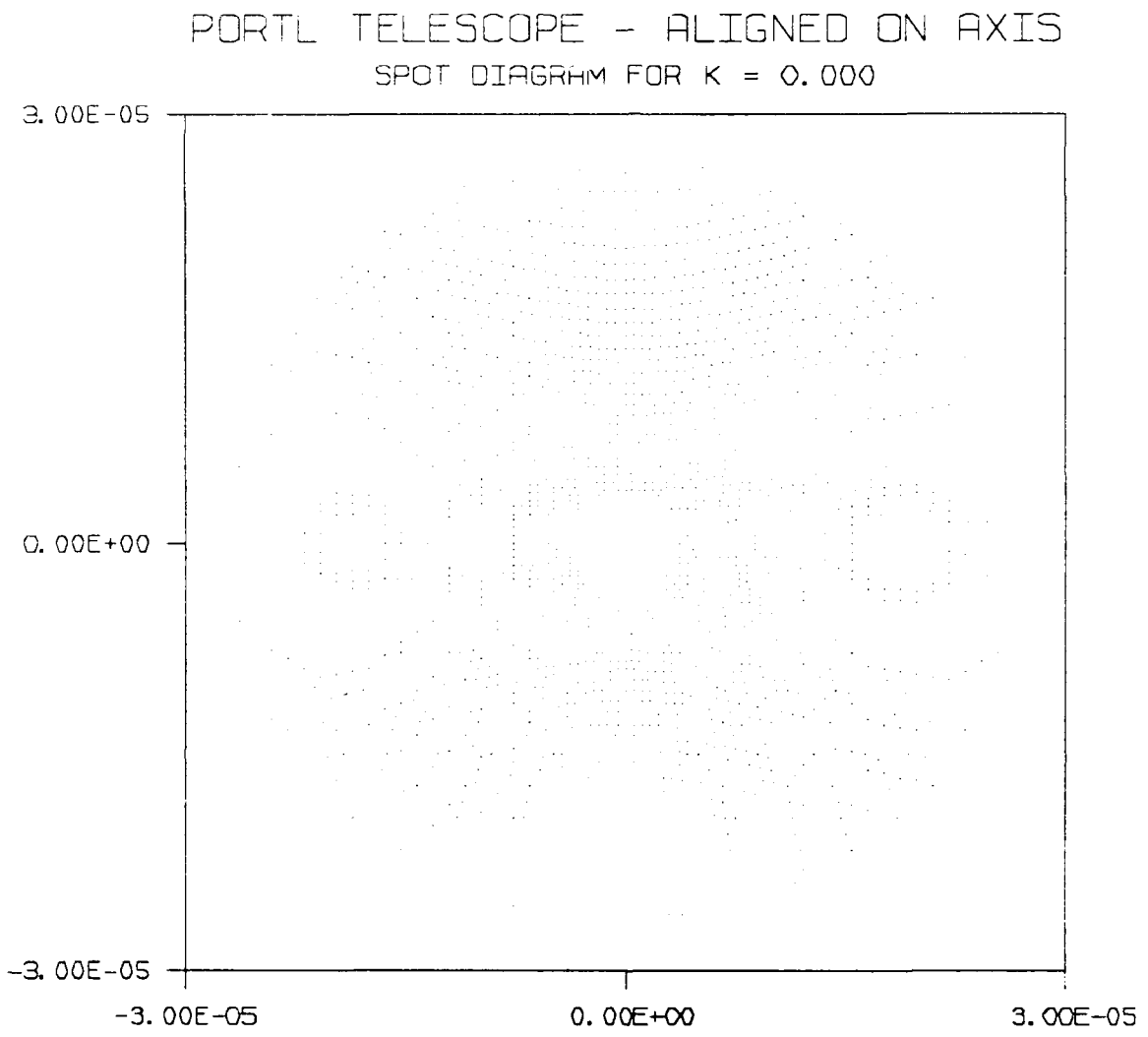

Figure A-1a

On-axis aligned optics - geometric spot diagram for object at infinity (displaced from point focal position to show spot structure)

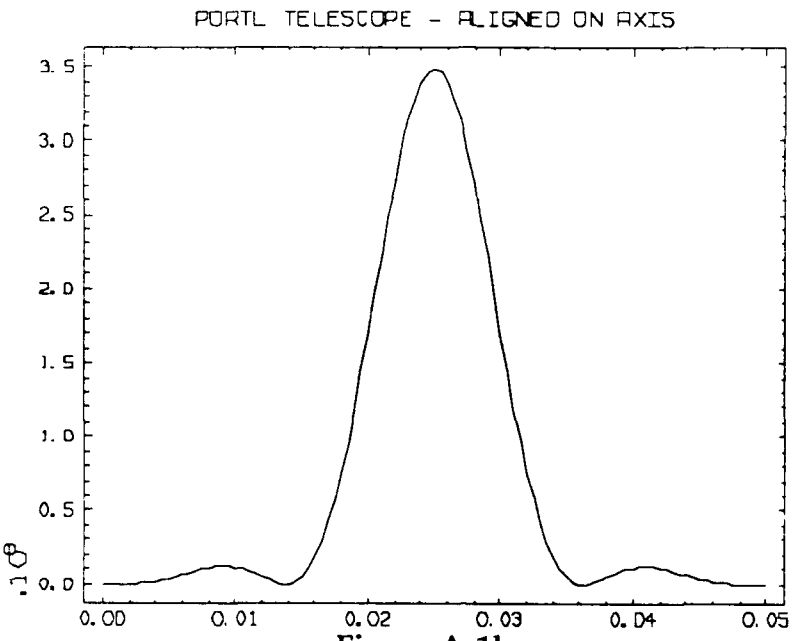

Figure A-1b
PSF - on axis infinity focus
X-axis slice

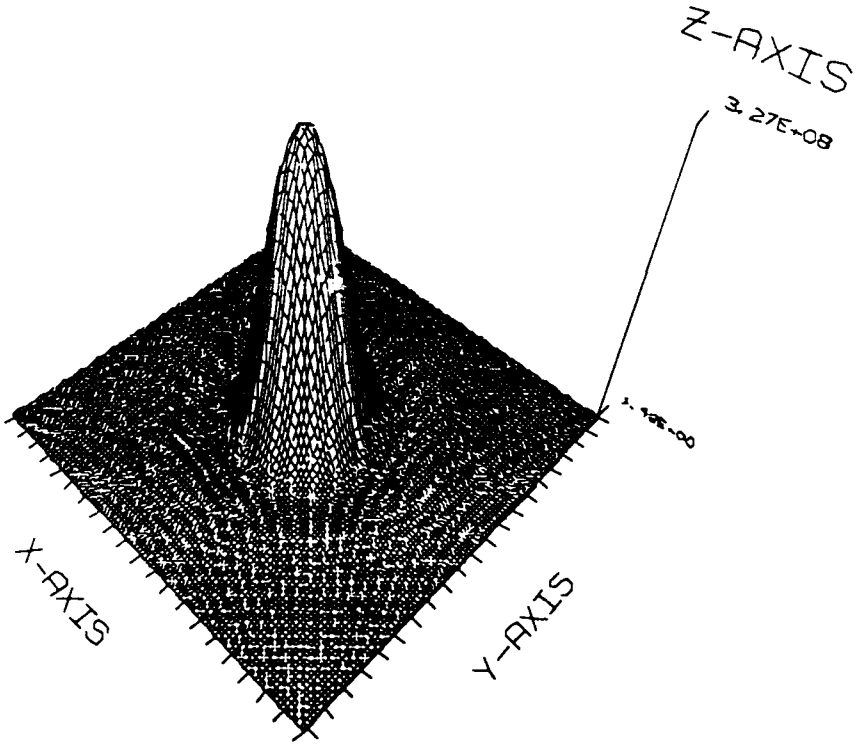

Figure A-1c
PSF - on axis infinity focus
Surface map

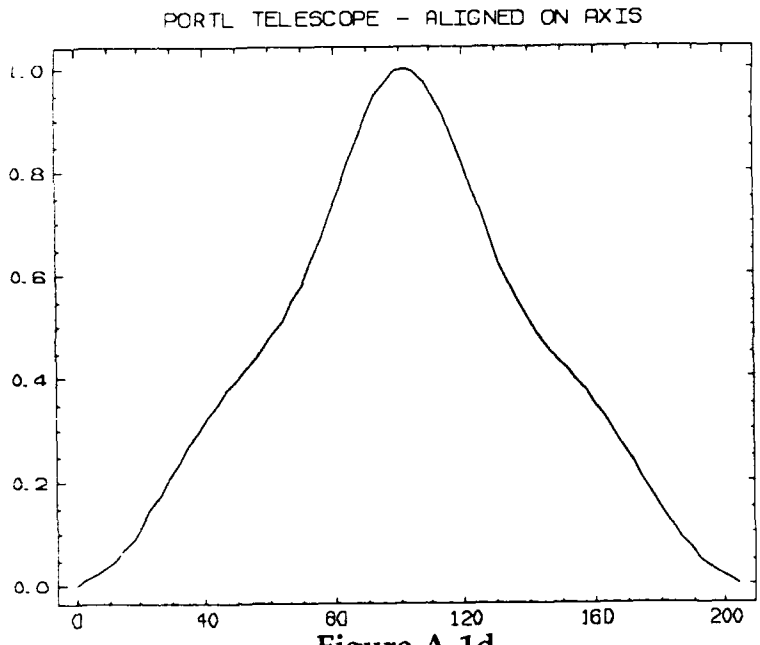

Figure A-1d
MTF - on axis infinity focus
X-axis slice

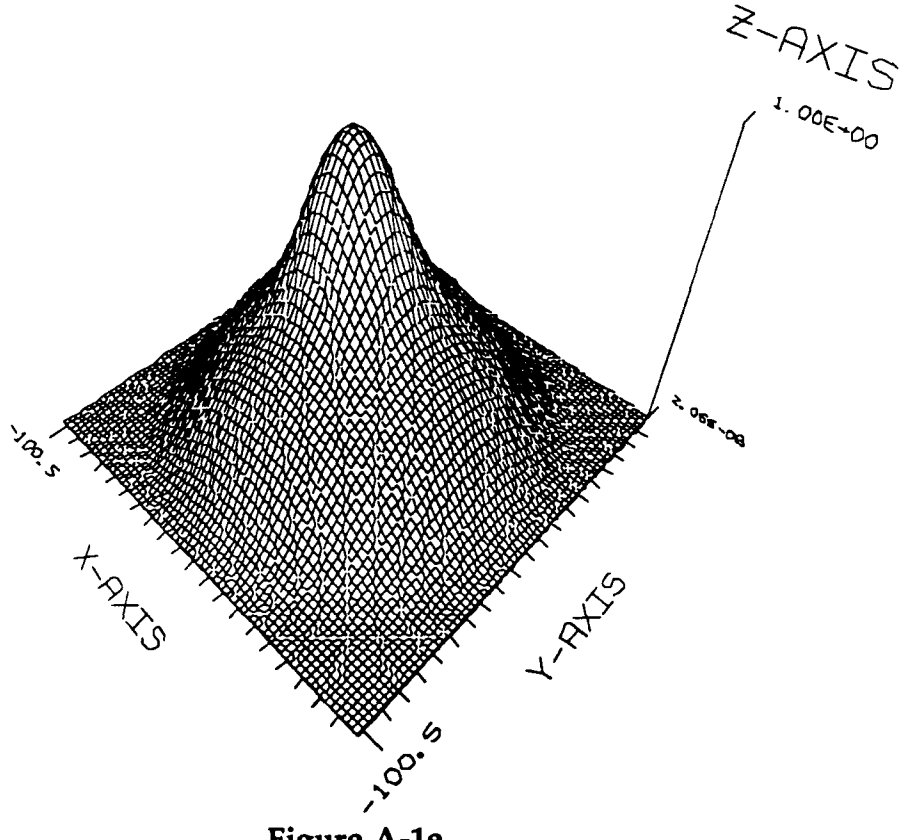

Figure A-1e
MTF - on axis infinity focus
Surface map

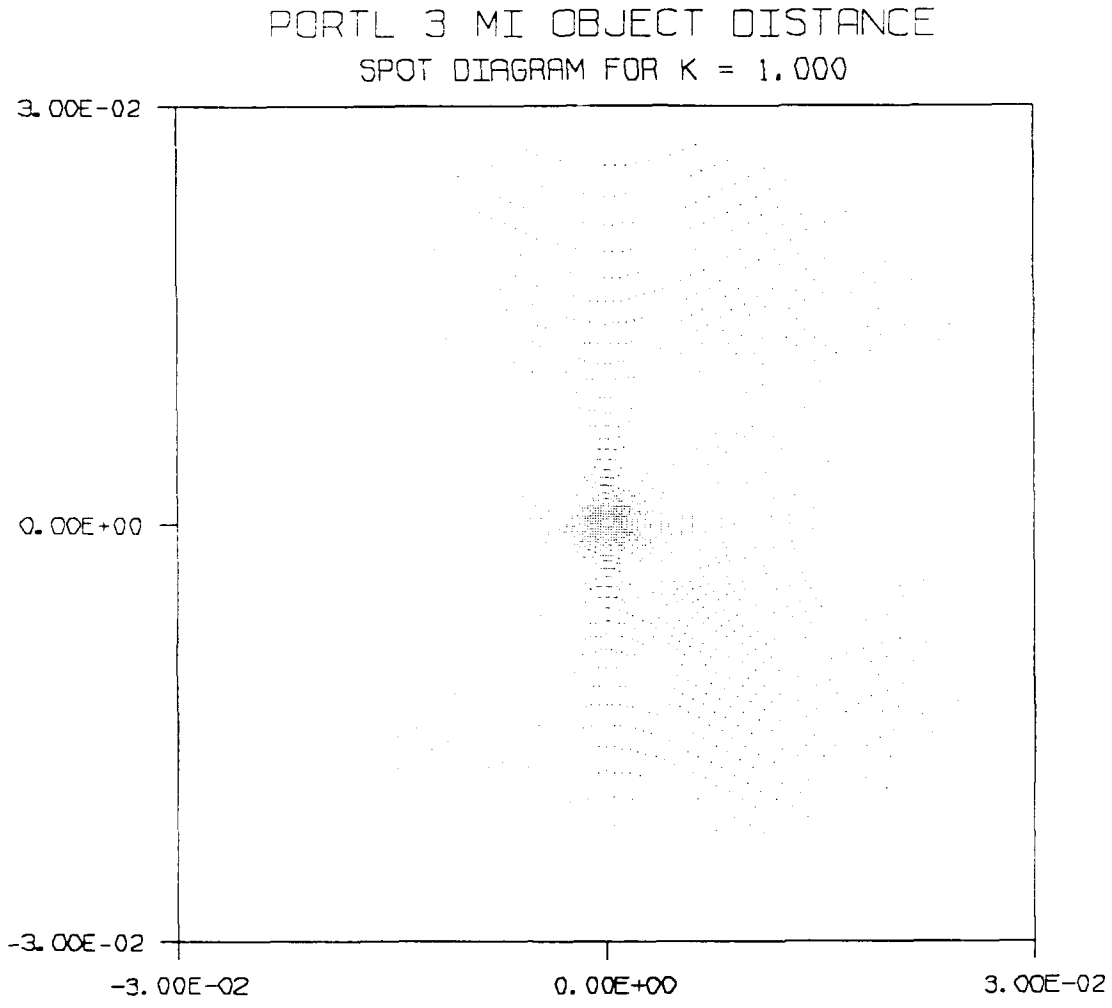

Figure A-2a

Spot Diagram for object at 3 miles range

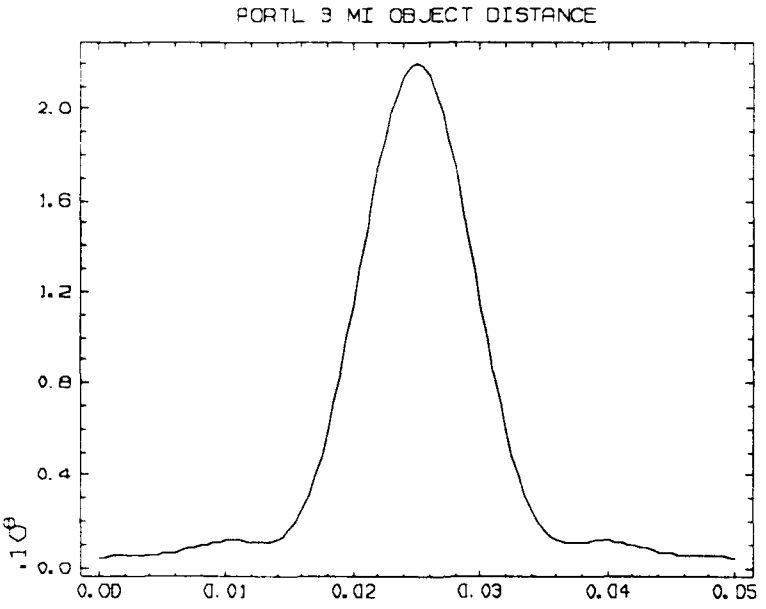

Figure A-2b
PSF - on axis aligned optics - 3 mile range
X-axis slice

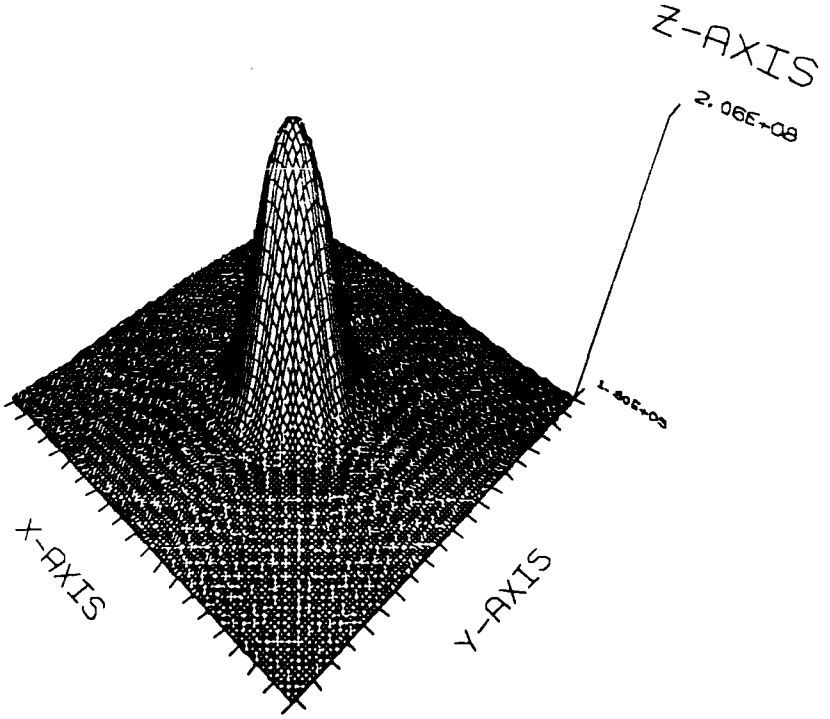

Figure A-2c
PSF - on axis aligned optics
Surface map

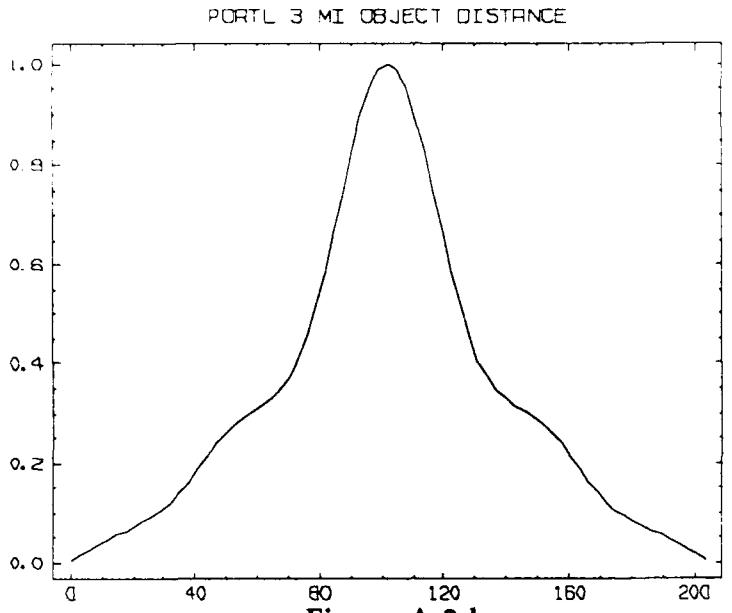

Figure A-2d
MTF - on axis aligned optics - 3 mile range
X-axis slice

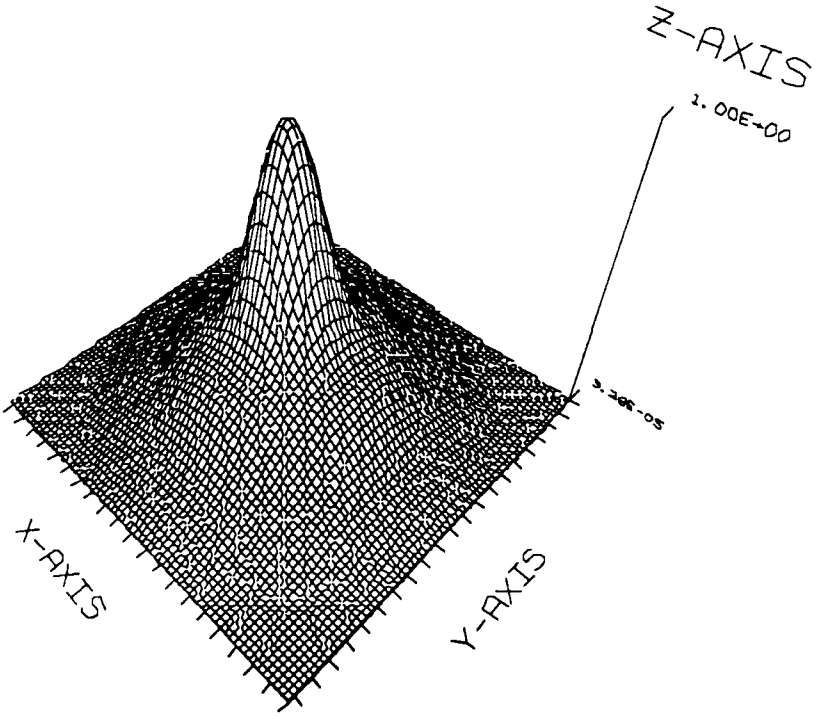

Figure A-2e
MTF - on axis aligned optics
Surface map

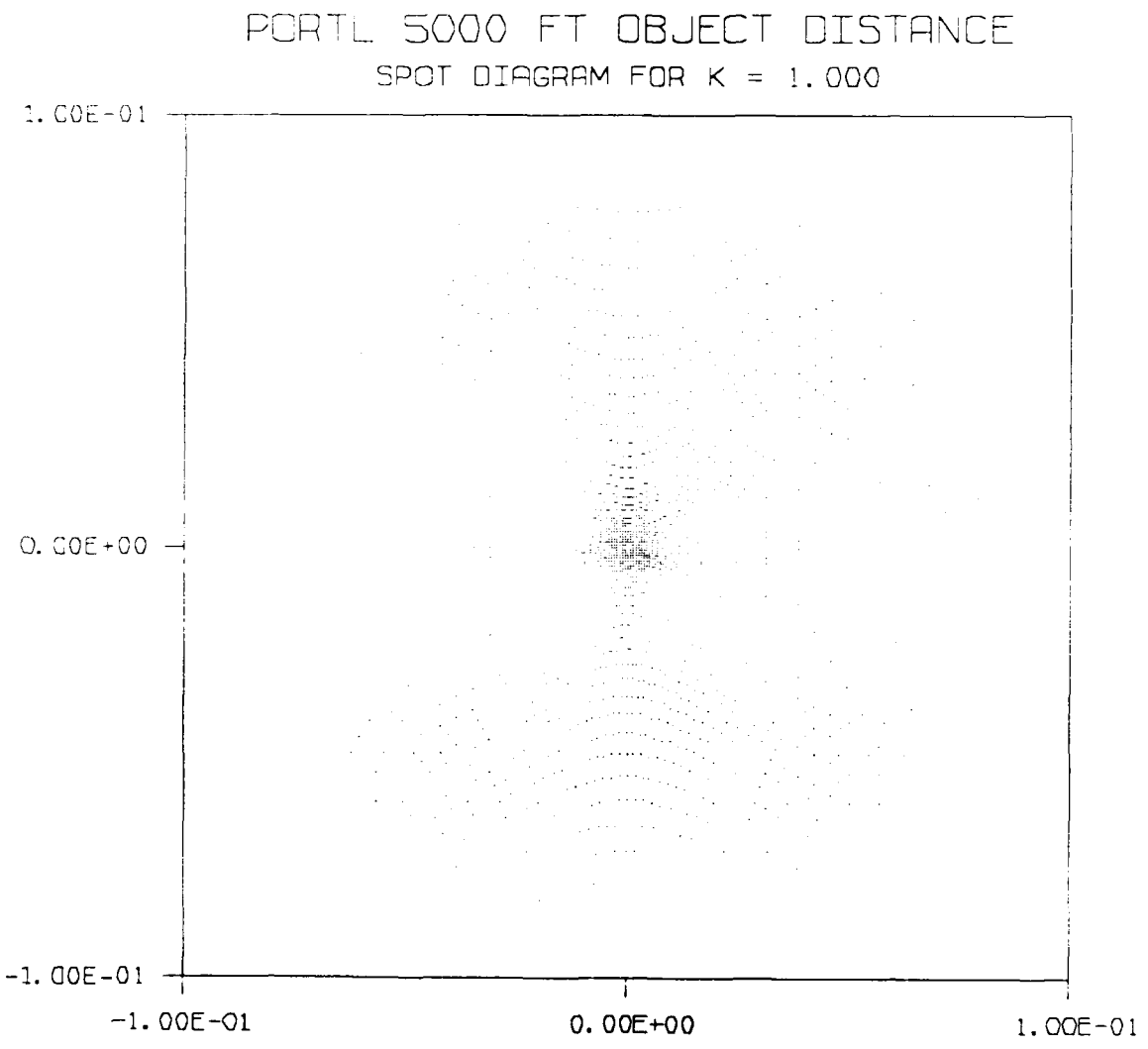

Figure A-3a

Geometric spot diagram for object at range of 5,000 feet

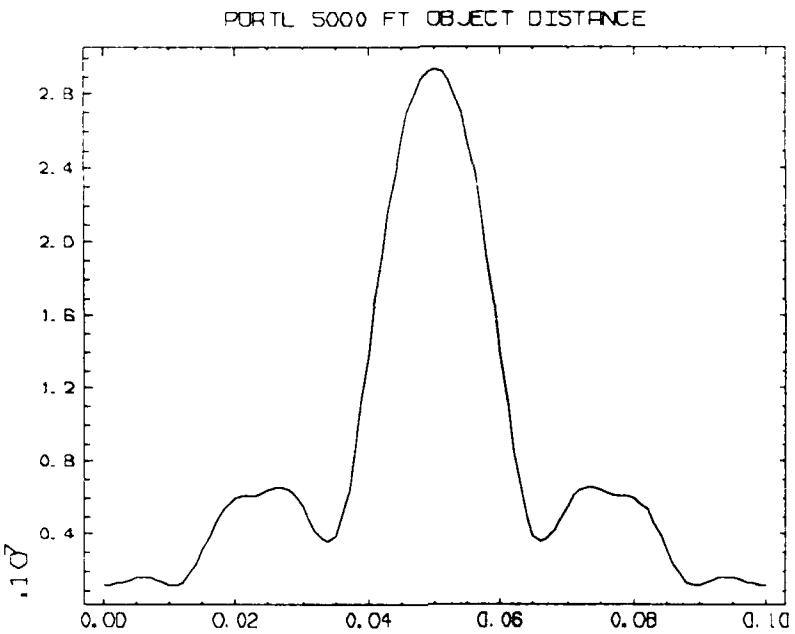

Figure A-3b
PSF - on axis aligned optics - 5,000 ft range
X-axis slice

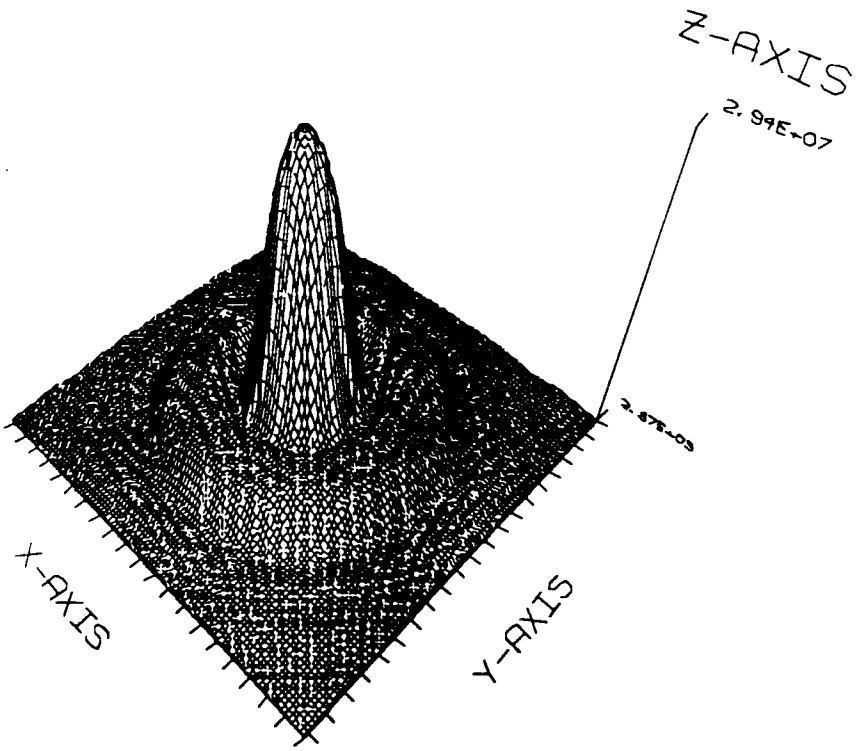

Figure A-3c
PSF - on axis aligned optics
Surface map

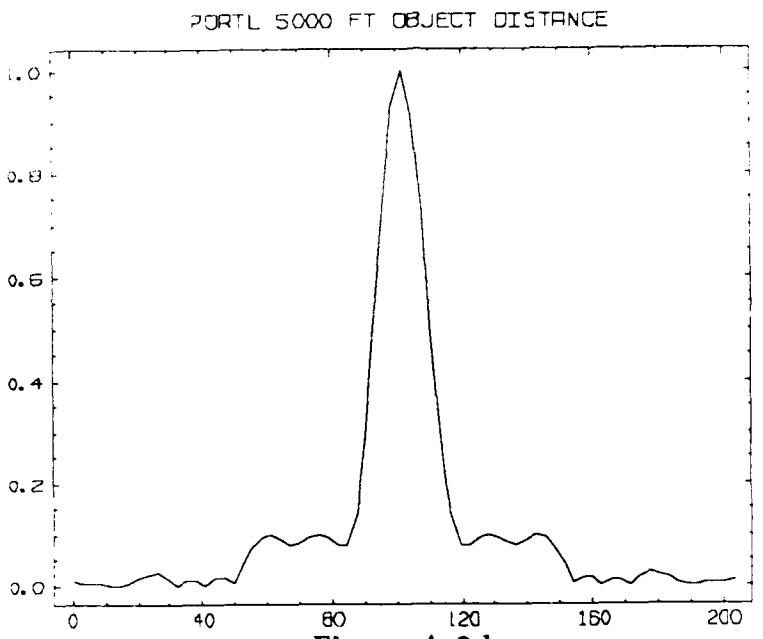

Figure A-3d
MTF - on axis aligned optics - 5,000 ft range
X-axis slice

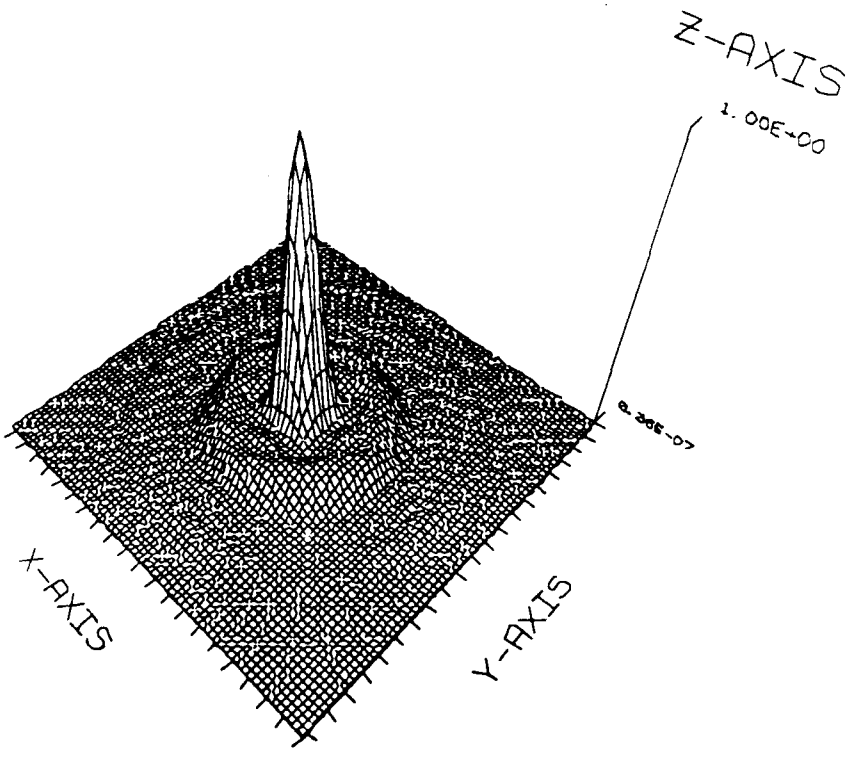

Figure A-3e
MTF - on axis aligned optics
Surface map

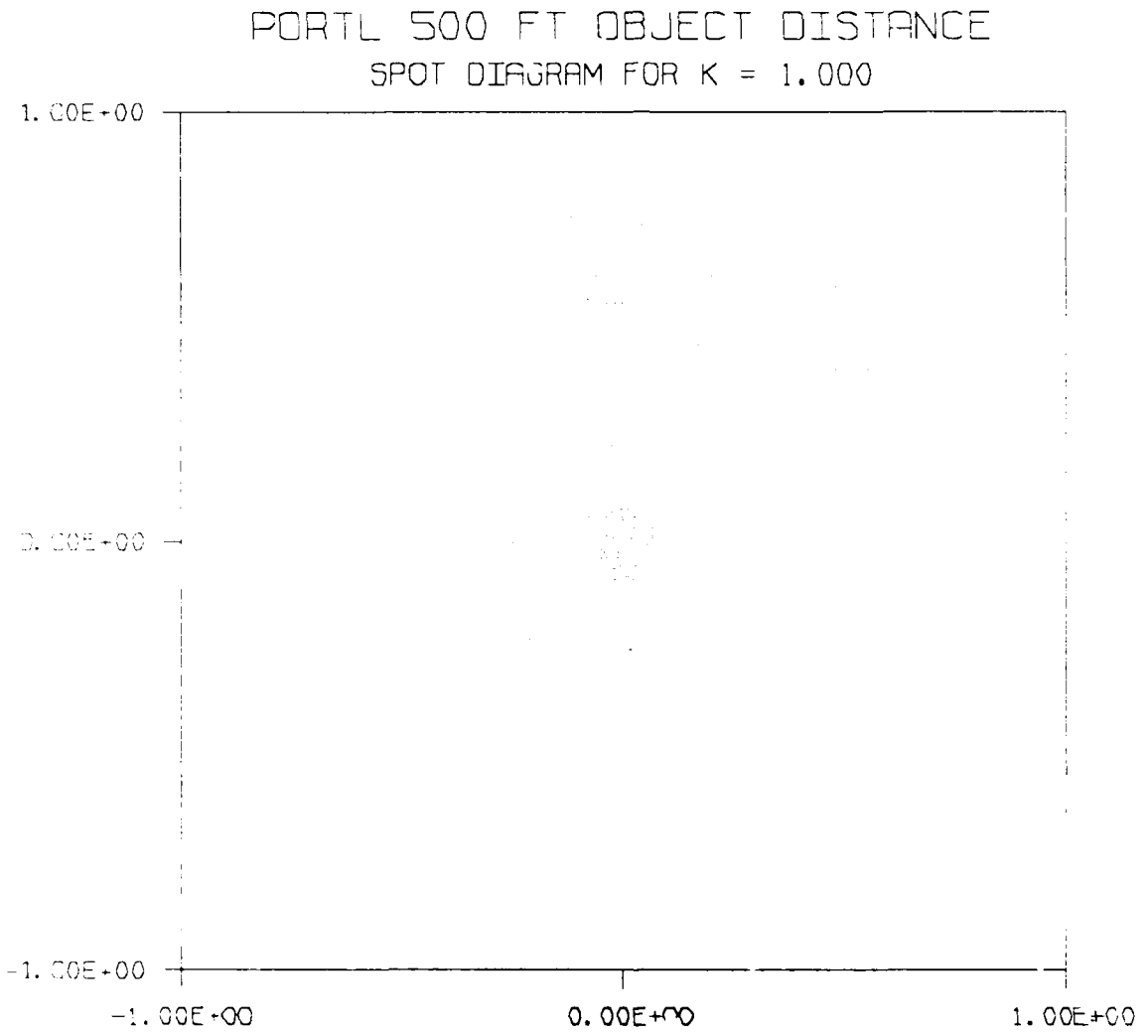

Figure A-4a

Spot Diagram for object at 500 feet range

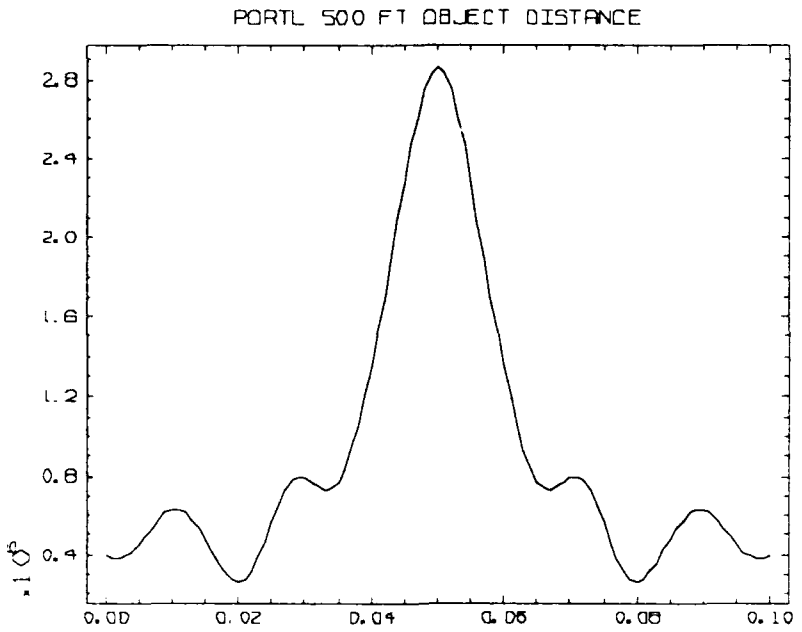

Figure A-4b
PSF - on axis aligned optics - 500 ft range
X-axis slice

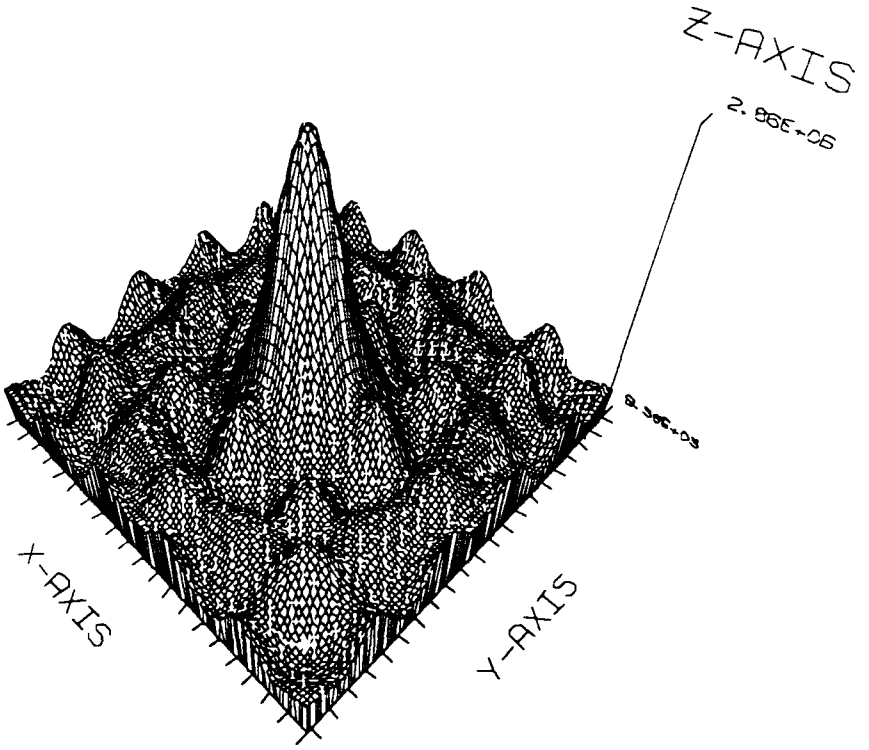

Figure A-4c
PSF - on axis aligned optics
Surface map

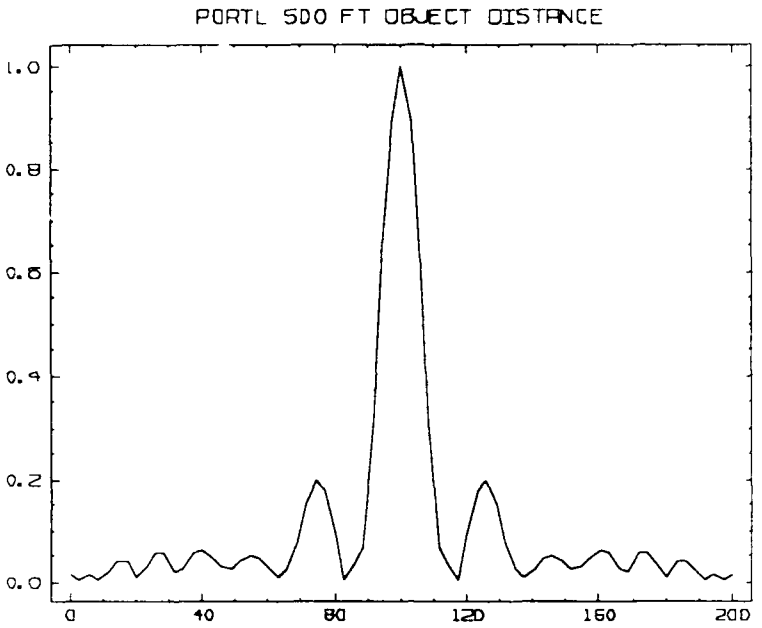

Figure A-4d
MTF - on axis aligned optics - 500 ft range
X-axis slice

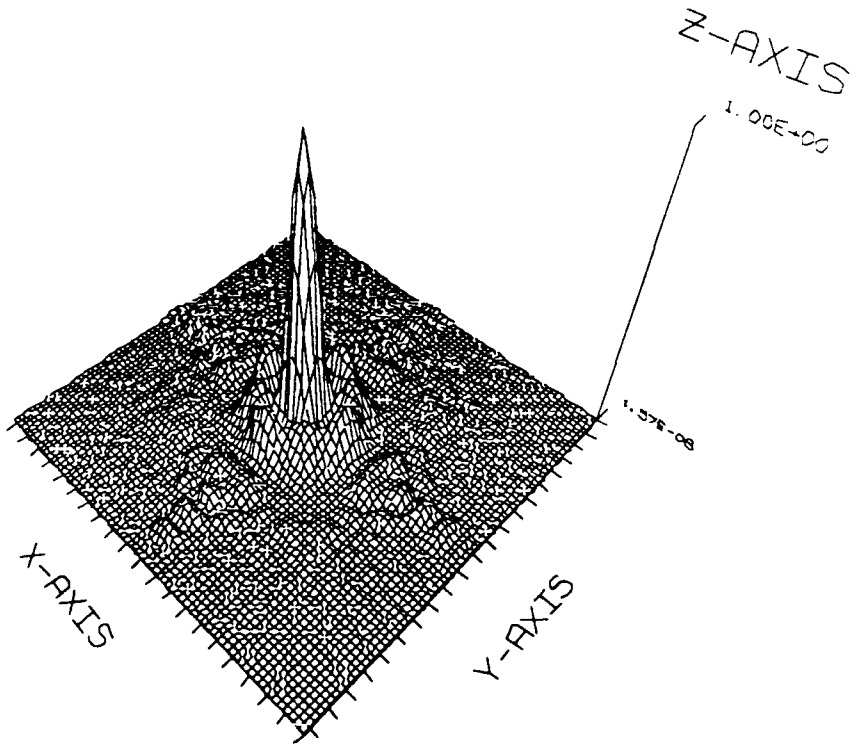

Figure A-4e
MTF - on axis aligned optics

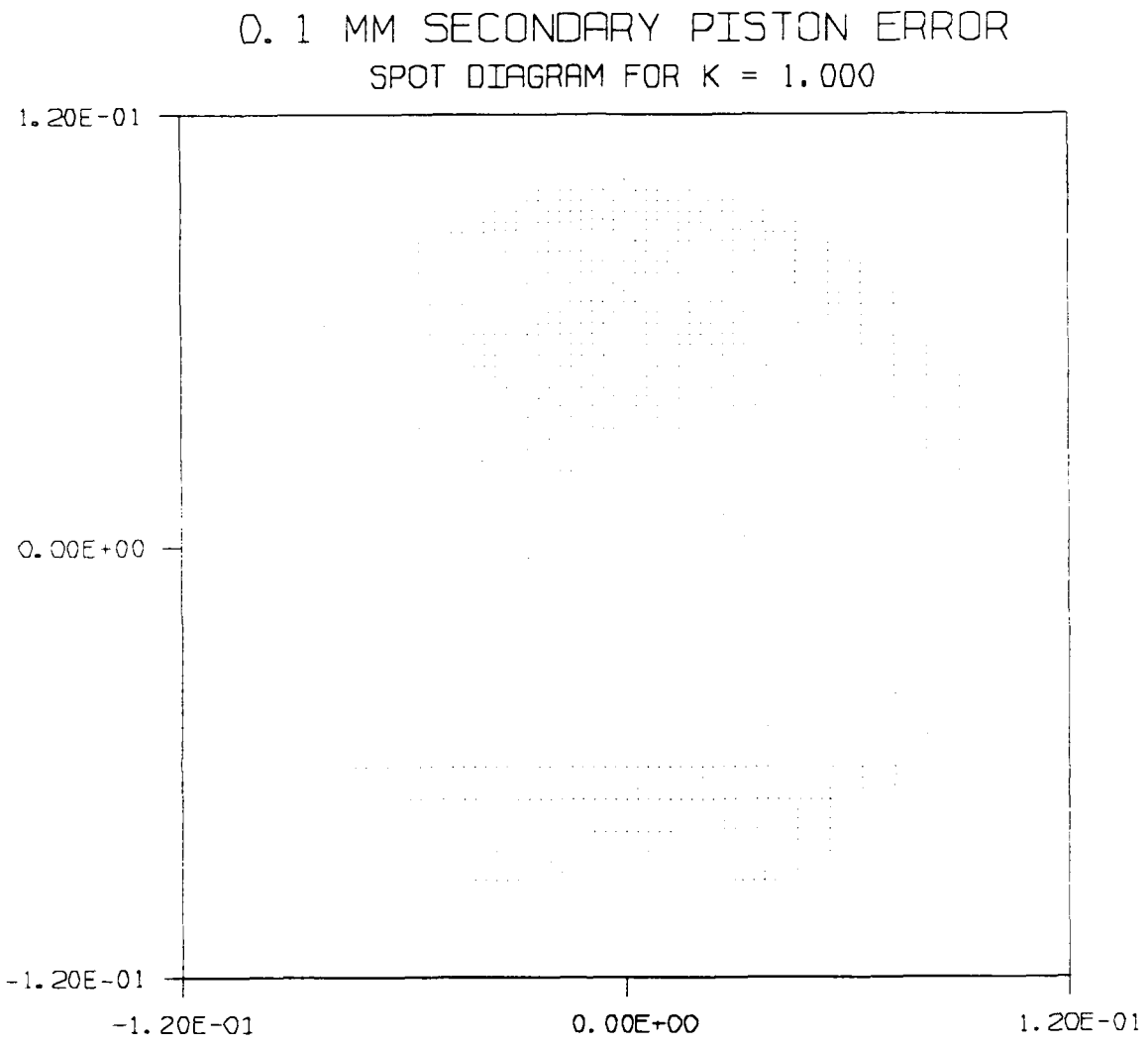

Figure A-5a

Spot diagram - Secondary mirror displaced 0.1 mm
No focal plane correction

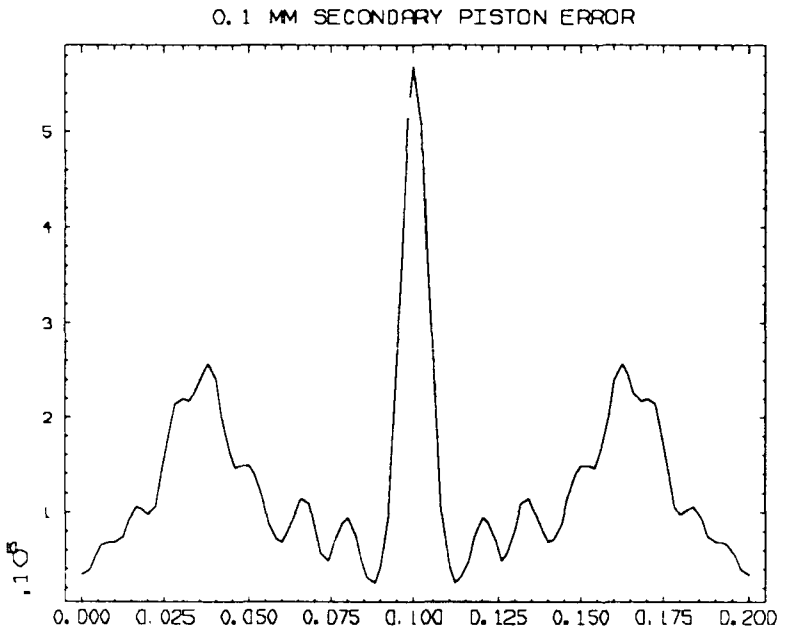

Figure A-5b
PSF - Secondary mirror displaced 0.1 mm
No focal plane correction - X-axis slice

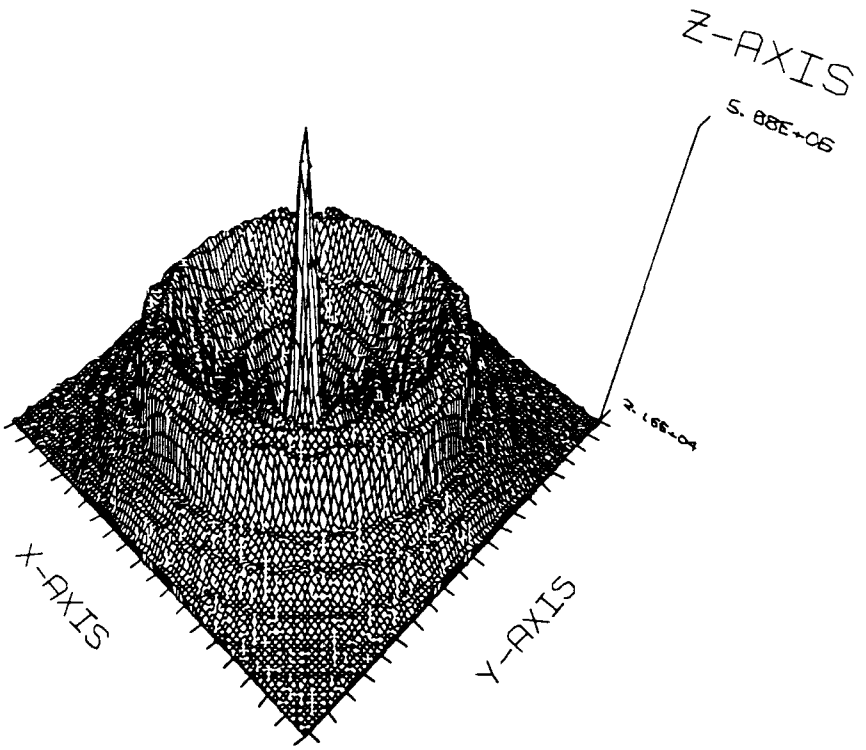

Figure A-5c
PSF - Secondary mirror displaced 0.1 mm
No focal plane correction - Surface map

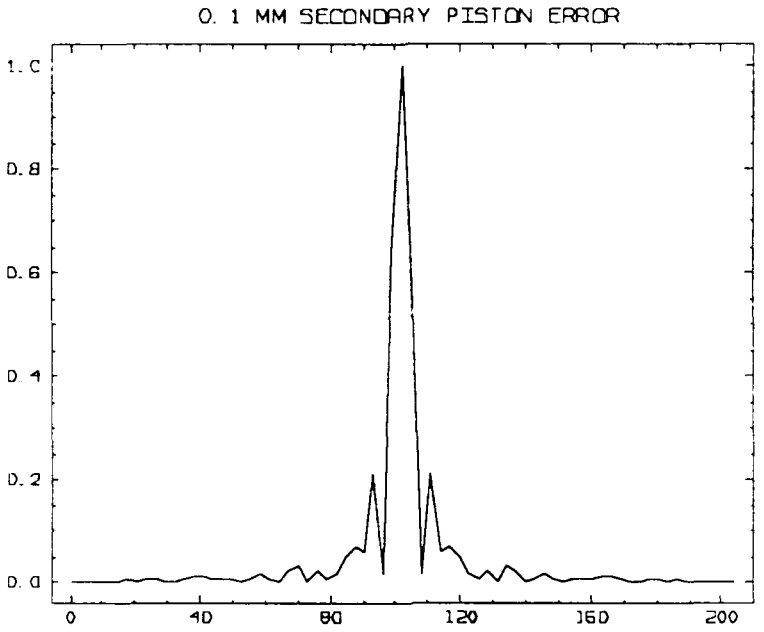

Figure A-5d
MTF - Secondary mirror displaced 0.1 mm
No focal plane correction - X-axis slice

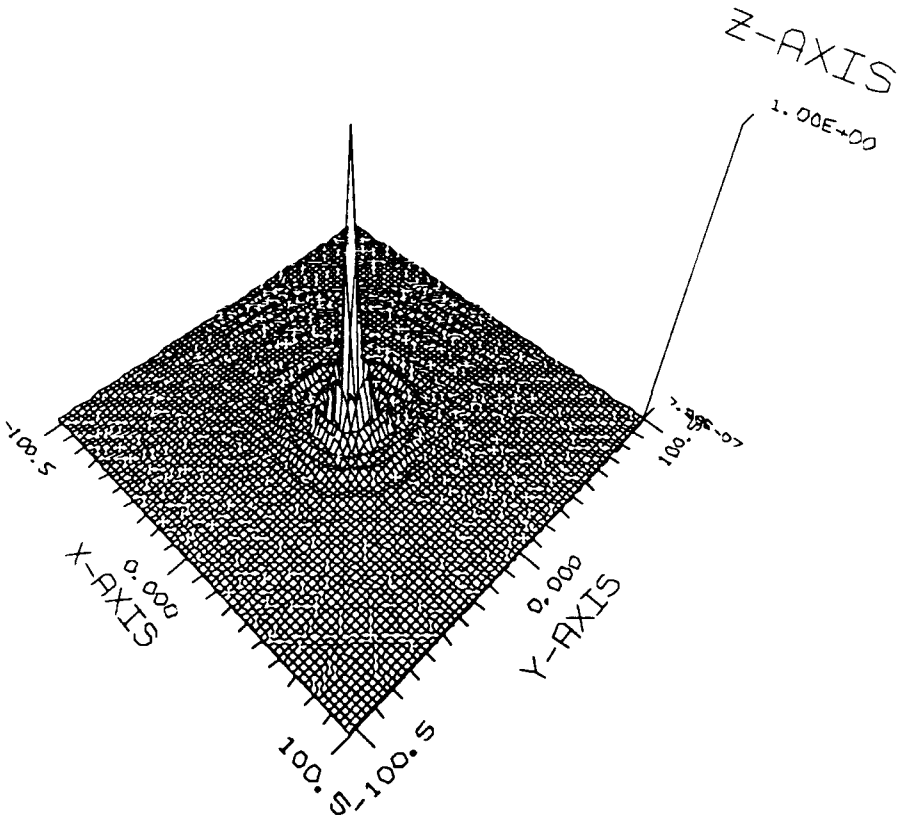

Figure A-5e
MTF - Secondary mirror displaced 0.1 mm
No focal plane correction - Surface map

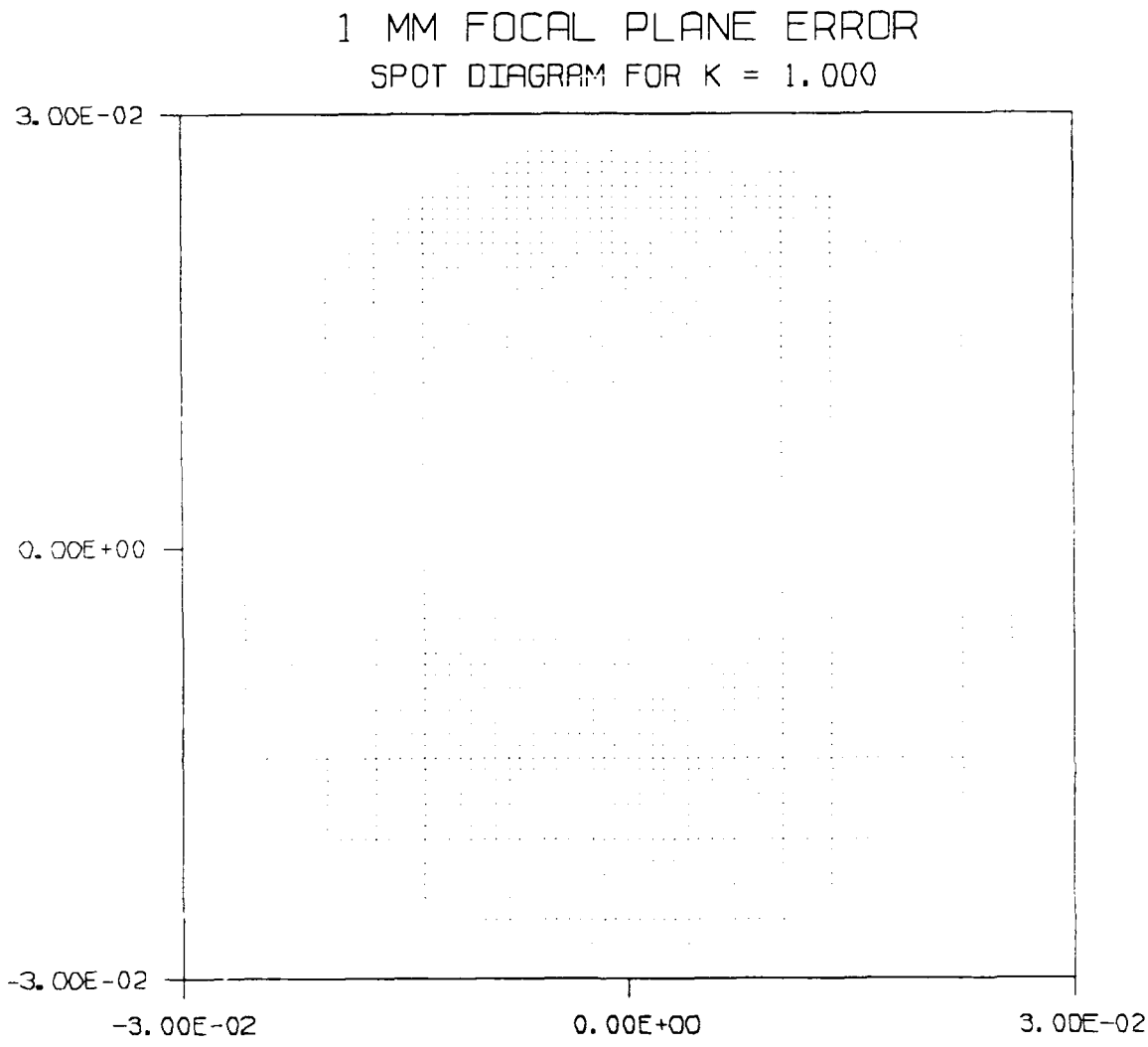

Figure A-6a

Spot Diagram for 1 mm focal plane defocus

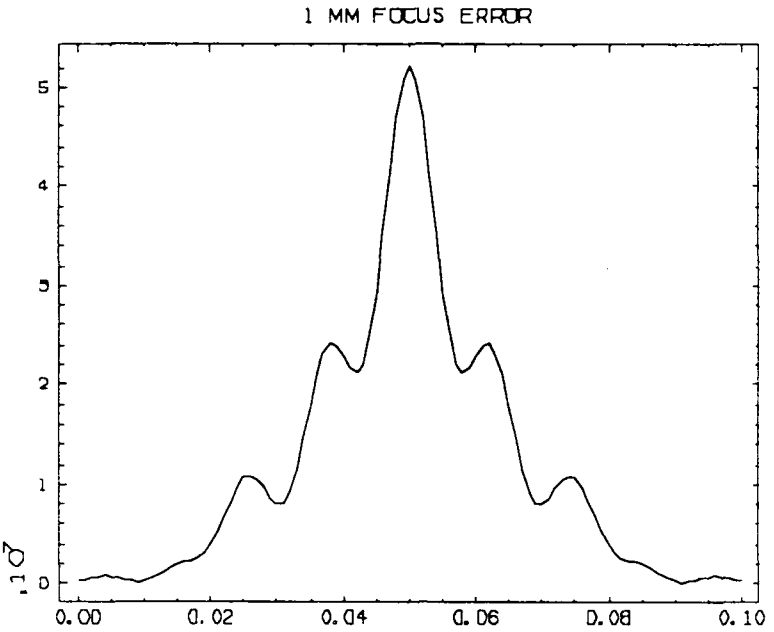

Figure A-6b
PSF - on axis aligned optics - 1 mm FP defocus
X-axis slice

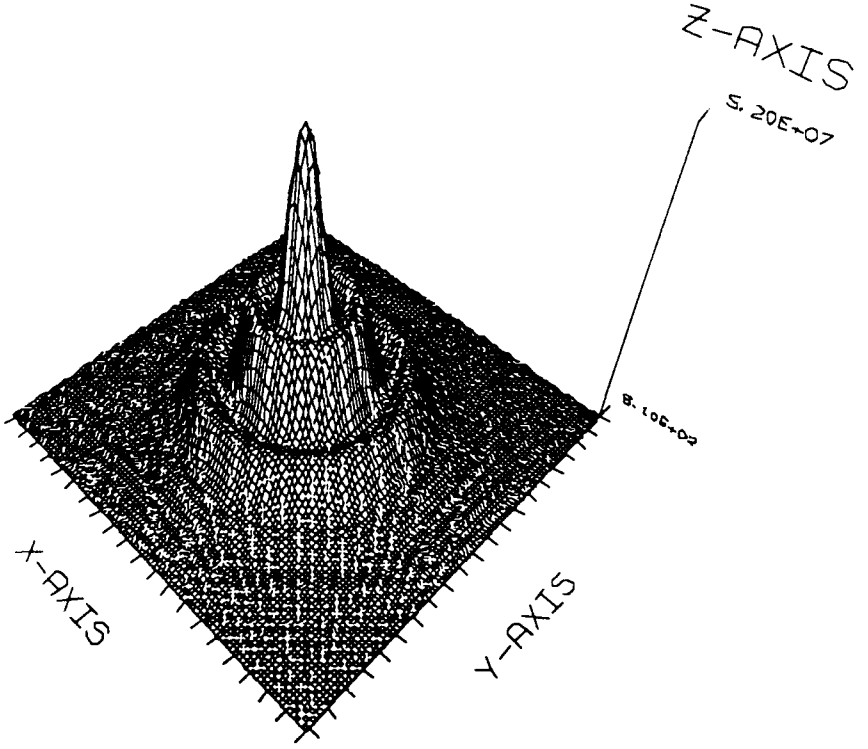

Figure A-6c
PSF - on axis aligned optics - 1 mm FP defocus
Surface map

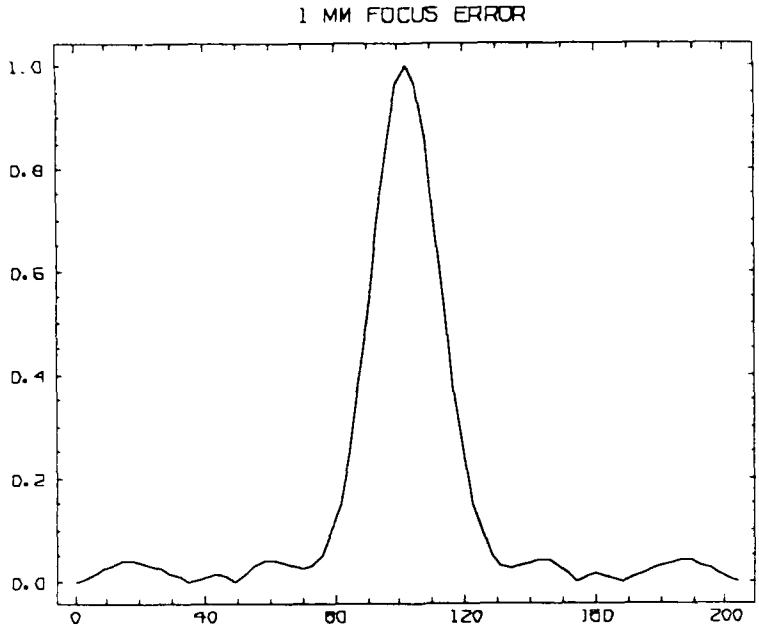

Figure A-6d
MTF - on axis aligned optics - 1 mm FP defocus
X-axis slice

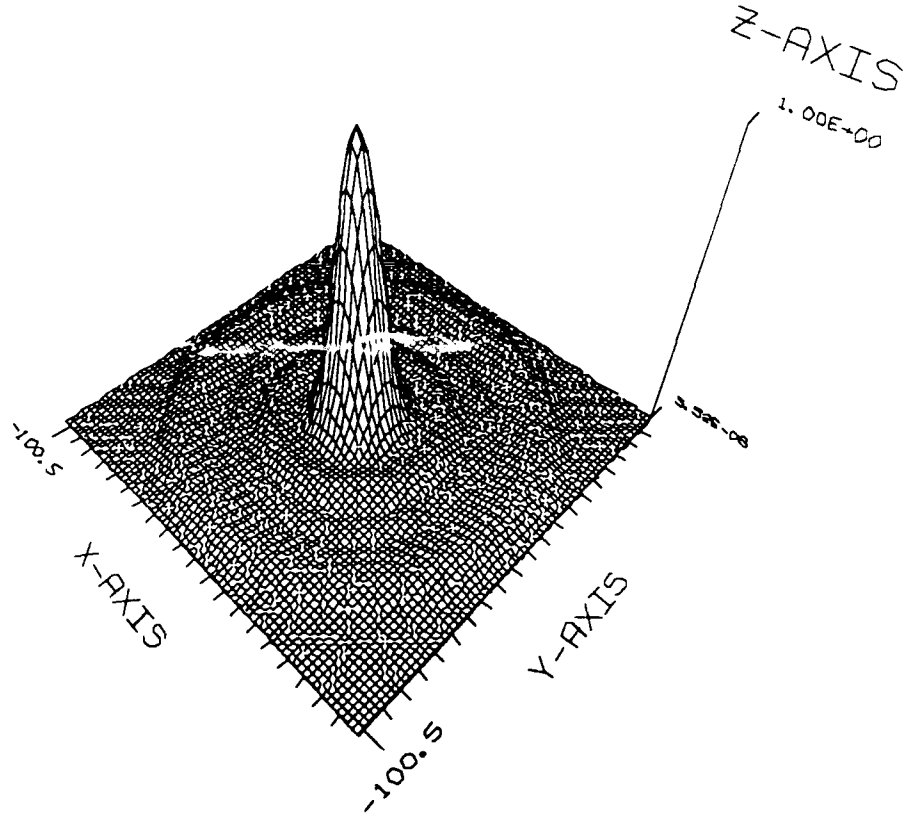

Figure A-6e
MTF - on axis aligned optics - 1 mm FP defocus

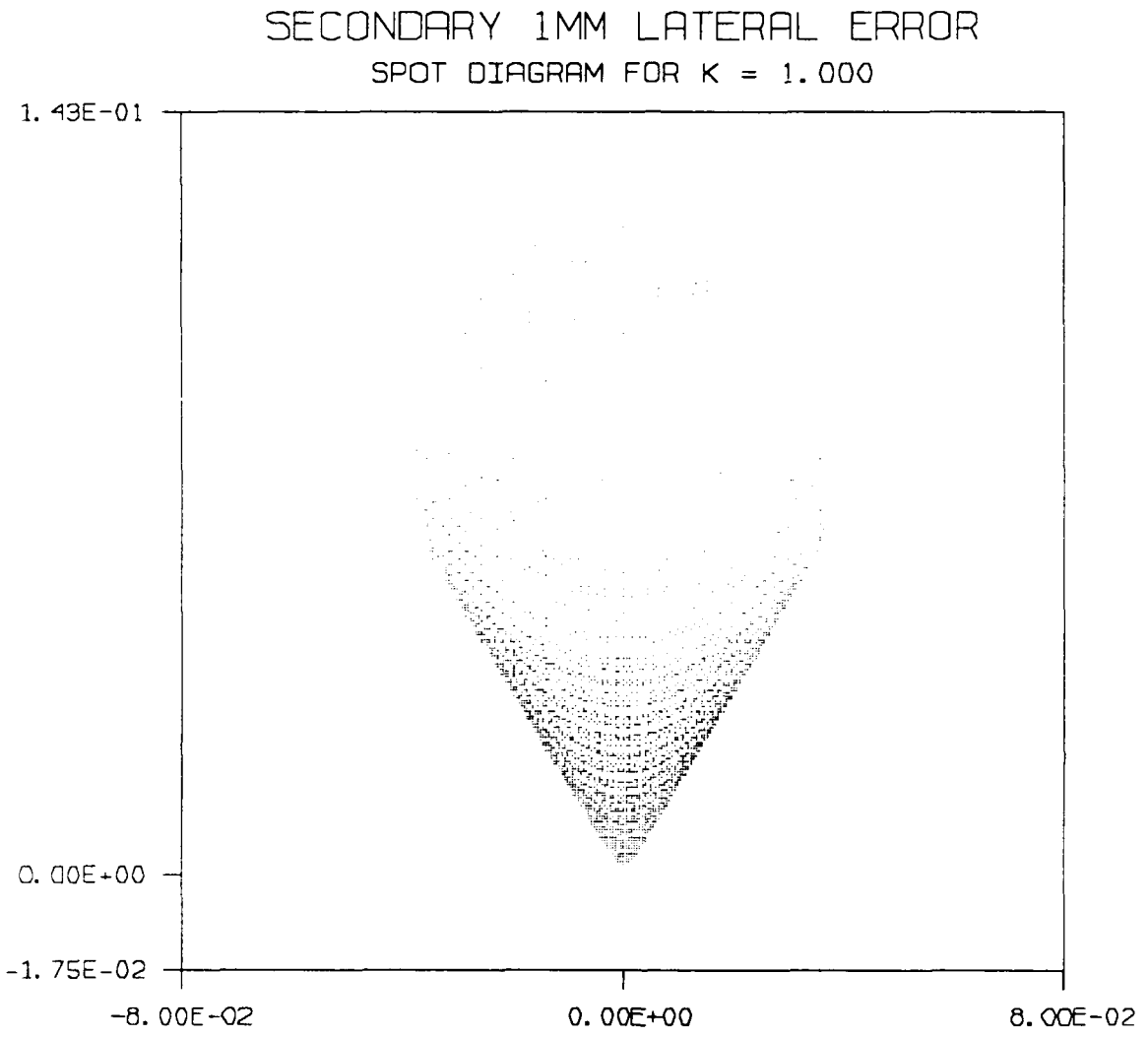

Figure A-7a

Spot Diagram for secondary 1 mm Y-axis lateral misalignment

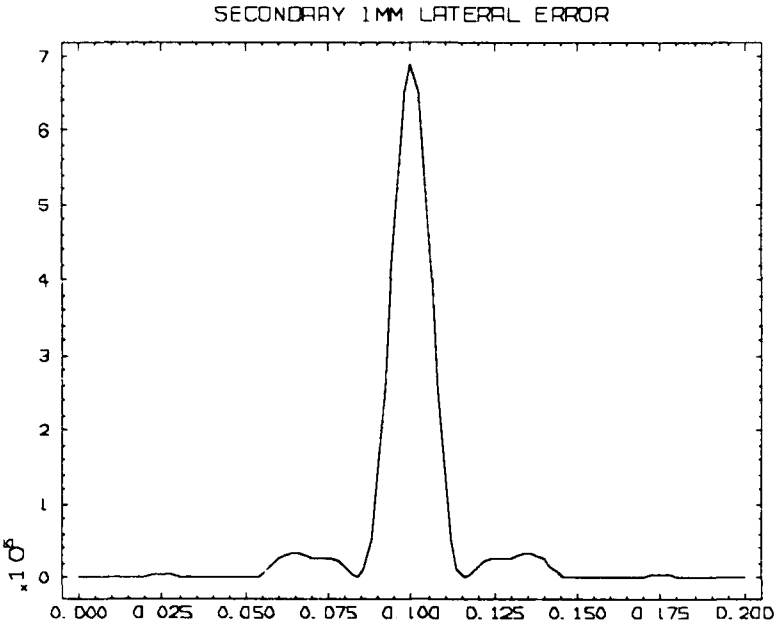

Figure A-7b
PSF - 1 mm secondary lateral displacement
X-axis slice

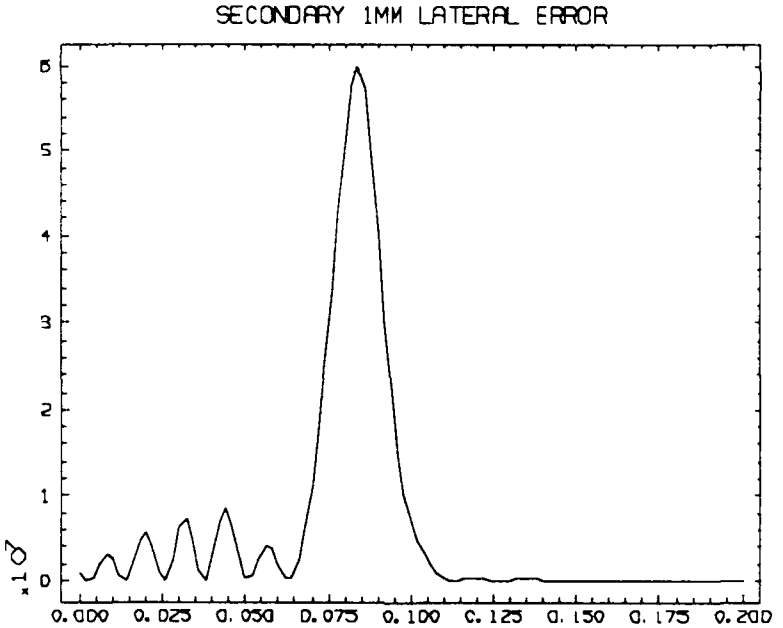

Figure A-7c
PSF - 1 mm secondary lateral displacement
Y-axis slice

Figure A-7d
PSF - 1 mm secondary lateral displacement
Surface contour

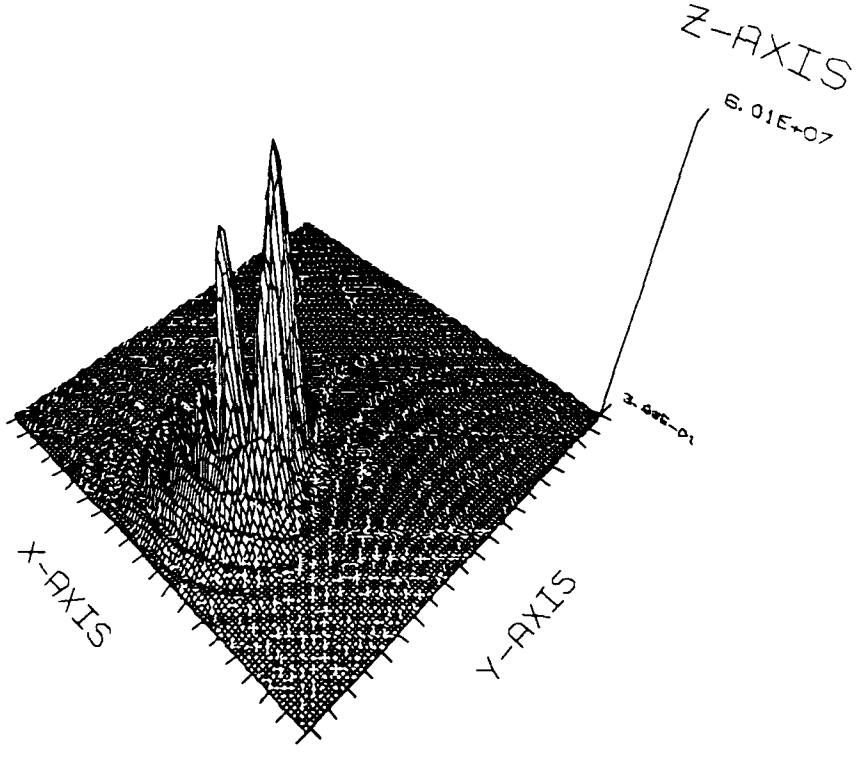

Figure A-7e
PSF - 1 mm secondary lateral displacement
Surface plot

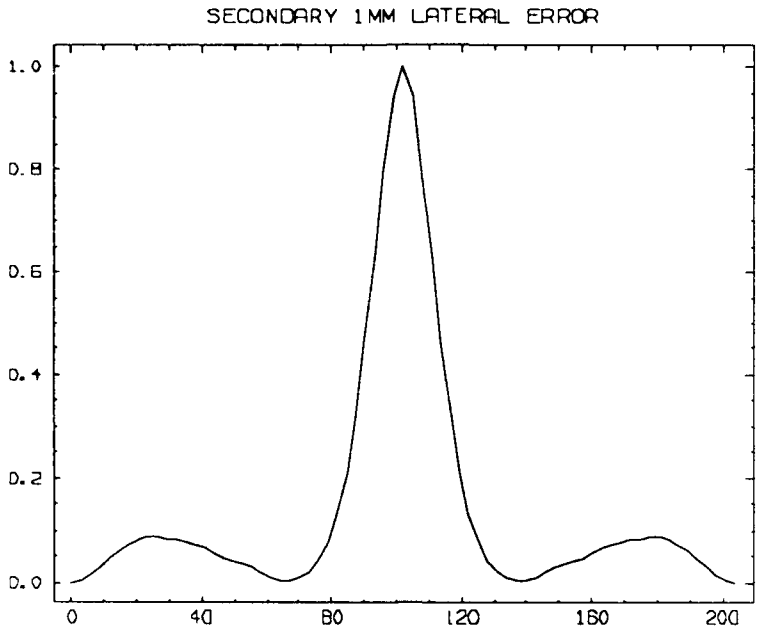

Figure A-7f
MTF - 1 mm secondary lateral displacement
X-axis slice

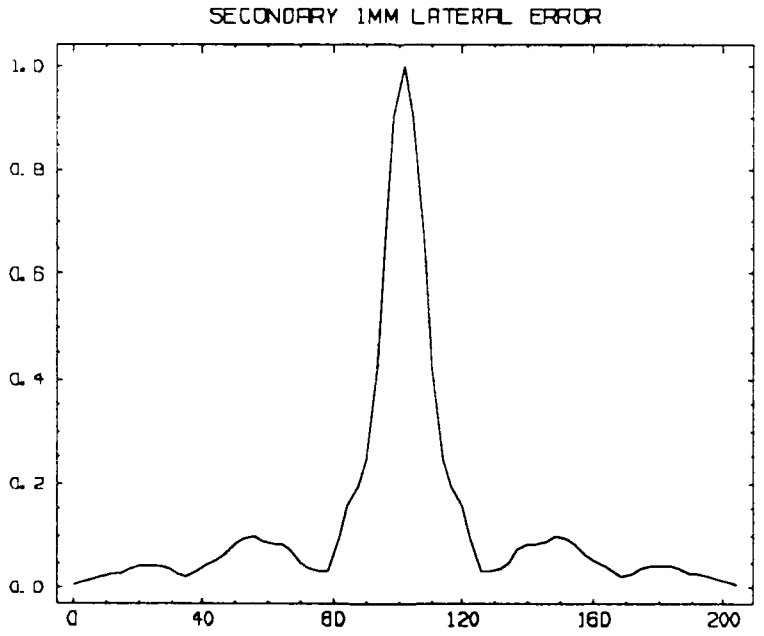

Figure A-7g
MTF - 1 mm secondary lateral displacement
Y-axis slice

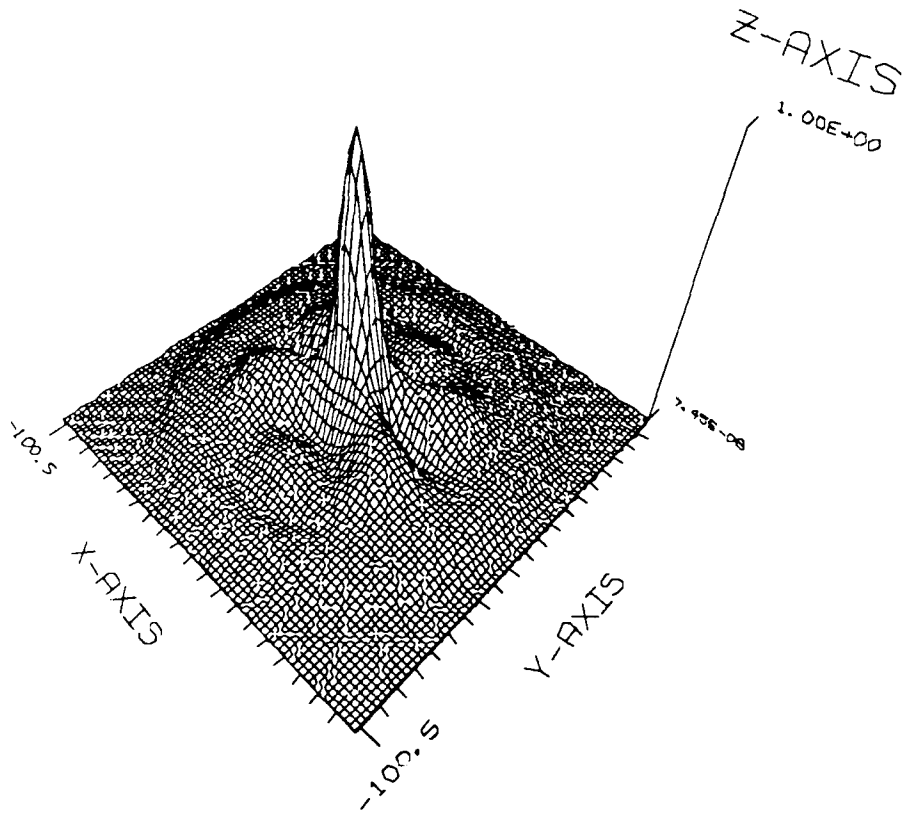

Figure A-7h
MTF - 1 mm secondary lateral displacement
Surface plot

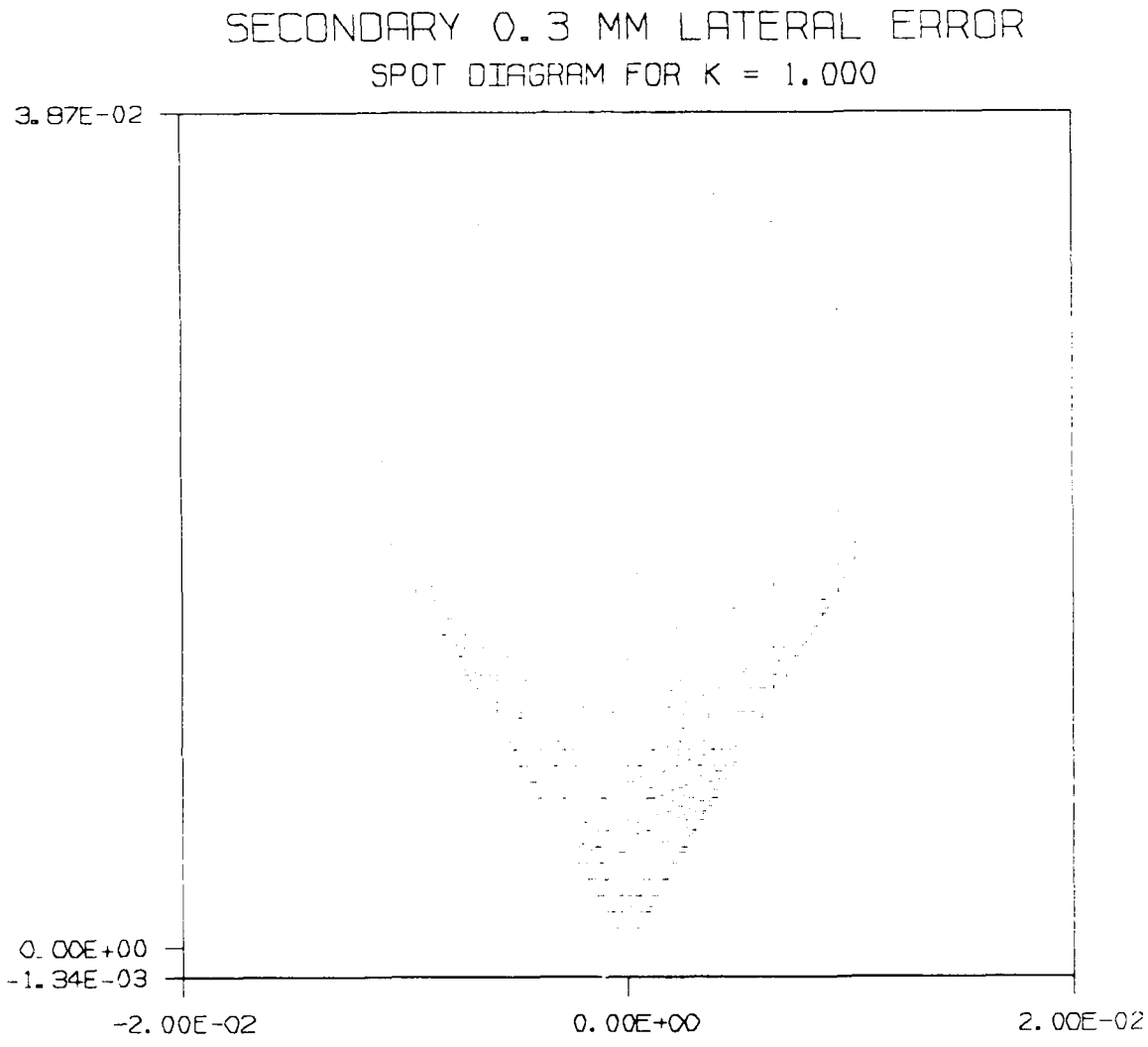

Figure A-8a

Spot Diagram for secondary 0.3 mm Y-axis lateral misalignment

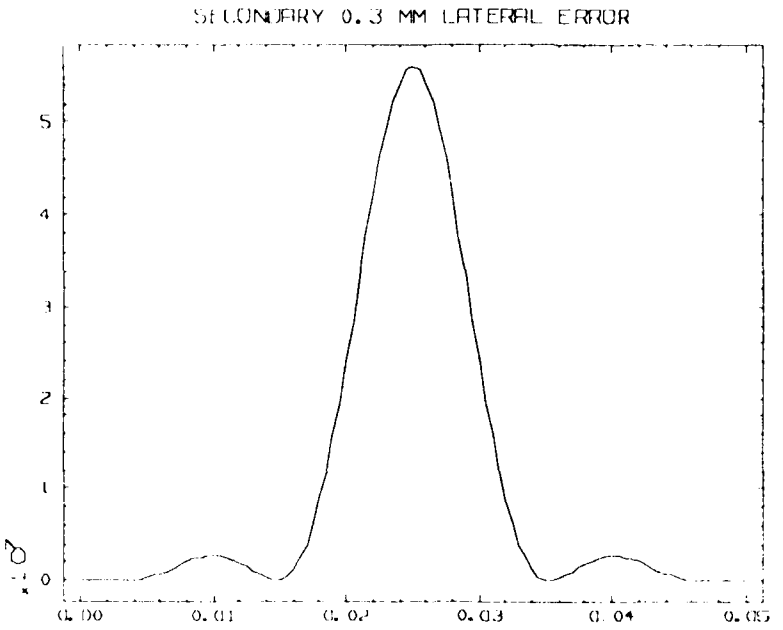

Figure A-8b
PSF - 0.3 mm secondary lateral displacement
X-axis slice

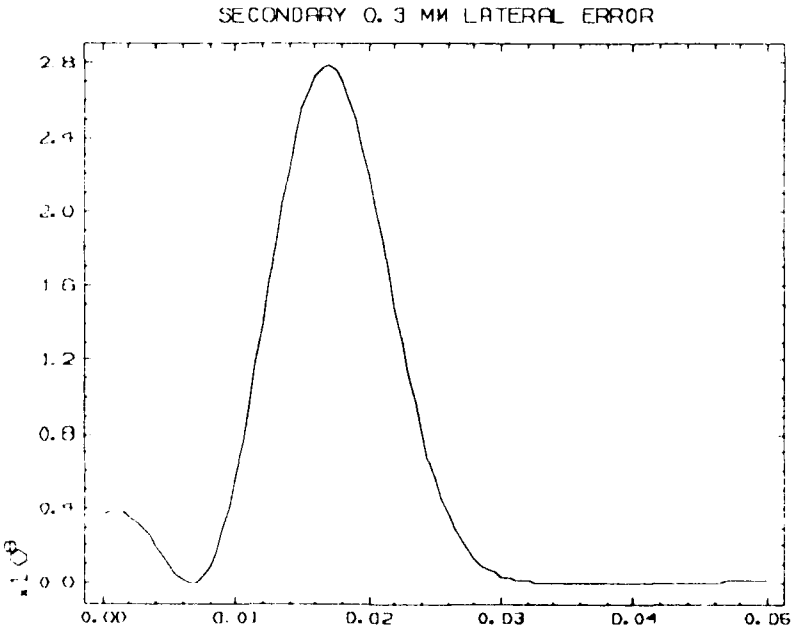

Figure A-8c
PSF - 0.3 mm secondary lateral displacement
Y-axis slice

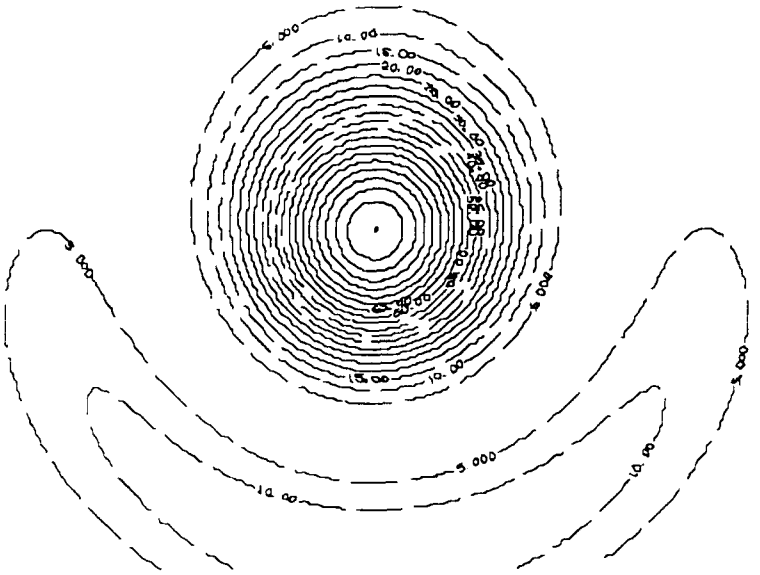

Figure A-8d
PSF - 0.3 mm secondary lateral displacement
Surface contour

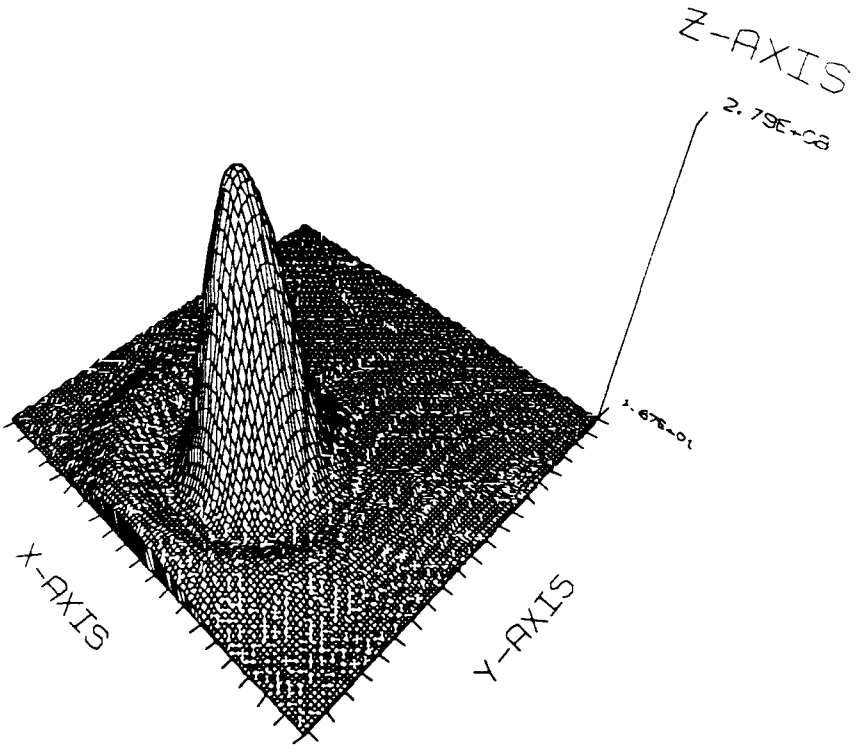

Figure A-8e
PSF - 0.3 mm secondary lateral displacement
Surface plot

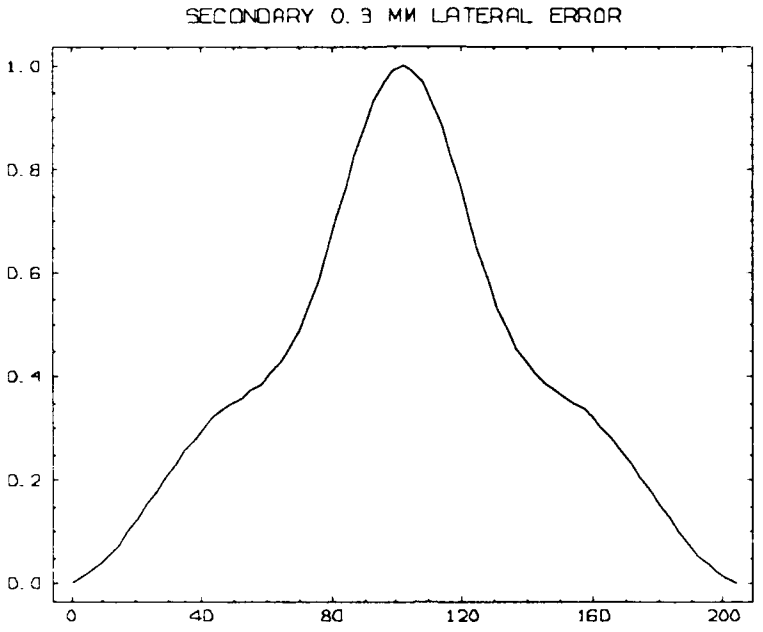

Figure A-8f
MTF - 0.3 mm secondary lateral displacement
X-axis slice

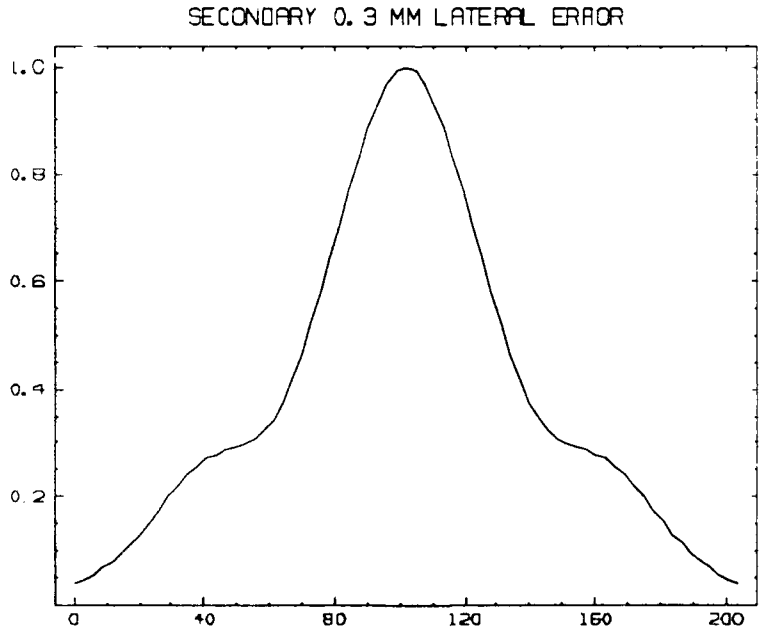

Figure A-8g
MTF - 0.3 mm secondary lateral displacement
Y-axis slice

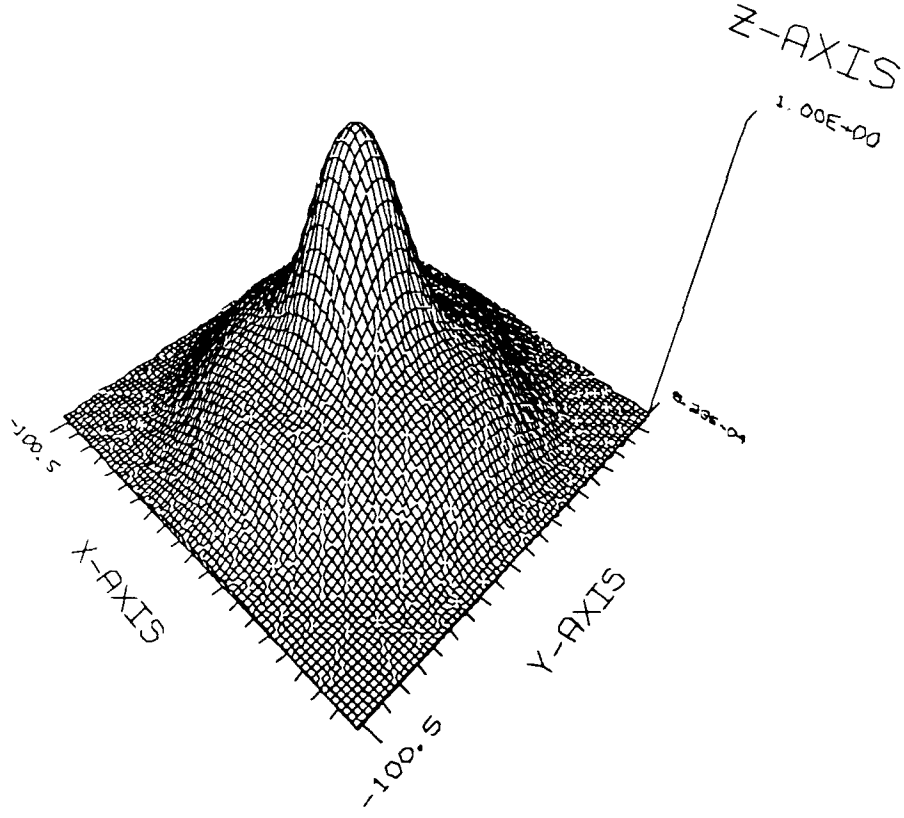

Figure A-8h
MTF - 0.3 mm secondary lateral displacement
Surface plot

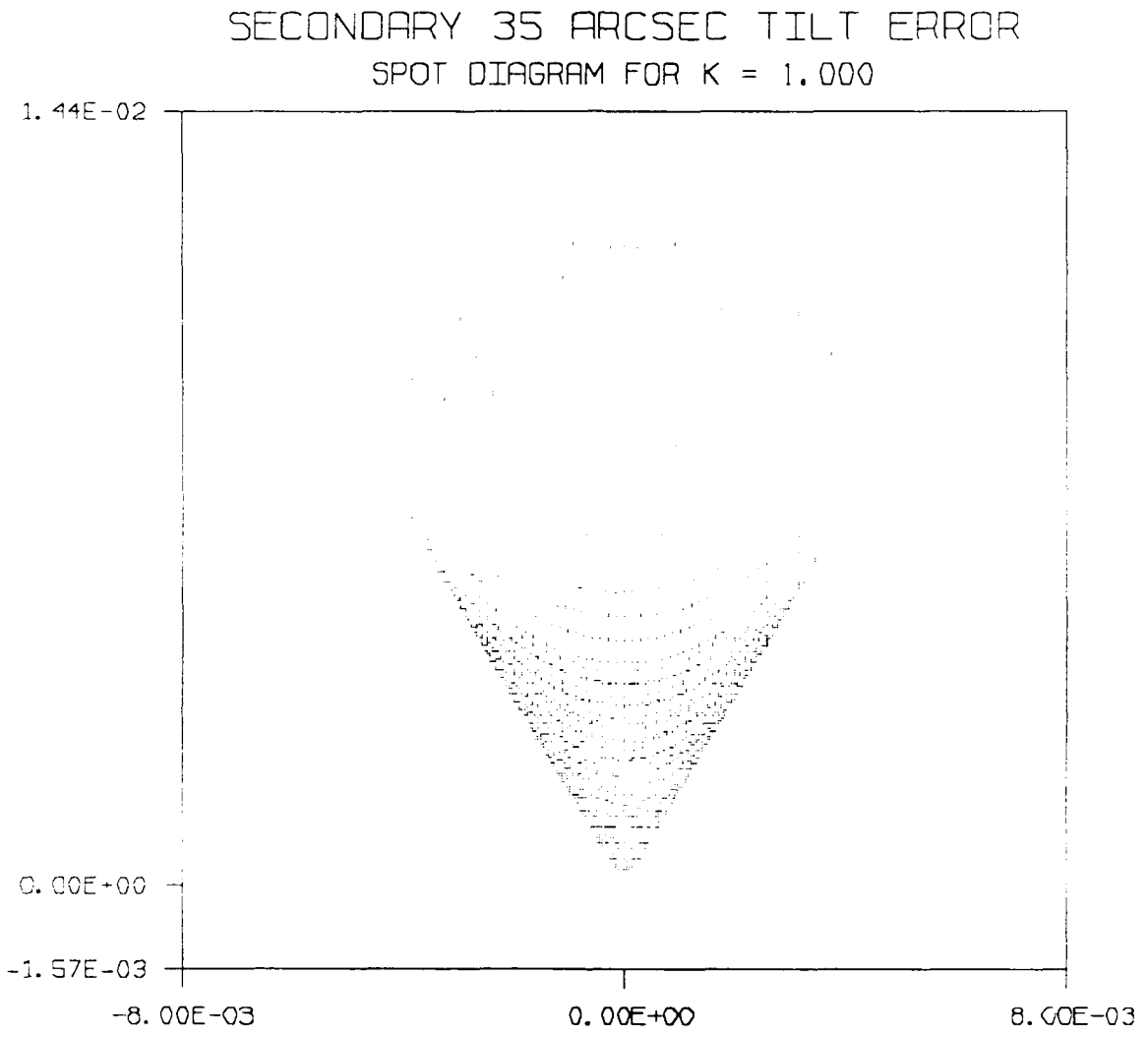

Figure A-9a

Spot Diagram - 35 arcsec Y tilt in secondary mirror

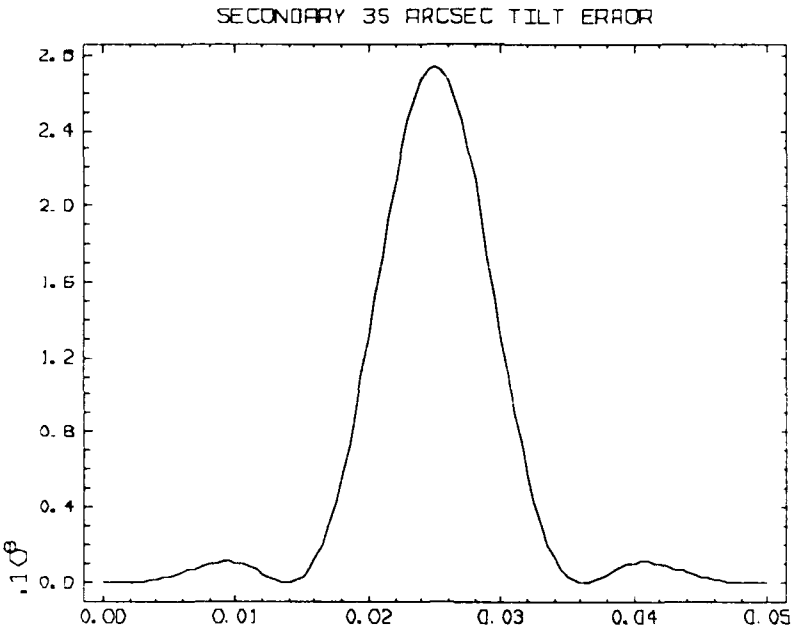

Figure A-9b
PSF - 35 arcsec Y tilt in secondary mirror
X-axis slice

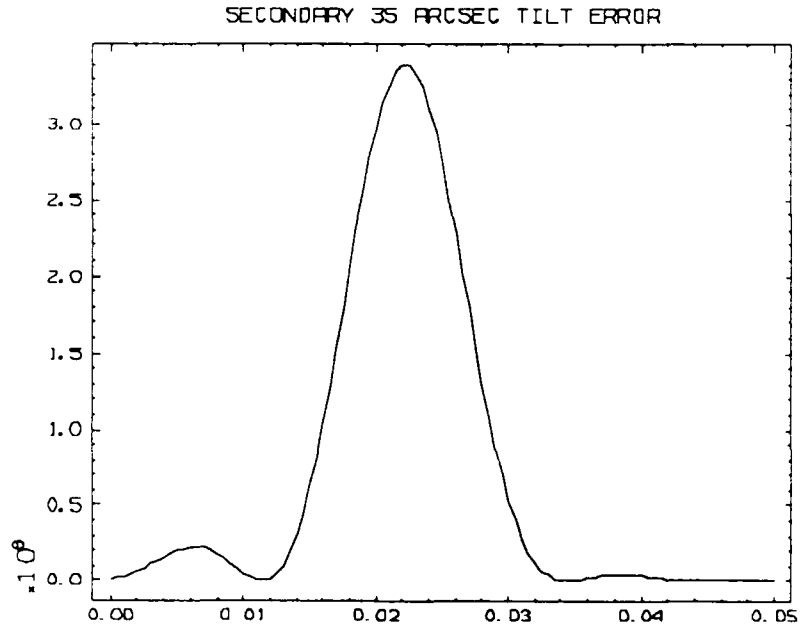

Figure A-9c
PSF - 35 arcsec Y tilt in secondary mirror
Y-axis slice

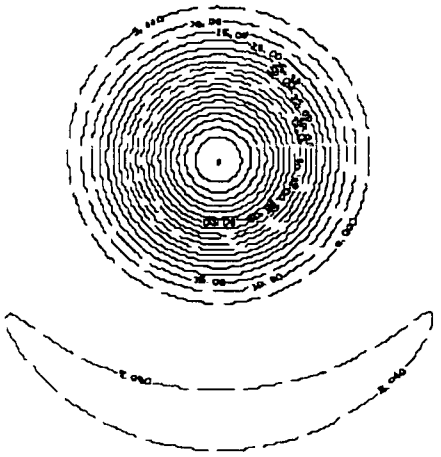

Figure A-9d
PSF - 35 arcsec Y tilt in secondary mirror
Surface contour

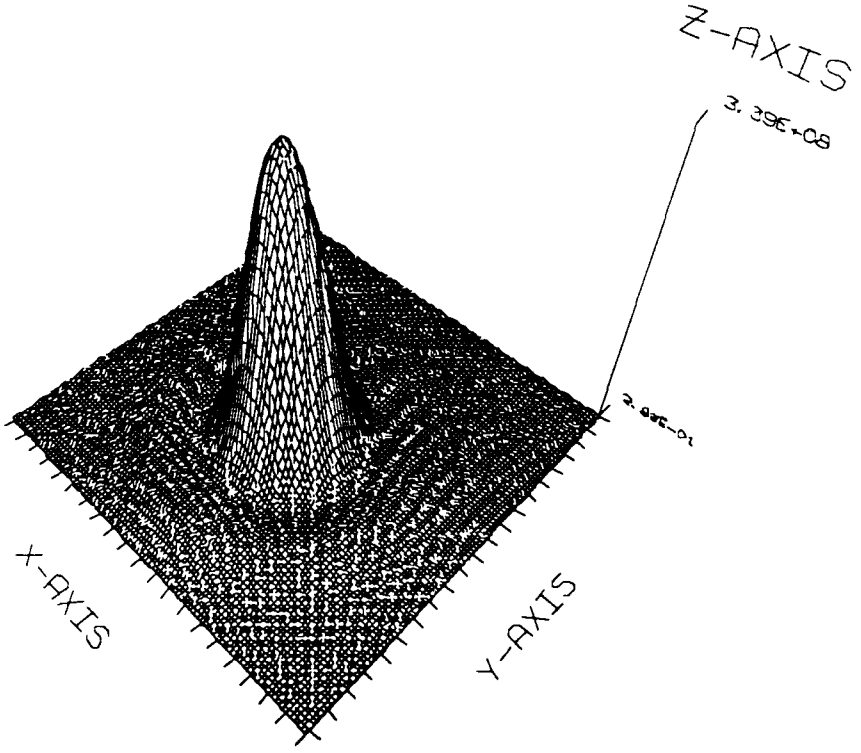

Figure A-9e
PSF - 35 arcsec Y tilt in secondary mirror
Surface plot

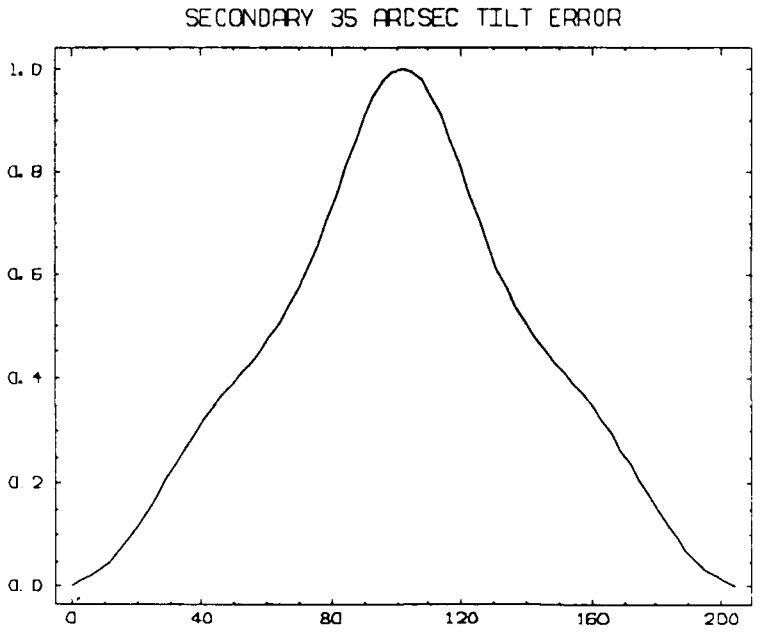

Figure A-9f
MTF - 35 arcsec Y tilt in secondary mirror
X-axis slice

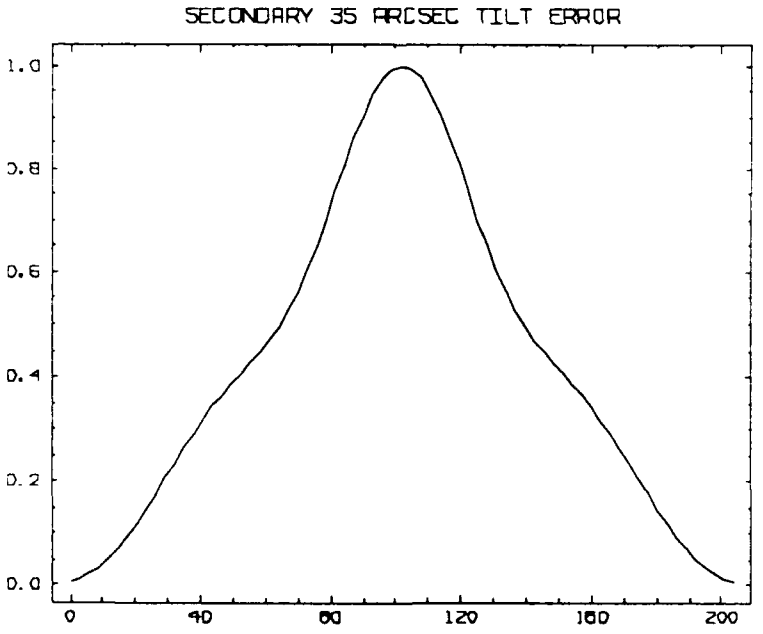

Figure A-9g
MTF - 35 arcsec Y tilt in secondary mirror
Y-axis slice

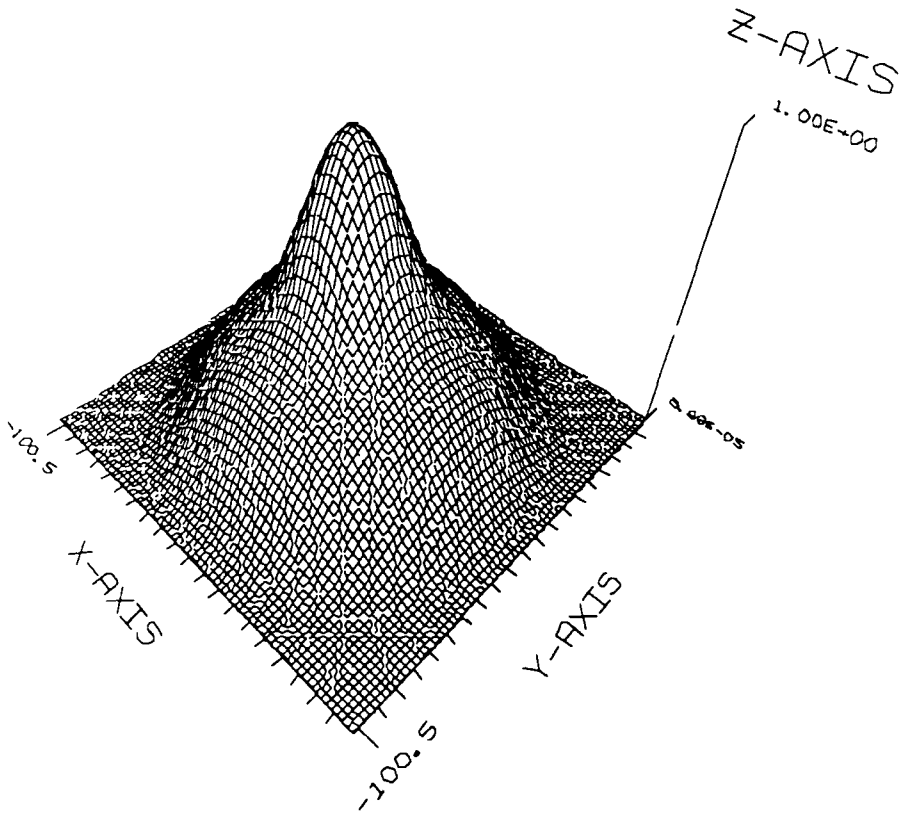

Figure A-9h

MTF - 35 arcsec Y tilt in secondary mirror
Surface plot

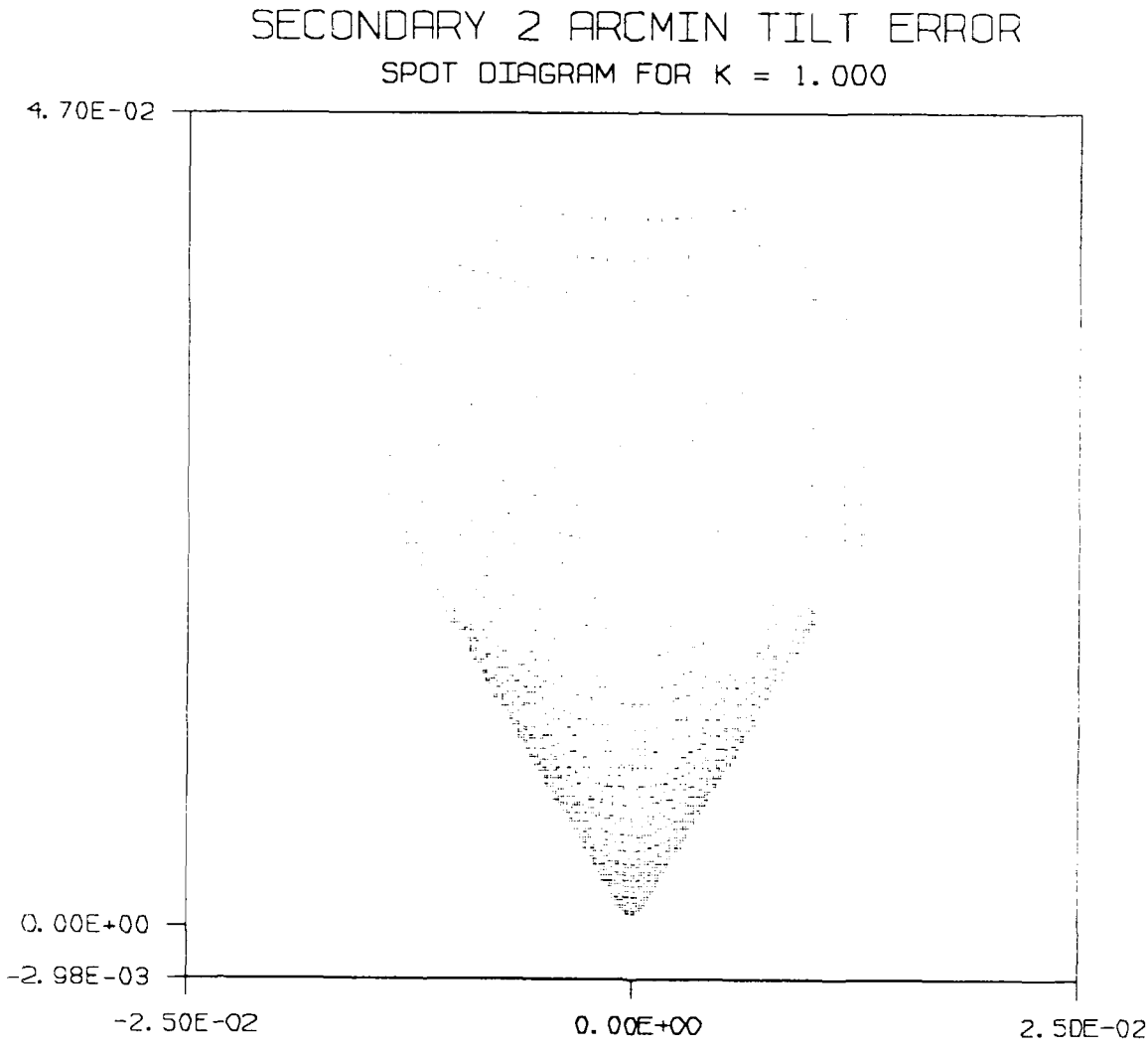

Figure A-10a

Spot Diagram - 2 arcmin Y tilt in secondary mirror

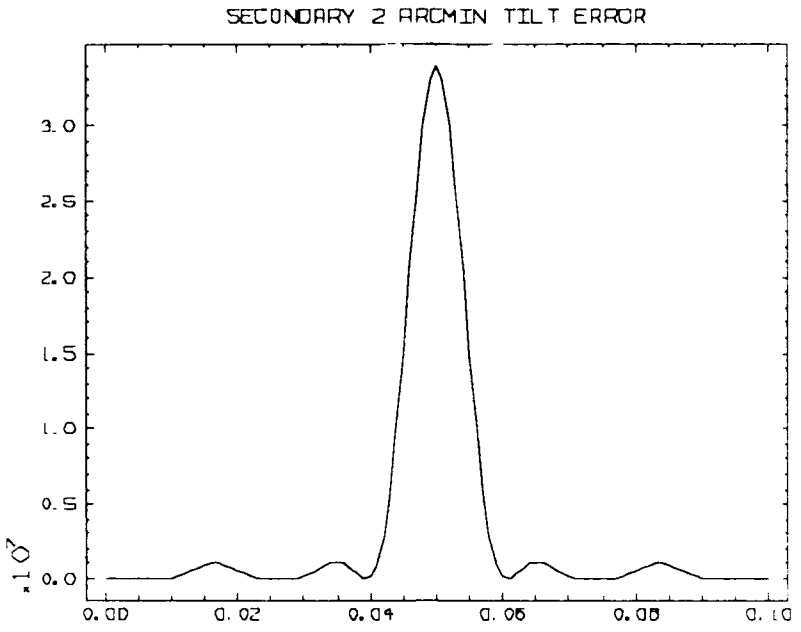

Figure A-10b
PSF - 2 arcmin Y tilt in secondary mirror
X-axis slice

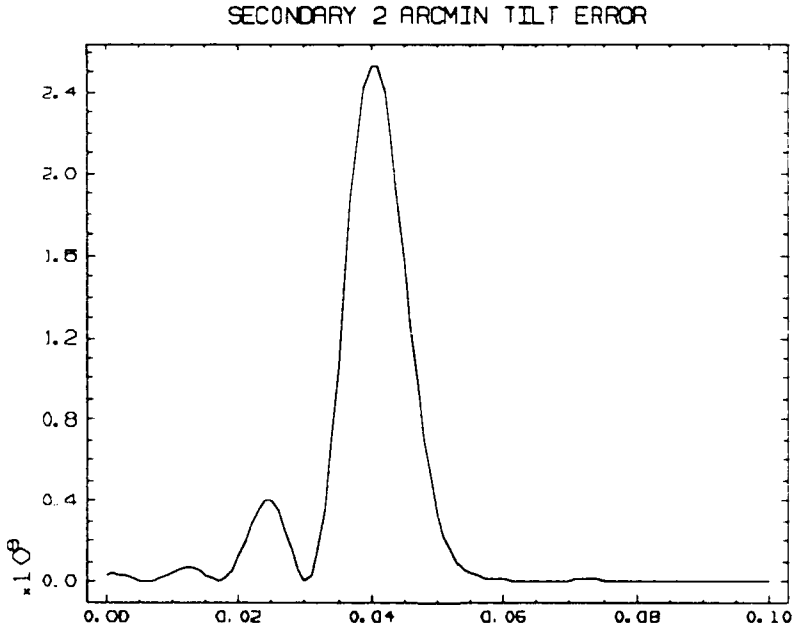

Figure A-10c
PSF - 32 arcmin Y tilt in secondary mirror
Y-axis slice

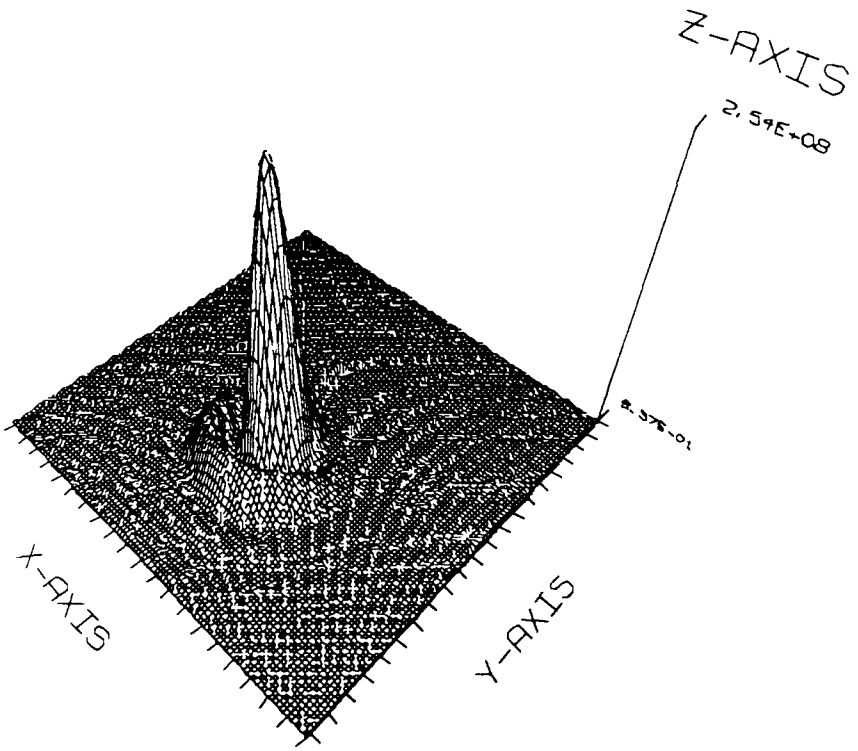

Figure A-10d

PSF - 2 arcmin Y tilt in secondary mirror
Surface plot

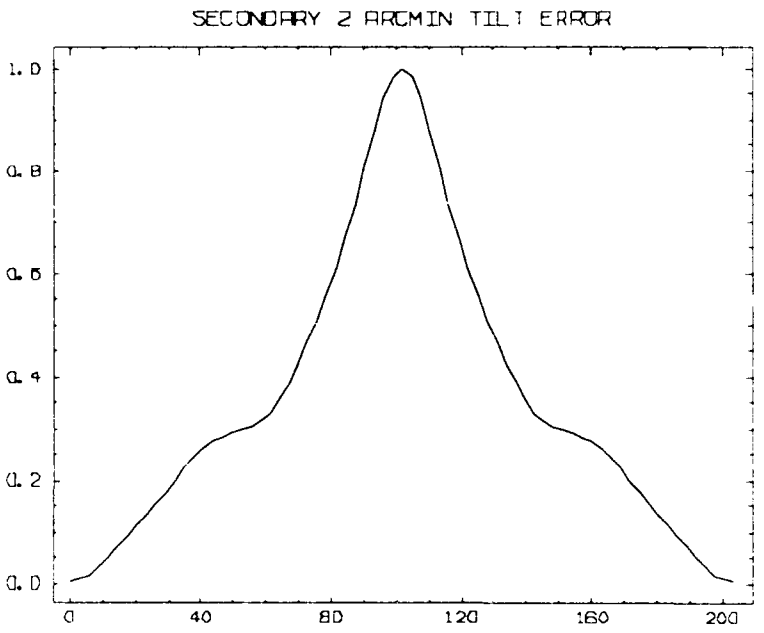

Figure A-10e
MTF - 2 arcmin Y tilt in secondary mirror
X-axis slice

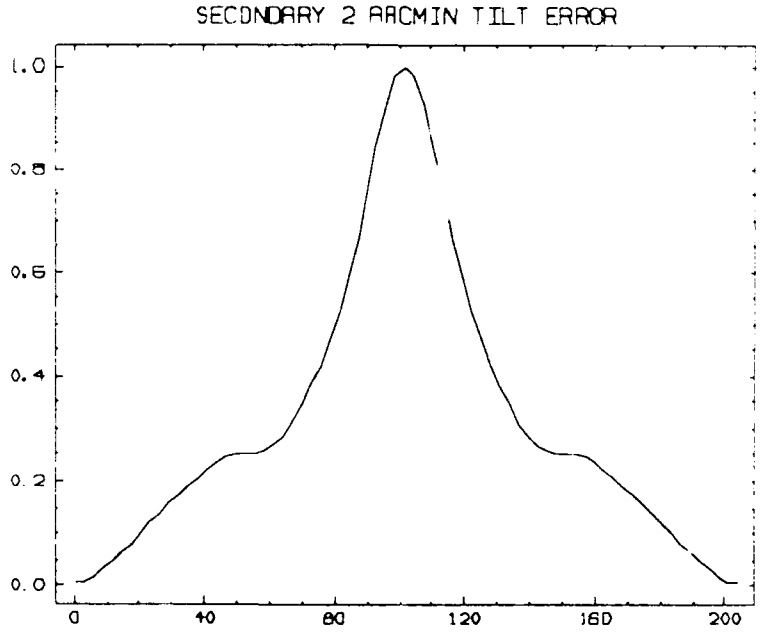

Figure A-10f
MTF - 2 arcmin Y tilt in secondary mirror
Y-axis slice

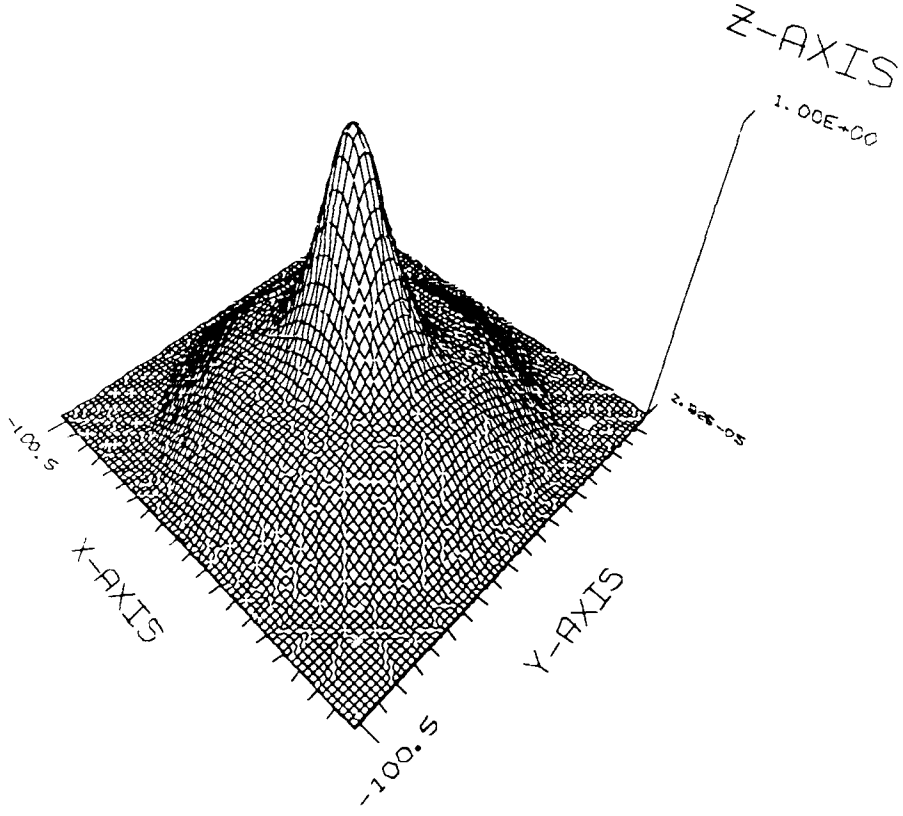

Figure A-10g
MTF - 2 arcmin Y tilt in secondary mirror
Surface plot

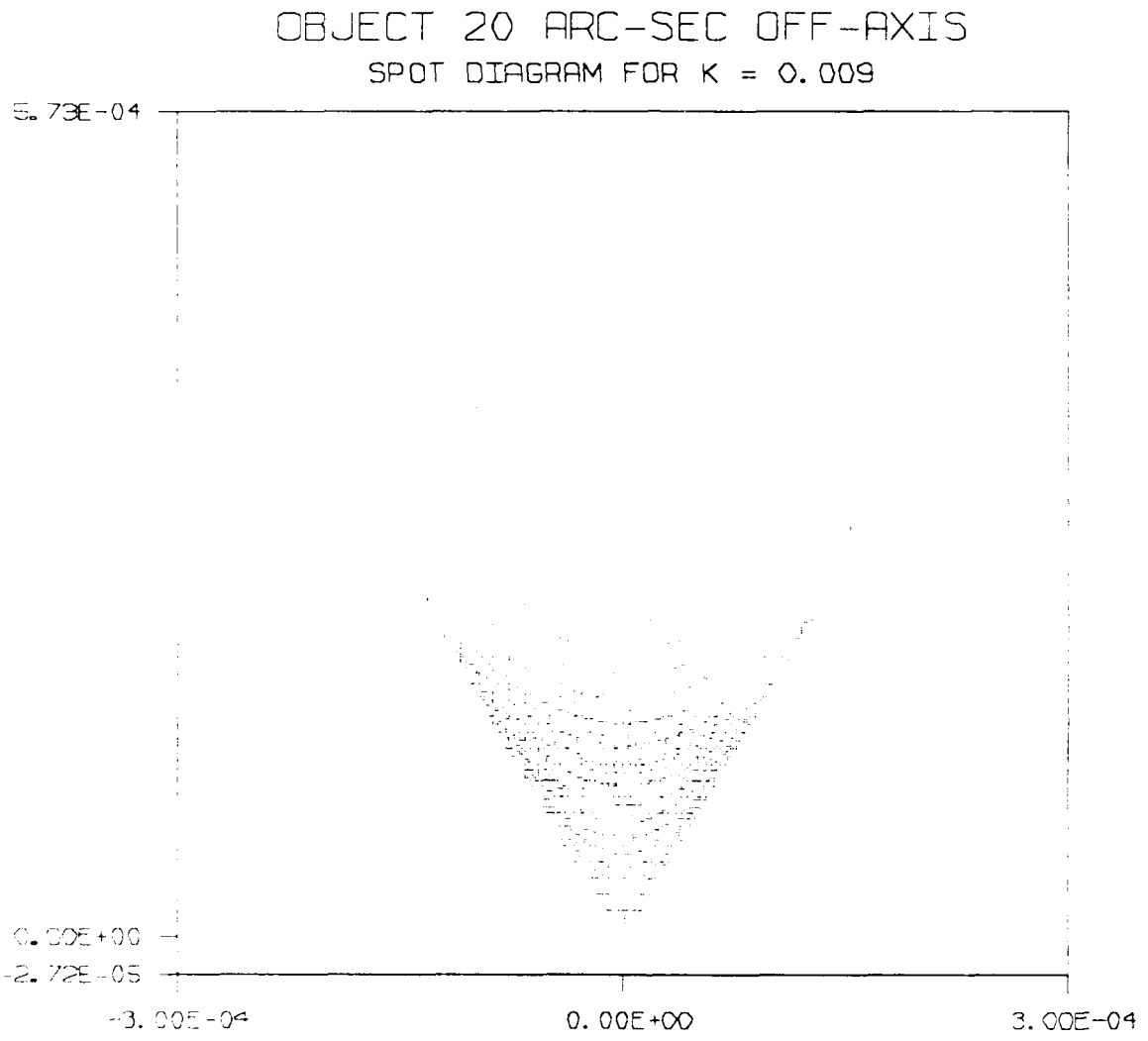

Figure A-11a

Spot diagram for object 20 arcsec off-axis

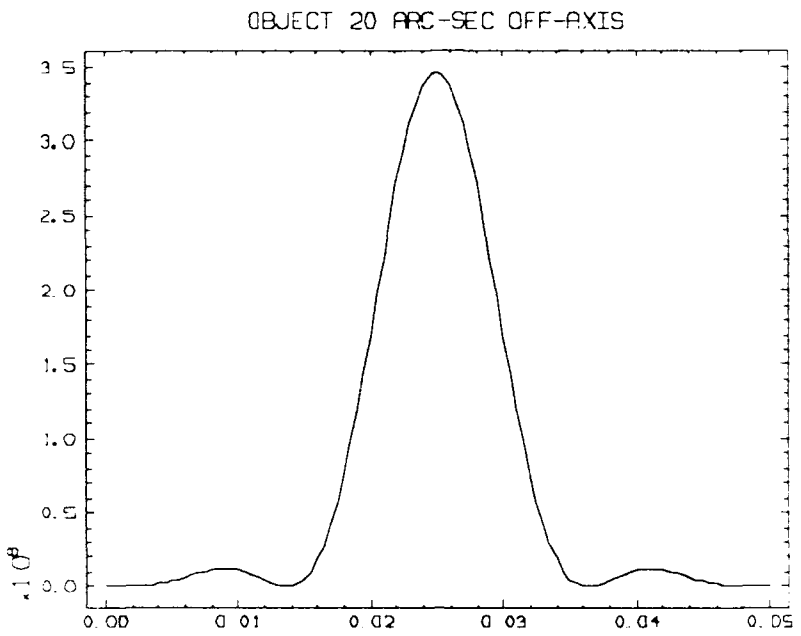

Figure A-11b
PSF - object 20 arcsec off-axis
X-axis slice

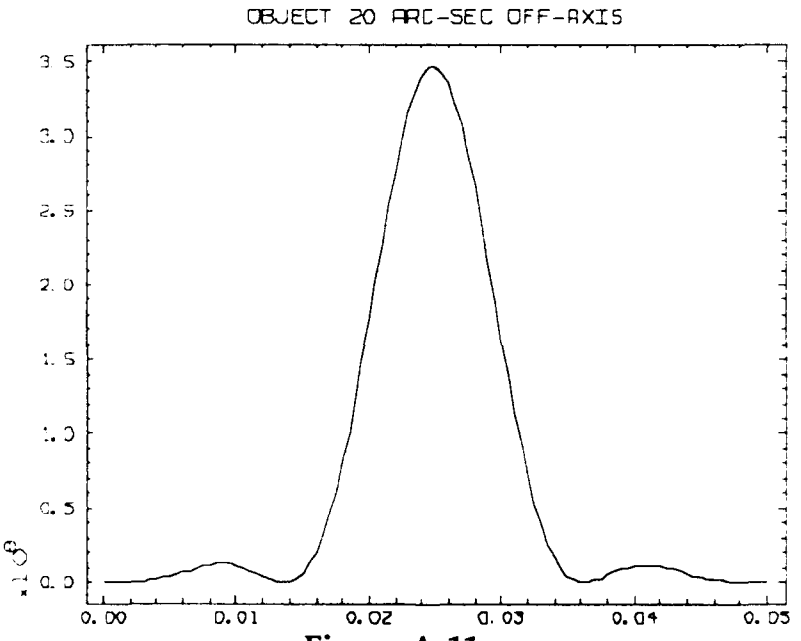

Figure A-11c
PSF - object 20 arcsec off-axis
Y-axis slice

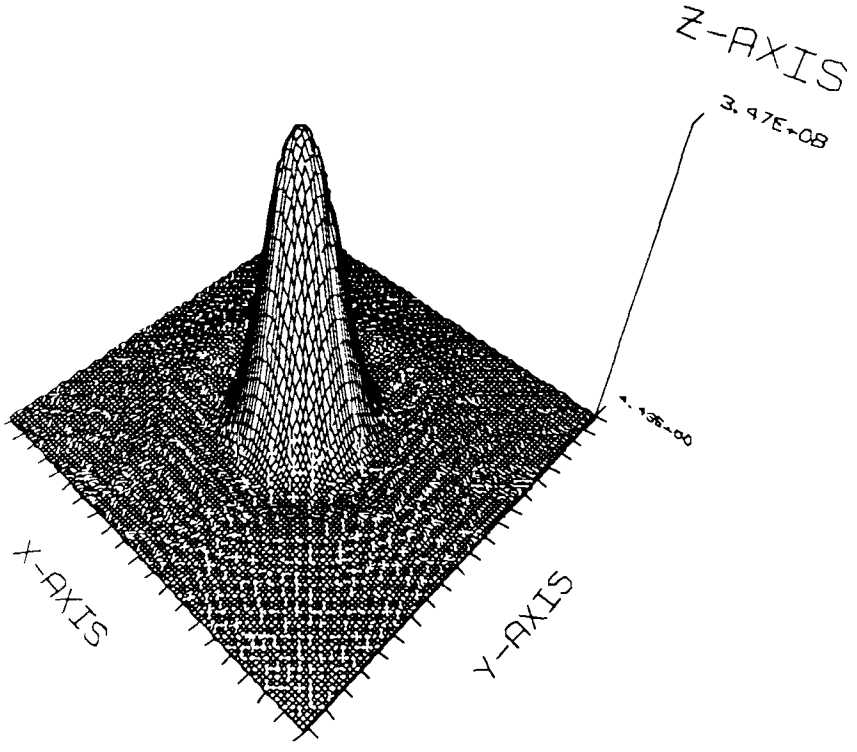

Figure A-11d

PSF - object 20 arcsec off-axis
Surface map

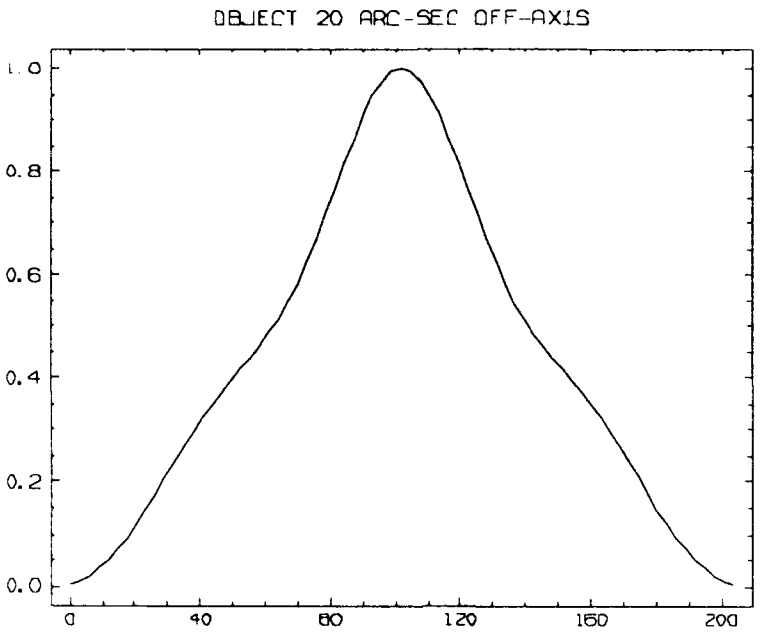

Figure A-11e
MTF - object 20 arcsec off-axis
X-axis slice

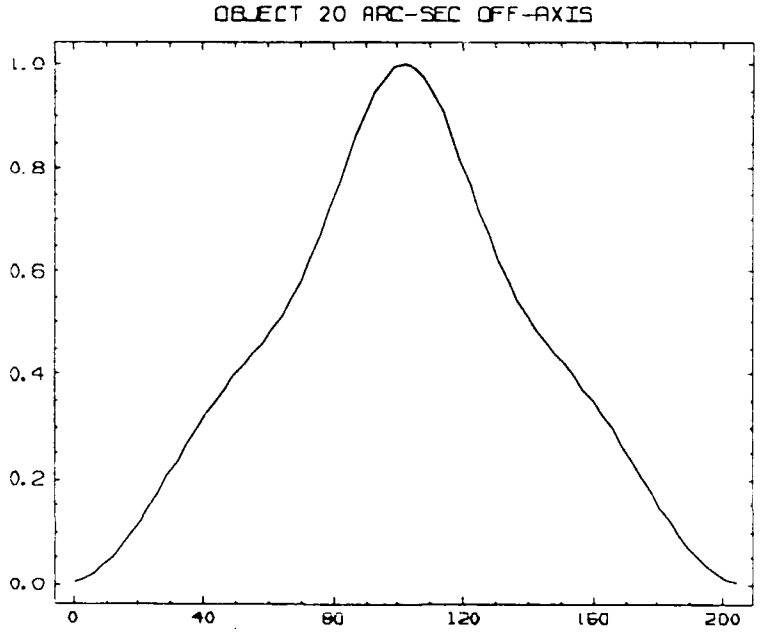

Figure A-11f
MTF - object 20 arcsec off-axis
Y-axis slice

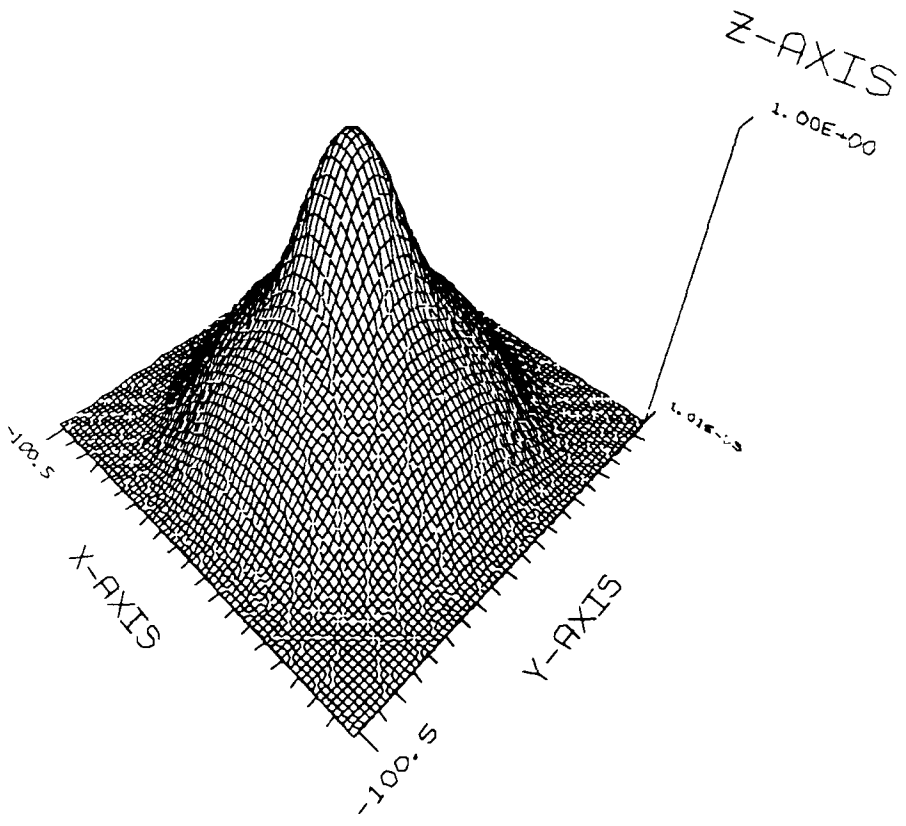

Figure A-11g

MTF - object 20 arcsec off-axis
Surface plot

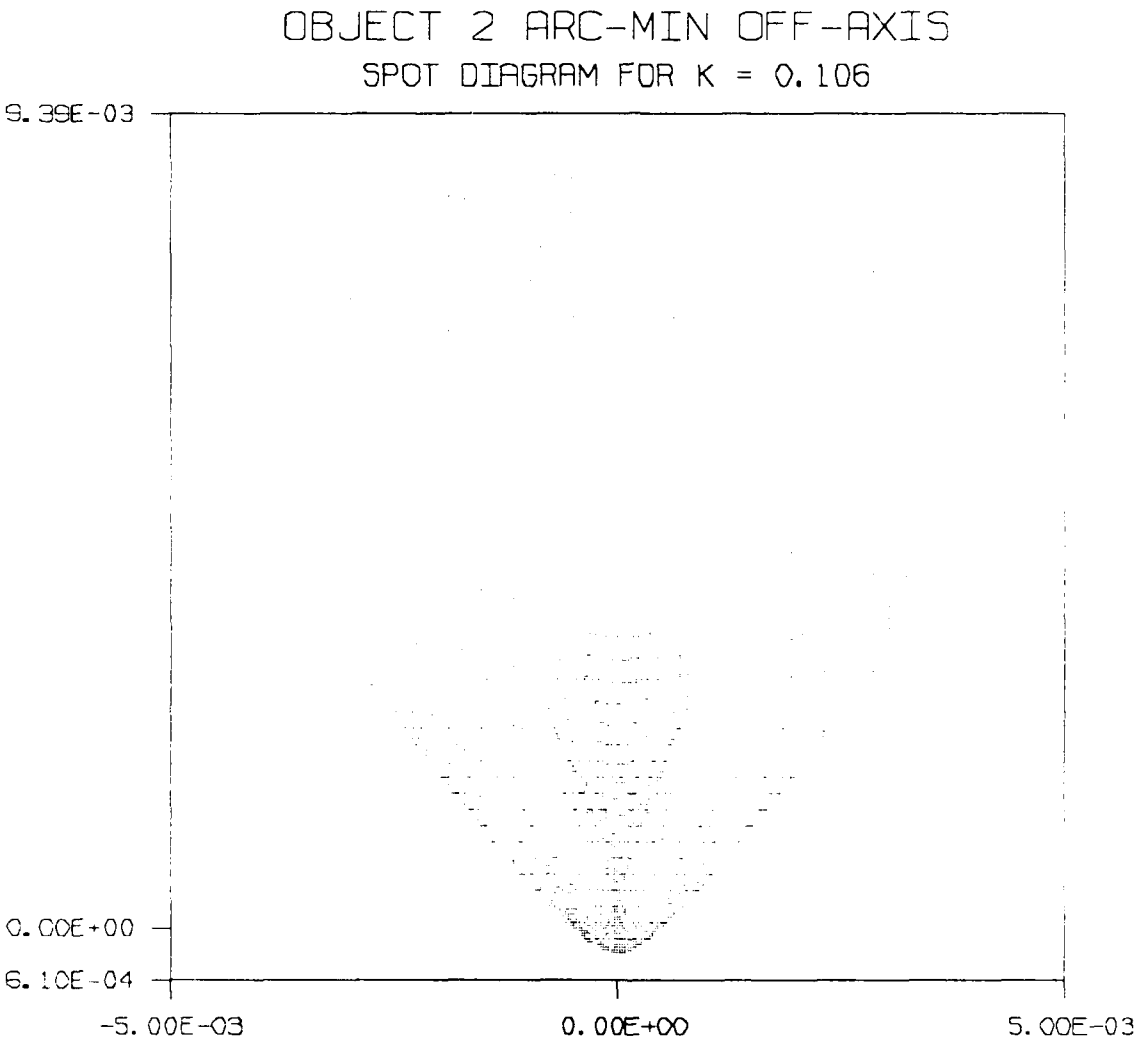

Figure A-12a

Spot diagram for object 2 arcmin off-axis

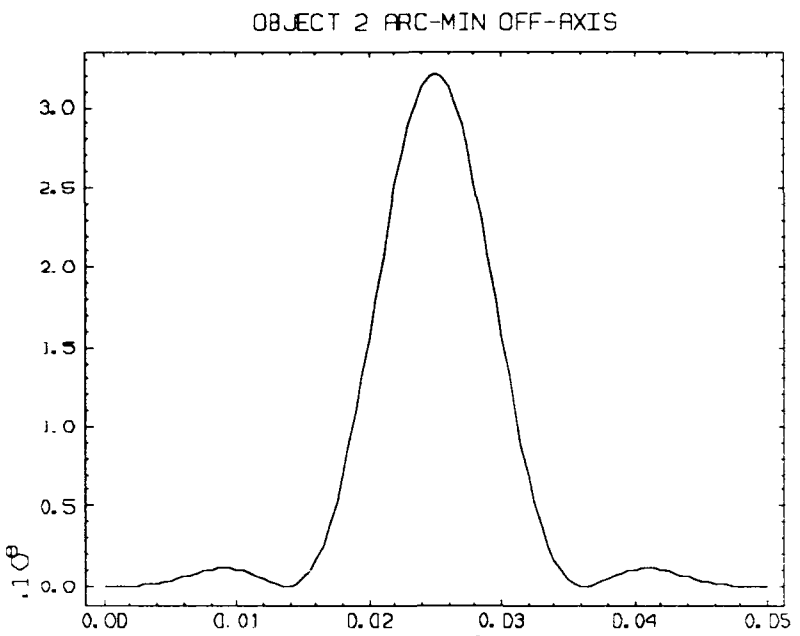

Figure A-12b
PSF - object 2 arcmin off-axis
X-axis slice

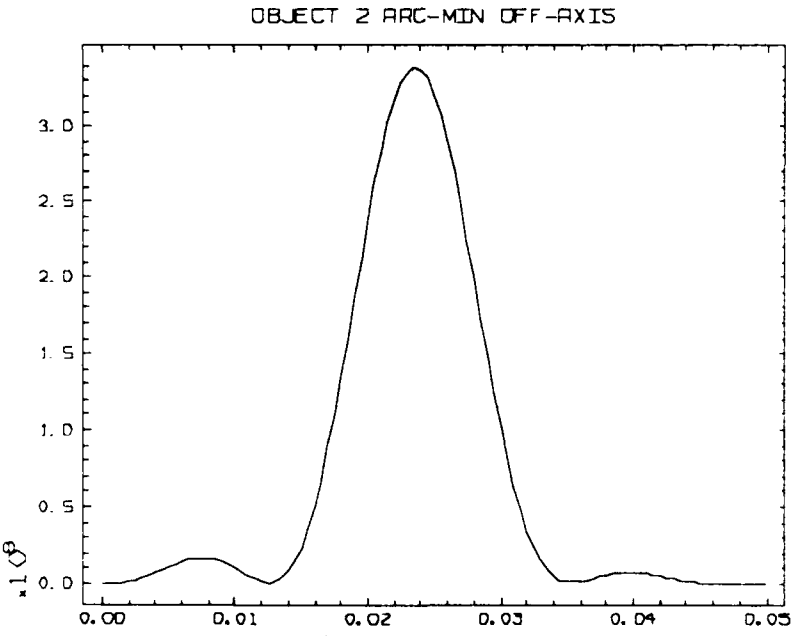

Figure A-12c
PSF - object 2 arcmin off-axis
Y-axis slice

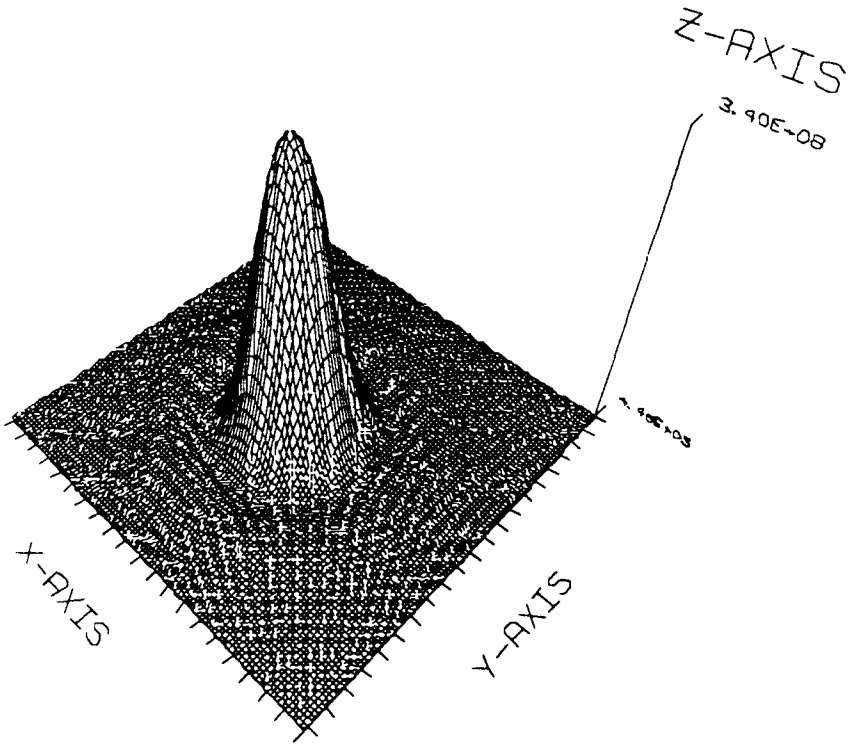

Figure A-12d

PSF - object 2 arcmin off-axis
Surface map

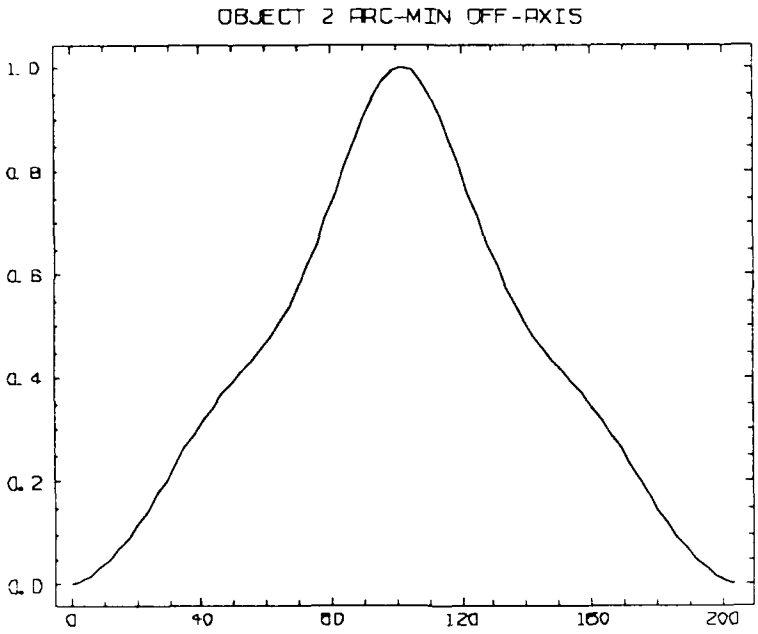

Figure A-12e
MTF - object 2 arcmin off-axis
X-axis slice

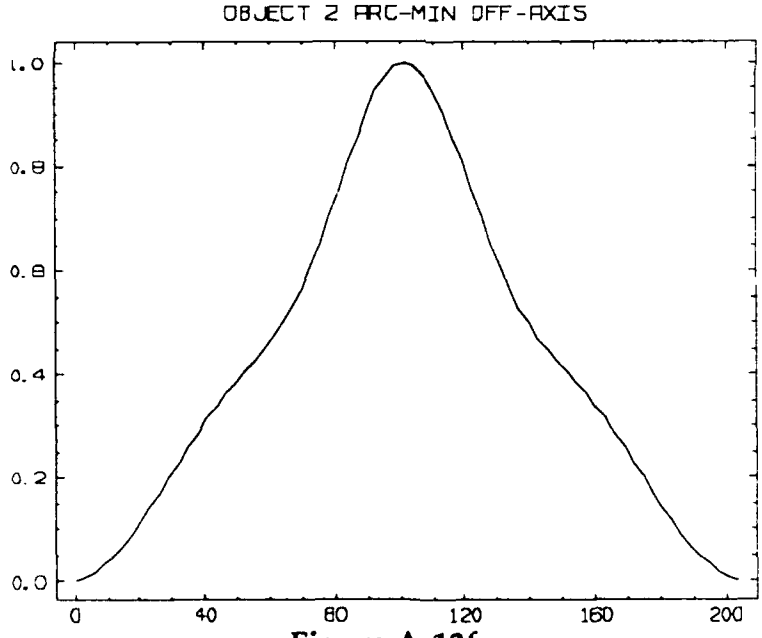

Figure A-12f
MTF - object 2 arcmin off-axis
Y-axis slice

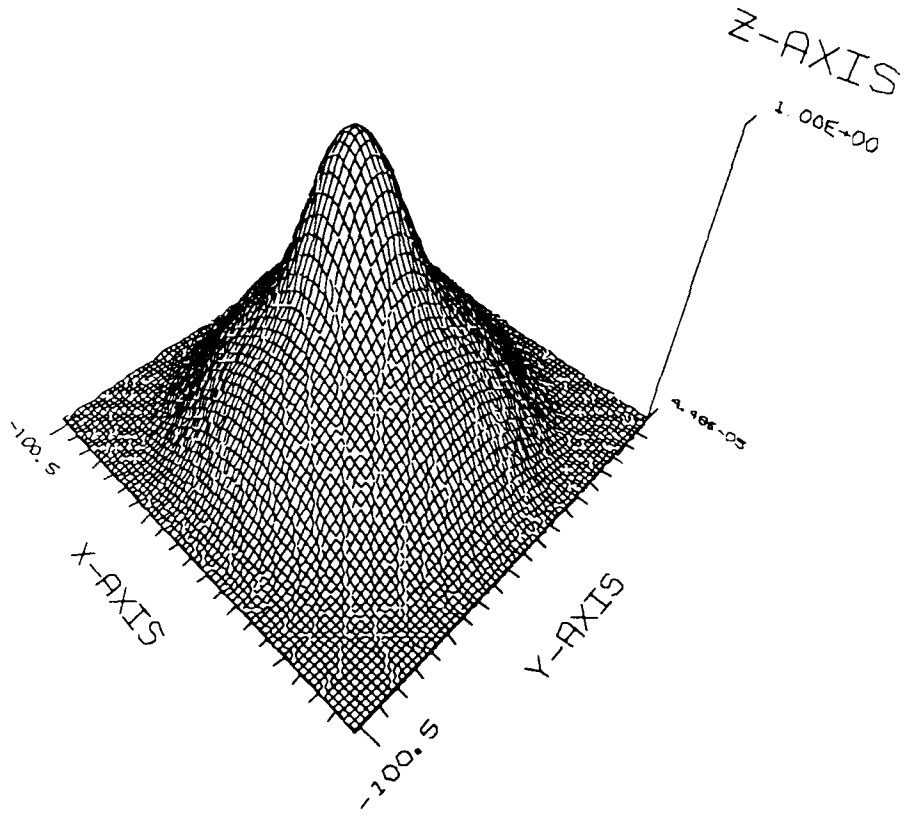

Figure A-12g

MTF - object 2 arcmin off-axis
Surface plot

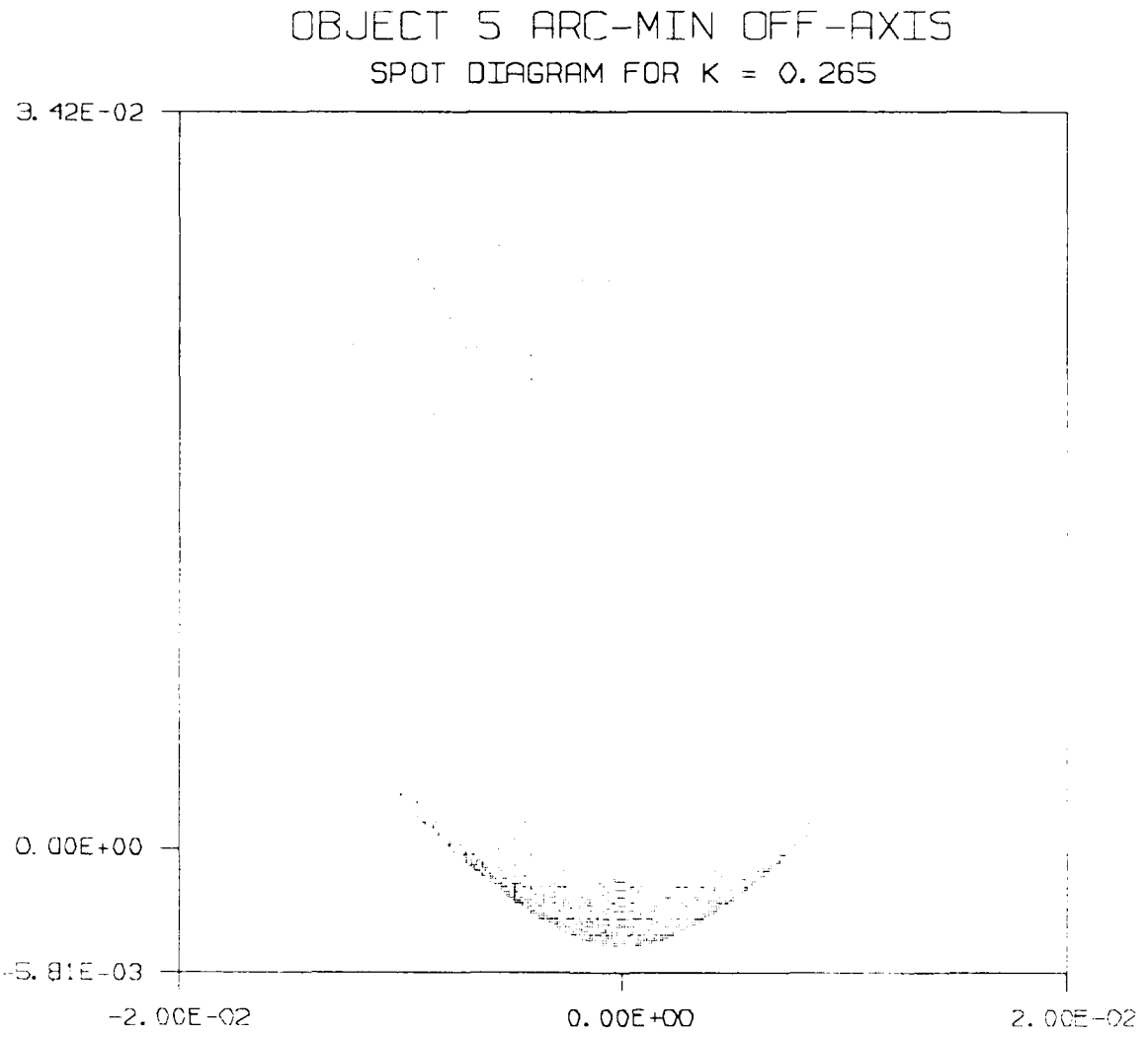

Figure A-13a

Spot diagram for object 5 arcmin off-axis

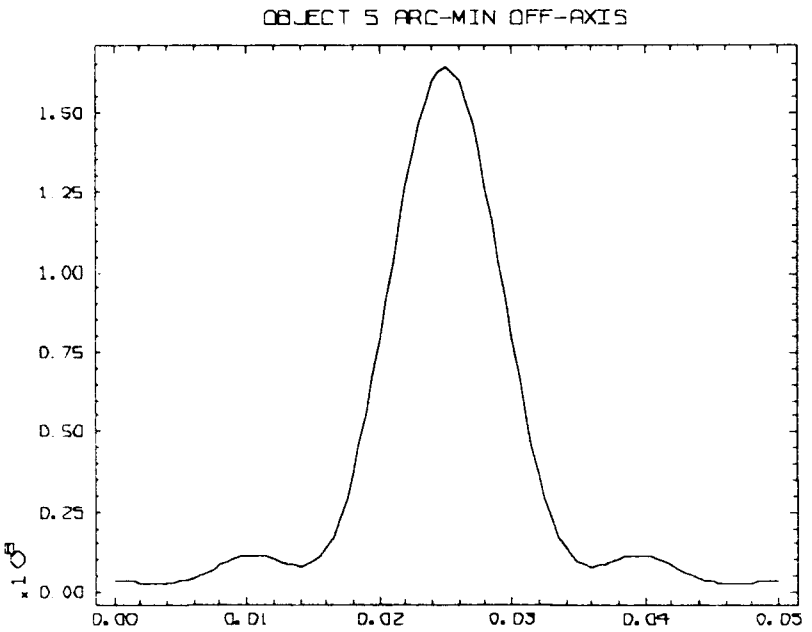

Figure A-13b
PSF - object 5 arcmin off-axis
X-axis slice

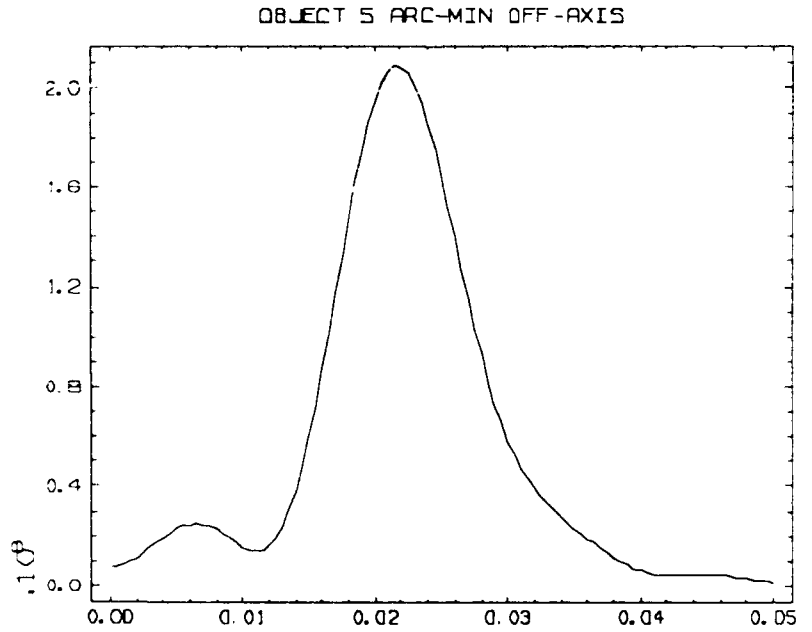

Figure A-13c
PSF - object 5 arcmin off-axis
Y-axis slice

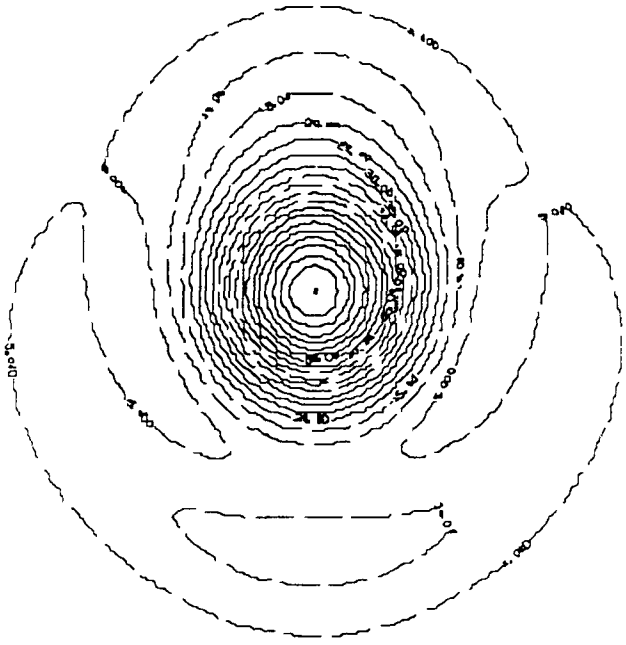

Figure A-13d
PSF - object 5 arcmin off-axis
Contour map

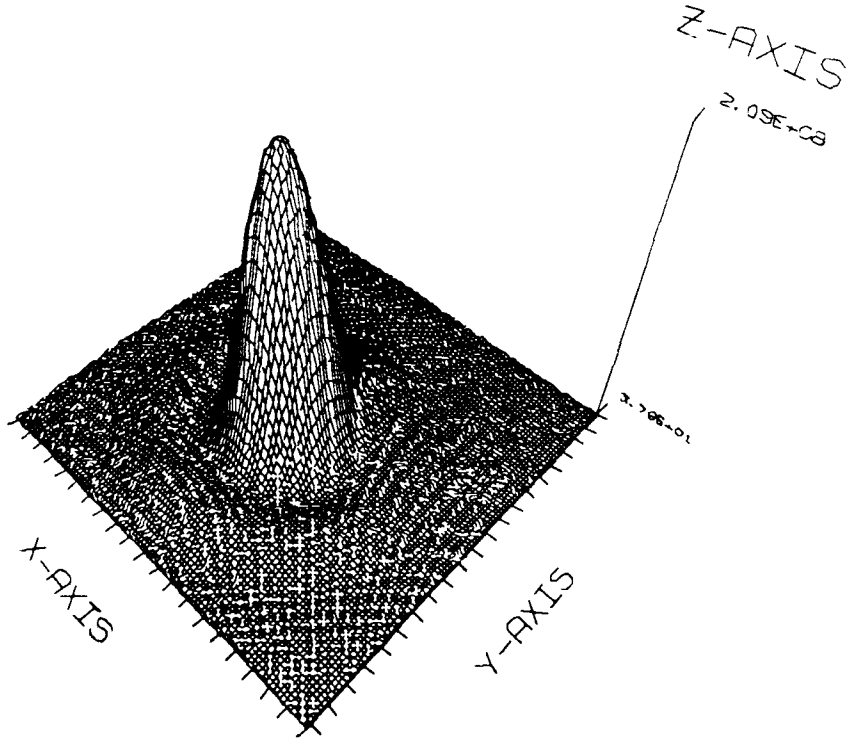

Figure A-13e
PSF - object 5 arcmin off-axis

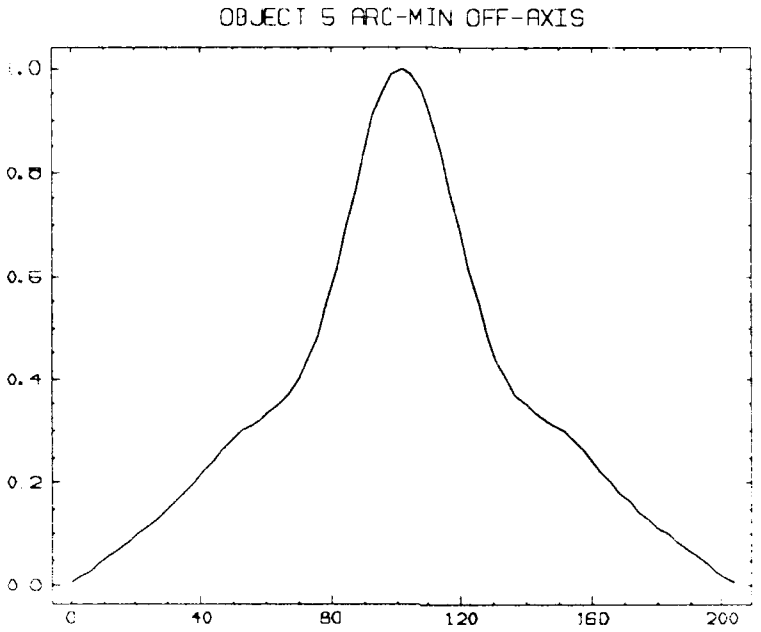

Figure A-13f
MTF - object 5 arcmin off-axis
X-axis slice

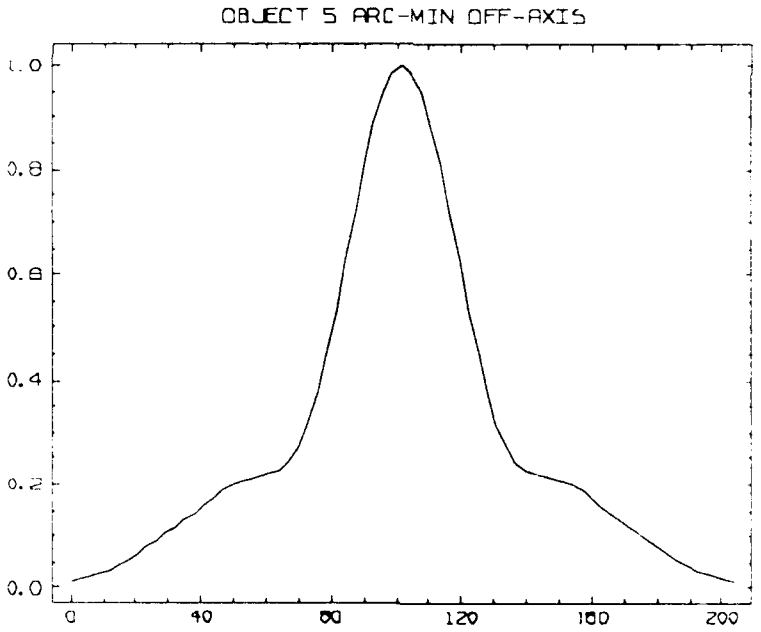

Figure A-13g
MTF - object 5 arcmin off-axis
Y-axis slice

AD-A235 604 OPTICAL PERFORMANCE ANALYSIS OF THE PRECISION OPTICAL RESEARCH AND TRACKING FACILITY (PORTF)(U) ROME LAB GRIFFISS AFB NY P L REPAK MAR 91 RL-TR-91-47 XF-RL* 2/2

UNCLASSIFIED NL

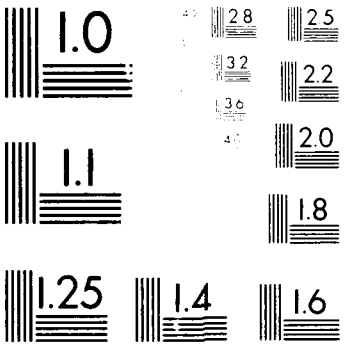

MICROCOPY RESOLUTION TEST CHART
NATIONAL BUREAU OF STANDARDS
STANDARD REFERENCE MATERIAL 1010a
(ANSI and ISO TEST CHART No. 2)

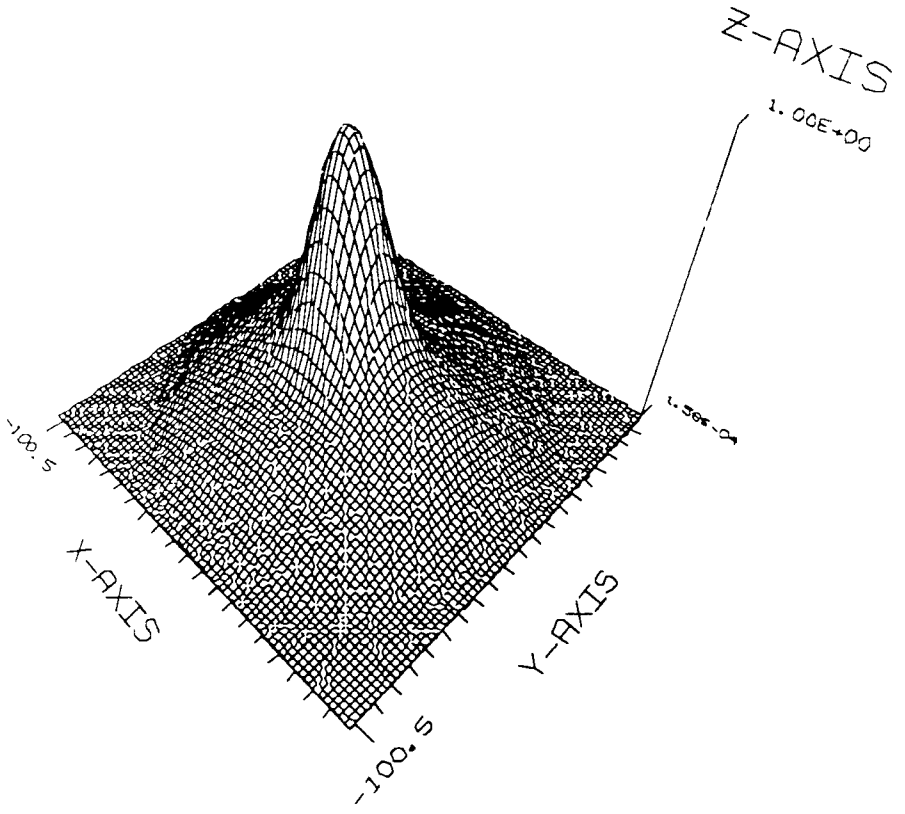

Figure A-13h

MTF - object 5 arcmin off-axis
Surface plot

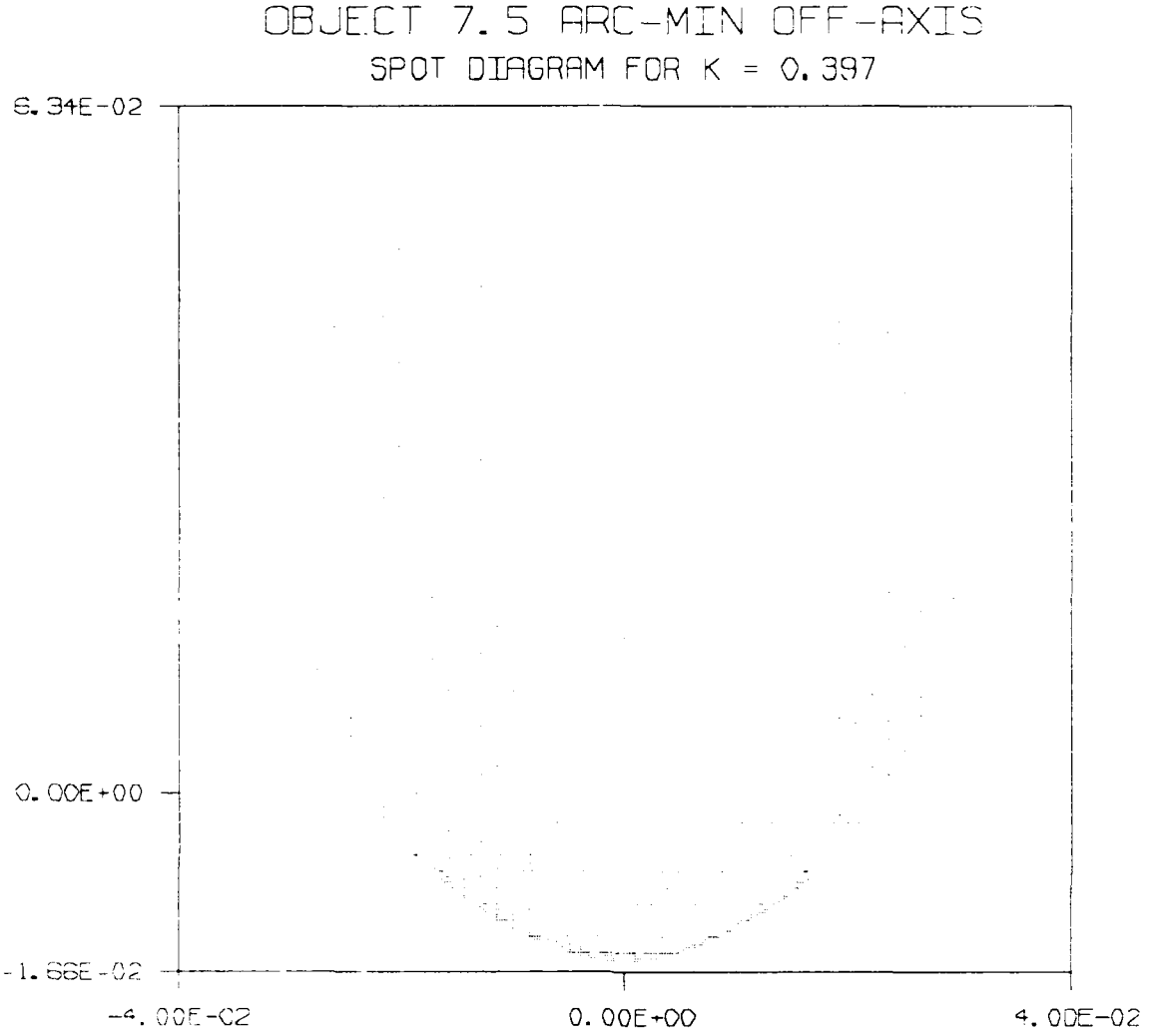

Figure A-14a

Spot diagram for object 7.5 arcmin off-axis

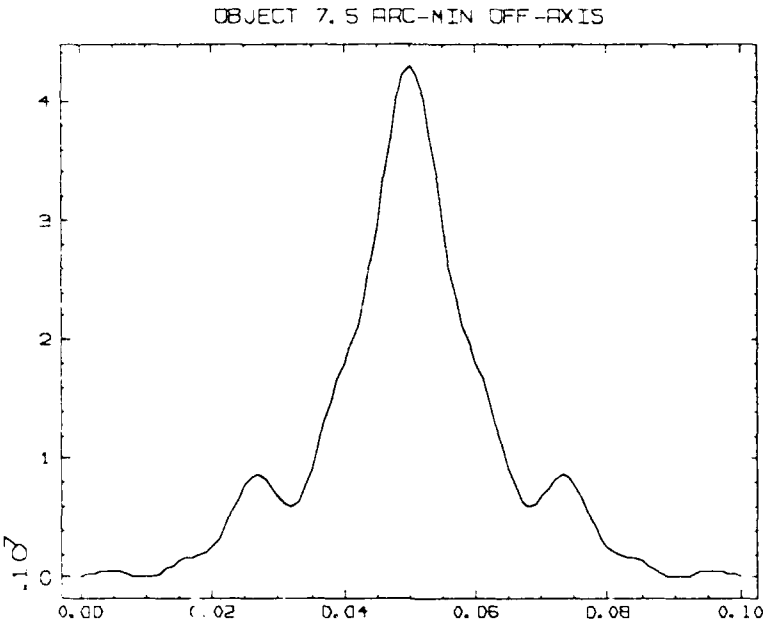

Figure A-14b
PSF - object 7.5 arcmin off-axis
X-axis slice

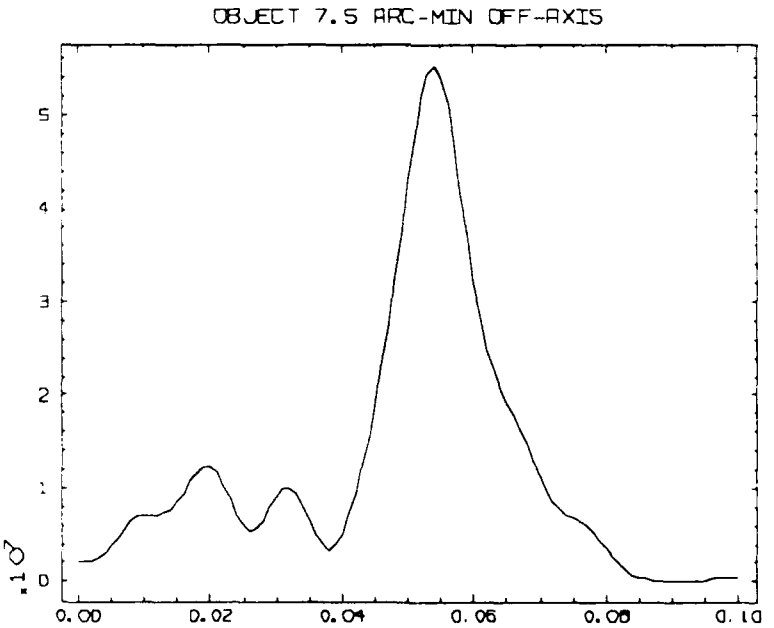

Figure A-14c
PSF - object 7.5 arcmin off-axis
Y-axis slice

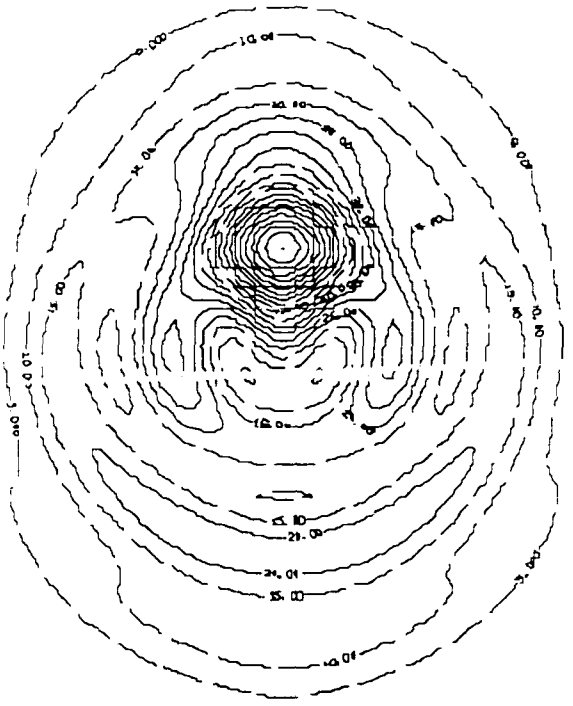

Figure A-14d
PSF - object 7.5 arcmin off-axis

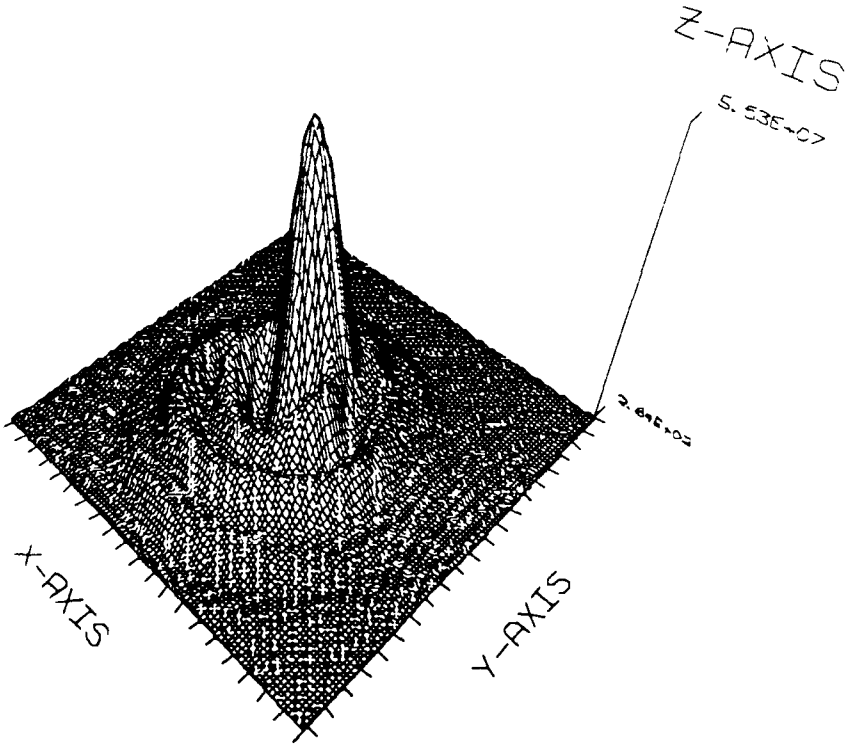

Figure A-14e
PSF - object 7.5 arcmin off-axis

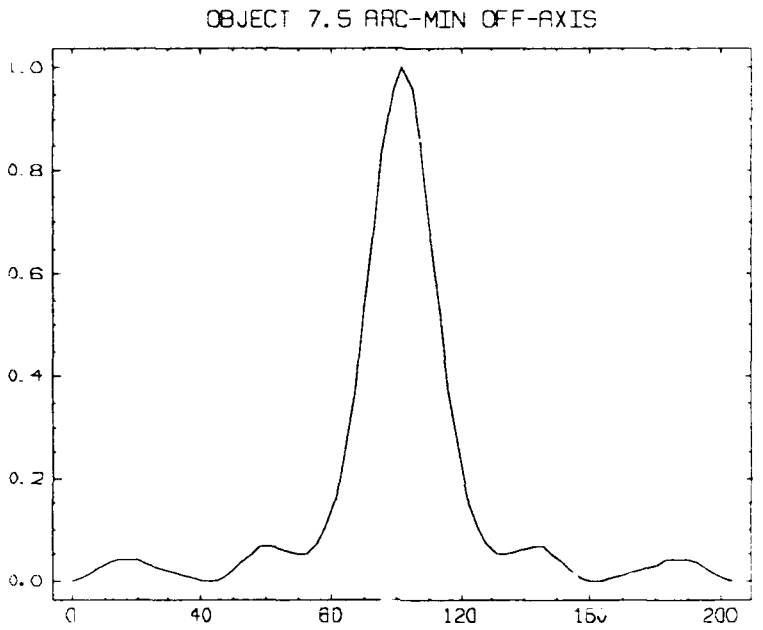

Figure A-14f
MTF - object 7.5 arcmin off-axis
X-axis slice

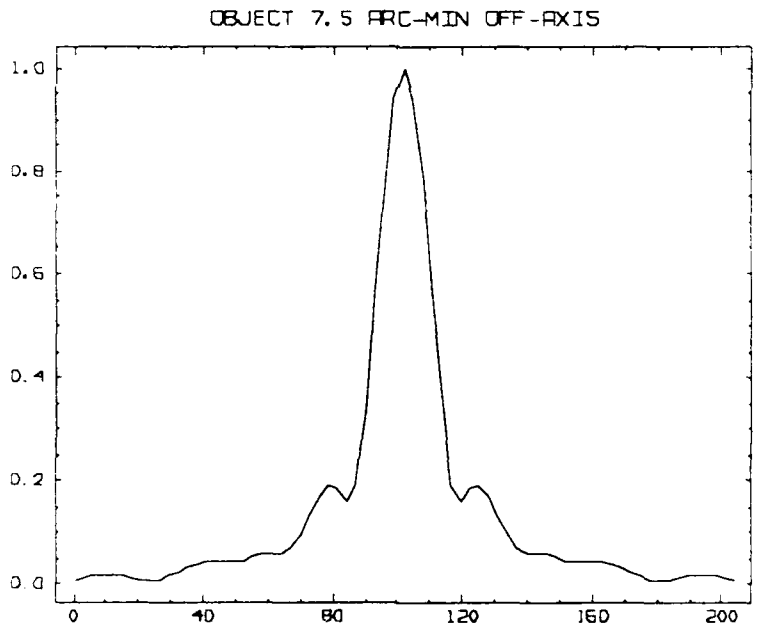

Figure A-14g
MTF - object 7.5 arcmin off-axis
Y-axis slice

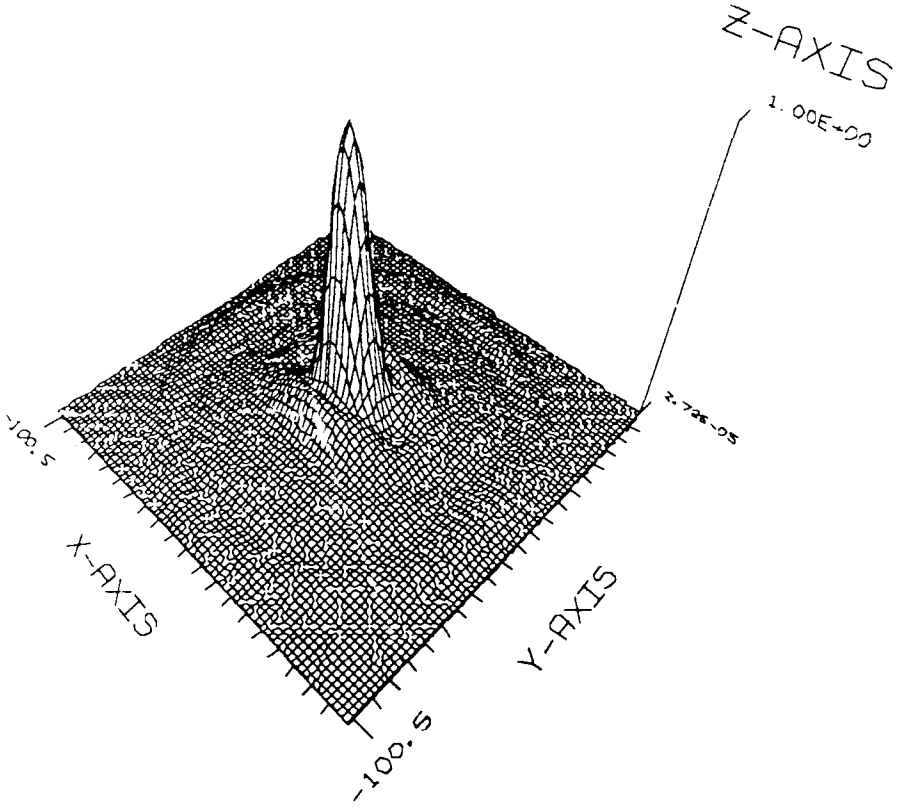

Figure A-14h

MTF - object 7.5 arcmin off-axis
Surface plot